



Jukka Siltanen

# LASER AND HYBRID WELDING OF HIGH-STRENGTH STRUCTURAL STEELS



Jukka Siltanen

## **LASER AND HYBRID WELDING OF HIGH-STRENGTH STRUCTURAL STEELS**

Thesis for the degree of Doctor of Science (Technology) to be presented with due permission for public examination and criticism in the Auditorium 1316 at Lappeenranta-Lahti University of Technology LUT, Lappeenranta, Finland on the 2<sup>nd</sup> of June, 2023, at noon.

Acta Universitatis  
Lappeenrantaensis 1076

Supervisor Docent Veli Kujanpää  
LUT School of Energy Systems  
Lappeenranta-Lahti University of Technology LUT  
Finland

Reviewers Professor Pasi Peura  
Faculty of Engineering and Natural Sciences  
Tampere University  
Finland

Associate Professor Morten Kristiansen  
Department of Materials and Production  
Aalborg University  
Denmark

Opponent Professor Pasi Peura  
Faculty of Engineering and Natural Sciences  
Tampere University  
Finland

ISBN 978-952-335-937-6  
ISBN 978-952-335-938-3 (PDF)  
ISSN 1456-4491 (Print)  
ISSN 2814-5518 (Online)

Lappeenranta-Lahti University of Technology LUT  
LUT University Press 2023

# Abstract

**Jukka Siltanen**

**Laser and hybrid welding of high-strength structural steels**

Lappeenranta 2023

89 pages

Acta Universitatis Lappeenrantaensis 1076

Diss. Lappeenranta-Lahti University of Technology LUT

ISBN 978-952-335-937-6, ISBN 978-952-335-938-3 (PDF), ISSN 1456-4491 (Print),

ISSN 2814-5518 (Online)

Laser and laser-arc hybrid welding processes are recognized as key joining methods in many industrial fields such as light and heavy machinery, ship-building and the automotive industry. In the early days of laser welding, the process was known as a special joining process. The term special is still valid to some extent but the process soon came to be placed in the group of normal welding processes without any speciality. The same and often named list of the advantages and disadvantages of the laser welding process still exists although the situation has partially changed and the list has seen some changes or at least the emphasis is different. The operating and investment costs of laser welding systems have decreased. The number of laser welding system suppliers and integrators has increased and the prices of the main components have dramatically decreased as well. One component of note is the laser resonator. Lasers of one micron wavelength dominate the laser market. The euro/kilowatt ratio has dropped to a level that makes investment possible for smaller companies too. This is especially true in laser cutting. The Covid pandemic had just a temporary influence on the laser technology market and now it is back on a growing curve, as shown by the market analysis reports.

Steelmaking is facing its biggest change since the whole mass production of steelmaking was born. First, the pressure of imported steel mainly from Asia and Eastern Europe forced European steel mills to focus more and more on the production of specialized steels and the reduction of production costs. This has led to the closure of unprofitable steel mills. In addition, one major change is imminent. Steelmaking is moving towards fossil-free production. The path will be a long and winding one but it will happen and most likely sooner rather than later. There is already a growing demand from customers for fossil-free steel. However, manufacturers have already managed to decrease the weight of products and reduce fuel consumption and are able to carry higher payloads by utilizing modern higher strength structural steels in structures.

The joining of high-strength and ultra-high-strength steel can be demanding with conventional welding processes, such as gas-metal-arc welding. The efficient utilization of steels in a welded condition requires the accurate following of recommendations set for example for the cooling rate and welding energy. Modern steels typically have limits set for a minimum and maximum value for the previously named characteristics. As precisely controlled and automated joining processes, laser welding and laser-arc hybrid

welding processes are suitable joining methods for joining modern steels and later for the joining of fossil-free steel as well. The total lifetime cost for a new product can be extremely favourable when combining a high-strength fossil-free structural steel and a laser-based joining process.

This doctoral dissertation contains the published key findings of several laser and hybrid welding studies made for selected high-strength structural steels of several thicknesses which can be utilized in many demanding industrial applications. The welded joints have been tested by non-destructive and destructive testing methods. Some non-standardized measuring methods have been used to some extent to produce scientifically valuable information for the publications. The results clearly show the connections between the welding parameters used and the achieved properties of the laser and hybrid welds. Equations to calculate some variables of welding, such as welding energy, heat input or cooling time were originally created to be used in conventional welding. Therefore, the special properties of laser welding or laser beam welding are not taken into account in these equations. One of these special properties is laser beam absorption, which is still a relatively demanding variable to measure absolutely correctly; for example it varies according to the welding speed and temperature. The doctoral dissertation addresses this topic and presents the utilization of the equations developed especially for laser welding, taking into account the previously mentioned special properties of the laser beam at least to some extent.

Keywords: cooling time, heat input, high strength structural steel, laser welding, laser-hybrid welding, welding energy, heat input, ultra-high strength steel

## **Acknowledgements**

The author would like to thank all of the people who made the writing of this doctoral thesis possible. The list of those persons is very long, making it therefore impossible to name all of them. The journey to writing and finalizing the thesis has been long and partly stony as well. Combining the writing work of the thesis with normal daily routines and work has been quite a demanding task. I am very grateful to my current employer SSAB and my manager Linda Petersson for the support and motivation they have given me to finalize my dissertation. I will allocate my special thanks to Professor Veli Kujanpää, who was my first supervisor when I was just starting my research career in 1995. He has encouraged me to finalize the thesis and gave me valuable advice during the writing process. I am thankful to the reviewers of the manuscript, Professor Pasi Peura from Tampere University (Finland) and Associate Professor Morten Kristiansen from Aalborg University (Denmark) for their time and suggestions that helped to improve this manuscript.

Finally, I will give my biggest thanks to my lovely family, who are always there when most needed. Thank you Sanna, Aada, Aamu and Leo!

This work was carried out in LUT School of Energy Systems at Lappeenranta-Lahti University of Technology LUT, Finland, between 2002 and 2023. It took almost twenty years but it was worth it.

Jukka Siltanen  
January, 2023  
Turenki, Finland



# Contents

**Abstract**

**Acknowledgements**

**List of publications** **9**

**Abbreviations and Symbols** **11**

**1 Introduction** **15**

- 1.1 Background and motivation..... 16
- 1.2 Scope and objectives ..... 16
- 1.3 Thesis structure ..... 18

**2 Presentation of the area** **19**

- 2.1 Laser and laser-hybrid welding..... 20
- 2.2 Laser welding parameters ..... 24
- 2.3 Laser weld quality, laser weld defects and imperfections ..... 28
  - 2.3.1 Porosity ..... 30
  - 2.3.2 Cracking..... 32
  - 2.3.3 Undercut..... 33
  - 2.3.4 Lack of fusion ..... 34
  - 2.3.5 Solidification flaw ..... 35
  - 2.3.6 Spatter..... 35
- 2.4 Laser and laser-hybrid welding of high-strength steel ..... 36
  - 2.4.1 Microstructure of laser and laser-hybrid welded joint ..... 38
  - 2.4.2 Hardness of laser and laser-hybrid welded joint ..... 39
  - 2.4.3 Strength properties of laser and laser-hybrid welded joint ..... 40
  - 2.4.4 Toughness and ductility of laser and laser-hybrid welded joint . 41
- 2.5 Laser welding applications ..... 42

**3 Research methodology** **47**

- 3.1 Materials and methods..... 47
- 3.2 Research limitations ..... 49

**4 Summary of the publications** **51**

- 4.1 Publication I..... 51
- 4.2 Publication II..... 52
- 4.3 Publication III ..... 54
- 4.4 Publication IV ..... 55
- 4.5 Publication V ..... 57

**5 Results and discussion** **59**



5.1	Role of welding parameters .....	59
5.2	Importance of steel grade.....	62
5.3	Testing of weld quality.....	63
5.3.1	Visual quality of welds.....	63
5.3.2	Weld cross-section, dimensions and microstructure .....	64
5.3.3	Hardness.....	65
5.3.4	Tensile strength .....	69
5.3.5	Bend tests.....	70
5.3.6	Toughness properties.....	72
5.3.7	Fatigue .....	74
<b>6</b>	<b>Conclusions</b>	<b>77</b>
<b>7</b>	<b>Future work</b>	<b>79</b>
	<b>References</b>	<b>81</b>
	<b>Publications</b>	

---

## List of publications

This dissertation is based on five (5) scientific publications. The publishers have granted the permission and rights to include these articles in the doctoral dissertation.

- I. Siltanen, J. (2019). Influence of welding parameters on the mechanical properties of a laser-welded joint. *Procedia Manufacturing*, 36, pp. 232-239.
- II. Siltanen, J., Tihinen, S., and Kömi, J. (2015). Laser and laser gas-metal-arc welding of 960 MPa direct quenched Structural steel in a butt joint configuration. *Journal of Laser Applications*, 27, pp. S29007-1-7. <https://doi.org/10.2351/1.4906386>.
- III. Siltanen, J., Skriko, T., and Björk, T. (2016). Effect of welding process and filler material on the fatigue behavior of 960 MPa structural steel at a butt joint configuration. *Journal of Laser Applications*, 28, pp. 1-9. <https://doi.org/10.2351/1.4943993>.
- IV. Farrokhi, F., Siltanen, J., and Salminen, A. (2015). Fiber laser welding of direct quenched ultra-high strength steels: Evaluation of hardness, tensile strength, and toughness properties at subzero temperatures. *Journal of Manufacturing Science and Engineering*, 37, pp. 061012-1-10.
- V. Siltanen, J., Minkkinen, A., and Järn, S. (2017). Laser welding of coated press-hardened steel 22MnB5. *Physics Procedia*, 89, pp. 139-147.

## Author's contribution

The author of the thesis has made the following contribution to the publications.

- I. Principal and only author of the publication. The author organized and supervised the welding experiments and analysed the test results.
- II. Principal author of the publication. The author collected and summarized the presented key findings of the reference articles. Participated as a team member on the reporting of the findings.
- III. Principal author of the publication. The author planned, organized and supervised the welding tests and the destructive testing of welded joints. Dr Tuomas Skriko from Lappeenranta University of Technology organized the fatigue testing of the welded joints, and also participated in writing the article.

- IV. Associate author of the publication. Participated in the finalizing of the publication and provided information for making the publication, such as the welding data for a high strength structural steel.
- V. Principal author of the publication. Planned, organized and supervised the welding experiments. The author analysed the test results of the welded joints and reported the key findings together with the project team inside SSAB.

## Supporting studies

Siltanen, J., Minkkinen, A., Lepikko, E., Järvenpää, M. (2015). Preliminary laser welding tests of 22MnB5 steel with a butt joint and lap joint configurations. ICALEO-conference proceedings, paper 799, <https://doi.org/10.2351/1.5063231>. LIA.

Siltanen, J., Kesti, V., Ruoppa, R. (2014). Longitudinal bendability of laser welded special steels in a butt joint configuration. ICALEO conference proceedings, paper 1127, <https://doi.org/10.2351/1.5063037>. LIA.

Laitinen, R., Tihinen, S., Siltanen, J., Kömi, J. (2013). Laser GMA-hybrid welding of high strength steels with the yield strength of 700 MPa. The 14th Nordic Laser Materials Processing Conference, pp. 193-203.

Karhu, M., Kujanpää, V., Leino, K., Siltanen, J. (2012). Laser-GMA hybrid welding of direct quenched steel in lap joint configuration- A preliminary study. ICALEO conference proceedings, pp. 486-493. LIA.

Siltanen, J., Tihinen, S. (2012). Position welding of 960 MPa steel. ICALEO conference proceedings, paper 464, <https://doi.org/10.2351/1.5062489>. LIA.

Siltanen, J., Kömi, J., Laitinen, R., Lehtinen, M., Tihinen, S., Jasnau, U., Sumpf, A. (2011). Laser-GMA hybrid welding of 960 MPa steels. ICALEO conference proceedings, paper 1502. LIA.

Siltanen, J. (2010). Utilizing laser-hybrid welding in industrial application. ICALEO conference proceedings, paper 53, <https://doi.org/10.2351/1.5062076>. LIA.

## Abbreviations and Symbols

### Abbreviation

AHSS	Advanced high-strength steel
BM	Base material / Base metal
BOP	Bead on plate
CGHAZ	Coarse-grained heat-affected zone
CEN	European Committee for Standardization
CEV	Carbon equivalent
CO <sub>2</sub>	Carbon dioxide
CR	Cold rolled
CVN	Charpy V notch
DQ	Direct quenched
DQ+T	Direct quenched + tempered
DT	Destructive testing
FAT	Fatigue resistance
FGHAZ	Fine-grained heat-affected zone
FZ	Fusion zone
GMA	Gas-metal-arc welding
GMAW	Gas-metal-arc welding
GMAG	Gas-metal-arc welding
HAZ	Heat-affected zone
HLAW	Hybrid-laser-arc welding
HPFL	High-power fibre laser
HPSSL	High-power solid state laser
HSS	High-strength steel
HV	Vickers hardness
ICHAZ	Inter critical heat-affected zone
ISO	International Organization for Standardization
LBW	Laser-beam welding
LHW, LAHW	Laser-hybrid welding
LME	Liquid metal embrittlement
LOF	Lack of fusion
LSS	Low-strength steel
LWTB	Laser-welded tailored blanks
MAG	Metal active gas
MC	Thermomechanical rolling and cold formability
MPNG	Multi-pass narrow-gap
MS	Martensitic steel
NDT	Non-destructive testing
Nd:YAG	Neodymium yttrium aluminium garnet
OK	Commercial name for Esab welding filler wire
PH	Press-hardened

QL	Quenching and tempering
RQ+T	Direct quenching and tempering
RT	Radiographic testing
S	Steel
SCHAZ	Sub-critical heat-affected zone
SEP	Stahl-Eisen-Prüfblätter
TIG	Tungsten inert gas
TMCP	Thermo-mechanically controlled processed
TR	Technical report
UHSS	Ultra-high-strength steel
VDA	German Association of the Automotive Industry
VDW	German Machine Tool Builders' Association
VT	Visual inspection
X-ray	Radiographic electromagnetic radiation
X80/100	American classification of high strength pipeline steel
X96	Welding wire manufactured by voestalpine Böhler Welding Austria GmbH
WM	Weld metal

<b>Symbol</b>	<b>Unit</b>	<b>Explanation</b>
A, A <sub>5</sub>	[%]	Elongation
A <sub>s</sub>	[mm <sup>2</sup> ]	Area of laser spot on the surface
D, d	[mm]	Laser beam diameter
E	[kJ/mm or kJ/cm]	Welding energy
E <sub>l</sub>	[J/mm]	Laser welding energy
I	[A]	Current
P, P <sub>l</sub>	[W]	Laser Power
Q	[kJ/mm or kJ/cm]	Heat input
Q <sub>laser</sub>	[J/mm]	Laser heat input
Q <sub>total</sub>	[J/mm]	Total heat input
R	-	Stress ratio
R <sub>a</sub>	[μm]	Roughness
R <sub>m</sub>	[MPa]	Tensile strength
R <sub>p0.2</sub>	[MPa]	Yield strength
t	[mm]	Thickness
T	[K, °C]	Temperature
U	[V]	Voltage
v	[mm/s or m/min]	Welding speed / Travelling speed
λ	[nm]	Wavelength
η, η <sub>l</sub> , η <sub>arc</sub>	-	Efficiency factor in welding
τ <sub>i</sub>	[s]	Interaction time
Δσ	[MPa]	Stress range

<b>Element</b>	<b>Explanation</b>
Al	aluminium
B	boron
C	carbon
Cr	chromium
Cu	copper
Mn	manganese
Mo	molybdenum
Nb	niobium
Ni	nickel
P	phosphorus
S	sulphur
Ti	titanium
V	vanadium
Zn	zinc
AlSi	aluminium-silicon
ZnFe	zinc-iron
ZnAl	zinc-aluminium



## 1 Introduction

The size of the global steel market is expected to grow. Utilization of steel will increase in all areas of industry. However, steelmaking itself is facing fundamental and almost revolutionary changes. The fossil-free production of steel will start within a few years and it seems that the deadline set for it is moving even closer, if we are to believe the news published by steel producers. The faster than expected and partly unpredictable climate change has been the ultimate trigger to initiate this change in the steel industry. World AutoSteel, the automotive group of the World Steel Association, recently published that the steel industry's share of CO<sub>2</sub> emissions represent about 7 % of the total global emissions. Therefore, steel producers in Europe and the US are starting many actions to reduce their emissions.

One steelmaker worth mentioning in this context is SSAB. SSAB owns steel mills in Sweden, Finland and in the United States of America. Originally, they announced that the first deliveries of a fossil-free steel would take place in 2026, but they rescheduled it to start as early as 2024. In addition, they have already published a long list of customers as the first to utilize a fossil-free steel in their products. The Swedish company Volvo released the very first vehicle made from SSAB fossil-free steel in 2021.

The change in expectations and thinking of customers regarding the use of steel, its origin and possible emissions has been extremely fast and has spread to other sectors of industry as well. Even more changes are expected to happen when customers start to calculate the total lifetime emissions of a product. It is not just steel which is facing these big changes. It is very likely to happen at every level of manufacturing processes, starting from product design and ending in the recycling of the final product. There are some examples that prove that the old way of thinking and ranking possible requests for quotations for a new product or project based solely on the price is about to change. For example, in Norway some decisions on construction investments have been based on the total emissions calculated for the total lifetime of a structure. The winner of that specific order was the company who showed the smallest emissions and that the price is important but not the primary criterion. The usage of modern manufacturing technologies, such as laser-based welding, is one option to support such a change. The high wall-plug efficiency and lower running costs of laser welding compared to conventional welding can offer high productivity with lower emissions. The laser welding process is precisely controlled and has high repeatability, making it suitable also for joining special steels which typically have tight tolerances set for heat input and cooling time.



## 1.1 Background and motivation

Currently, the share of laser beam welding is less than one percent of all welding activities (Unt, 2018). However, industrial fields utilizing laser-based welding in different applications are increasing and the portfolio of processed material is large (Dyley, 1998; Ion, 2005; Steen, 2003; Ready, 2001; Olsen, 2009; Charschan, 1993). Many applications presented in the previous references are from a time when mainly CO<sub>2</sub> and Nd:YAG lasers were used in manufacturing. The birth of the fibre laser was a game changer. Especially the high-power fibre laser opened the door for some new applications. Fibre laser is a solid-state laser operating at close to one-micron wavelength and extremely high maximum laser powers can be reached. Fibre lasers have boosted the usage of laser technology in industry. Laser cutting is very good example of this development. Multi-kilowatt laser powers are utilized in laser cutting, nitrogen is used as a cutting gas and the result is an extremely high cutting speed for thick steel sections while retaining a good cut edge quality (roughness and perpendicularity).

At the same time, the number of welding applications has increased but not as fast as the number of fibre lasers used in laser cutting. Laser cutting machines are quite standardized and not tailor-made. In contrast, laser welding systems are often tailor-made, requiring deep knowhow of laser technology and the welding process. As a result, the number of laser welding system suppliers is quite limited compared to the number of laser cutting machine suppliers. However, laser welding with its different combinations can be seen as a normal joining process and is utilized in many industrial applications.

Fundamentally, the technology of laser welding still has some so-called grey areas with a limited amount of scientifically reliable and exact information. These areas at least partially include the calculation of exact welding energy, heat input, cooling time or even laser beam absorption. Nevertheless, the main challenges to overcome are derived from the special features of laser light.

## 1.2 Scope and objectives

This doctoral dissertation contains a wide spectrum of results regarding laser welding and the laser-hybrid welding of high-strength structural steels. In this dissertation laser-hybrid welding refers to the combination of laser and gas-metal-arc welding processes, unless otherwise mentioned.

The main objective of this research was the laser weldability of high-strength structural steels and the examination of laser-welded joints using non-destructive (NDT) and destructive (DT) testing. Laser welding is used in the automotive industry and the laser-welding results of steel used in automotive applications is presented as part of the doctoral dissertation.

The results of this research can be utilized by steel producers both when developing new steel grades and if there is a need to provide research information to support customers in utilizing laser welding and high-strength structural steels.

The approach to the topic is very practical and almost all of the publications included in this dissertation are the results of the daily work of the author of this doctoral thesis.

The doctoral dissertation focuses on the laser and laser-hybrid welding of high-strength structural steels in order to provide information of relationship between the welding parameters used and the mechanical properties achieved in laser and laser-hybrid welded joints in ultra-high strength steels. The examinations of the mechanical properties of welded joints included both static and dynamic examinations. The properties of laser and laser-arc hybrid welded joints were evaluated by non-destructive and destructive methods. The doctoral dissertation deepens understanding of the laser and laser-hybrid welding of ultra-high strength steels used in demanding applications.

### 1.3 Thesis structure

The doctoral dissertation is based on a general section and five (5) research publications. The first part describes the status of laser welding technology with some sub-themes, such as the laser and laser-hybrid welding processes, welding parameters, weld imperfections, special features of the welding of high-strength steels and finally applications utilizing laser welding technology. The second part of the dissertation presents the publications with the main research findings and analysis.

## 2 Presentation of the area

The history of laser and laser processing has already been detailed in a relatively long list of books and publications; articles describing the first laser beam flame are also numerous. The history of laser and laser technology is not repeated in this dissertation. The pioneers working with early lasers paved the way for remarkable process and nowadays this unique technology is used in countless numbers of applications. Instead of focusing on the past, the present situation of laser technology and welding is described here and attention is paid to laser welding parameters, weld quality and weld defects. Finally, the wide spectrum of applications utilizing laser technology in welding is presented.

This doctoral dissertation focuses on the laser welding of structural steel and especially the joining of high-strength structural steels. This group of steel includes steels used in the automotive industry and in many white goods; often termed advanced high-strength steels (AHSS), steels used in heavy engineering which are called high-strength structural (HSS) or even ultra-high-strength (UHSS) structural steels. These steels can have a very complex microstructure and be challenging to manufacture at the steel mill, because of their unique mechanical properties which make their further processing quite demanding.

The European steelmaking industry will soon face the biggest changes in its history. The transition to a low-emission green economy has started and the speed of the development is increasing thanks to the demand for decision-makers to start taking action, for example by setting strict limits for harmful emissions.

One example of a steelmaker who has started to act to reduce emissions dramatically is SSAB, the steelmaker from Scandinavia. SSAB has published an extremely ambitious plan to initiate fossil-free steel production. The original deadline to go for zero emissions of CO<sub>2</sub> was set for the year 2045 but it was then decided to bring it forward to 2035. The reduction of CO<sub>2</sub> emissions will be eight million metric tons annually. The reduction will cut total CO<sub>2</sub> emissions in Sweden by 10 percent and in Finland by 7 percent. There are still many challenges to overcome on the way before the target is reached. An enormous amount of electricity produced fossil-free and hydrogen for mill processing is needed. However, the recycling rate of steel is already above 85 per cent globally and this can be done without any loss of quality in the steel made from this recycled raw material. However, the amount of recycled steel is not high enough for total steel production and some mined iron ore is still needed. Therefore, fossil-free production with zero emissions is a combination of fossil-free mining, fossil-free electricity and fossil-free steel.

It is not just steelmaking that is facing big changes. There are examples showing the change in thinking when calculating the product lifetime cost and ranking steel products on that basis. There is an increased need to calculate the carbon footprint for a steel product starting from the mining of raw materials (iron ore) and ending up with the recycling of the final steel product. There are also many other processes between the

above-mentioned stages: laser welding or laser-hybrid welding can be one of these processes.

## 2.1 Laser and laser-hybrid welding

Laser welding can be divided into three different welding modes depending on the laser power density and depth of penetration used: conduction, transition and keyhole (penetration) mode, see Figure 2.1. Conduction welding as a welding process is similar to gas tungsten arc welding. It is performed by using a low energy density, typically around  $0.5 \text{ MW/cm}^2$  and the shape of the formed weld nugget is shallow and wide. The heat to create the weld in the material occurs by conduction from the surface. The thickness of the welded material in conduction laser welding is small and no deep penetration is achieved. The laser beam quality needed in conduction welding can be much lower than that used in keyhole welding. The early versions of the diode laser were used in conduction welding because of its low beam quality. The power intensity and beam quality were not good enough for deep penetration keyhole welding. Keyhole laser welding or penetration laser welding, as it is sometimes called, is similar to electron beam welding. In keyhole welding, laser beams form a vapour cavity tunnel inside the steel and the required laser power density is much higher ( $1.5 \text{ MW/cm}^2$ ) than in laser conduction welding. The formed keyhole can have a different shape and behave differently. The keyhole modes are named trap, cylinder and kaleidoscope, and there are some sub-types as well (Vänskä, 2014). The third mode, transition mode, is not mentioned so often in the literature. It occurs at medium power density, around  $1 \text{ MW/cm}^2$ . The penetration depth is relatively low and the weld depth/width ratio is close to one.

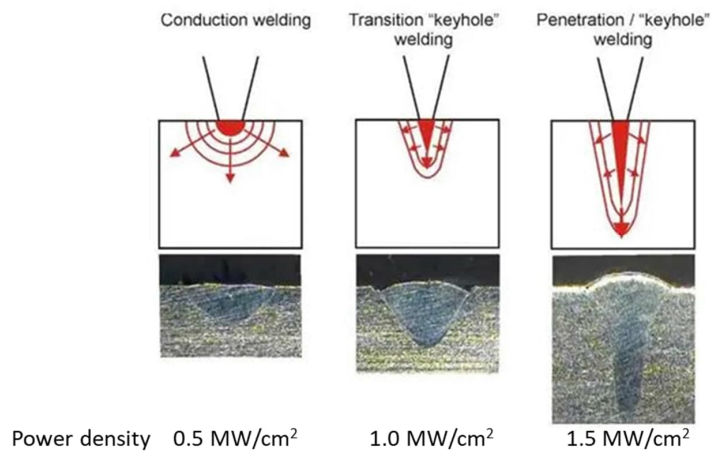


Figure 2.1: Principle of conduction, transition and keyhole laser welding (modified from the reference <https://amadaweldtech.com/blog/laser-welding-modes-conduction-transition-keyhole-welding/>).

Nowadays laser welding is a relatively common welding method and its plusses and minuses are well-known. When looking at the list of disadvantages and high investment costs in laser welding, it is worth mentioning that the field of industrial production and application has a huge influence on whether that statement is true or not. In mass production, such as the automotive industry, it is quite safe and common to invest in laser welding technology. The high production rate of the system can be fully utilized and used to achieve high-level automation. If we look instead at a typical engineering industry, for example, in Finland, the situation is totally different. The amount of articles produced may be large but the series size is small. Therefore, the time taken for a new set-up can be long and real production time is wasted, most likely making the investment unprofitable. It is also possible that laser welding based production is so efficient that the whole yearly production of the unit can be made in such a short time that there is not enough work for the laser welding system. This could be solved by intensive sales work to fill the line with new products.

Utilizing laser welding for joining steels has had a positive influence on the mechanical properties of welded joints. The welding test made for automotive steels showed good results when compared to the weld results of conventional gas-metal-arc welding. In the laser welding test made for martensitic high-strength steel ( $R_m=1200$  MPa), the strength properties showed just a slight decrease after welding from the properties of the base material. The width of the heat-affected zone (HAZ) was just 0.2 mm whereas in MAG welding it was 10 times wider and the microstructure of the HAZ did not show any dramatic grain coarsening (Nemecek et al., 2012).

The welding process is known as hybrid laser welding when an additional process is added to laser welding. This additional process is typically gas-metal-arc welding and the process can be named laser-arc hybrid or laser-hybrid welding. Laser-hybrid welding is

a more flexible and robust welding process, providing higher productivity and quality when compared to pure laser welding and conventional arc welding (Lawrence et al., 2010). The addition of an extra process to laser welding can have some benefits compared to laser beam welding with or without filler wire (cold or hot wire).

Laser-hybrid welding can improve productivity (+10 - +40%) compared to keyhole laser welding and it can reduce the formation of some weld imperfections (Kah, 2011; Eriksson et al., 2013). A higher speed is achieved when compared to conventional laser welding (Wouters, 2005).

Professor Steen invented the early version of laser-hybrid welding in 1980. At that time, the gas tungsten arc (TIG) process was combined together with a laser beam. Later, the process was developed and the laser-hybrid welding process took its current form. The development of the laser-hybrid welding process happened in three stages. The first stage was the invention of the hybrid process in the seventies (Steen, 2003). Steen described the process and some of its benefits, such as a more stable welding process when two welding methods are combined. The second stage of development occurred when the focus was on laser radiation and the efficiency of the process was increased. However, the utilization of the laser-hybrid process in industrial applications was still lacking and finally happened in the third stage of development (Mahrle et al., 2006). One of the first applications utilizing the laser-hybrid welding process was the joining of tailored blank steel sheets used in the automotive industry. A laser-welded tailored blank steel sheet is one of the applications that has its own standard. The standard gives instructions for the manufacturing, quality and inspection of laser-welded blanks. Shipbuilding was another of the first applications, starting testing of the laser-hybrid welding process to join steel sensitive to cracking. They also noticed that laser-hybrid welding can correct some of the disadvantages of laser beam welding.

Joint preparation before actual laser welding is a very important work phase. The conditions of the edges, such as roughness on the edges and the air gap between them, play an important role in deep penetration keyhole welding. The preparation of an edge surface to a roughness of  $6.3 \mu\text{m}$  ( $R_a$ ) and the usage of a controlled air gap (0.1-0.2 mm) have resulted in deeper penetration welds and better overall weldability (Sokolov, 2015). Common cutting methods, such as laser, plasma and abrasive water jet cutting and also milling have proved to be suitable edge preparation methods for laser and laser-hybrid welding (Farrokhi et al., 2015; Üstündag et al., 2022). The orientation of a cut kerf in a plasma-cut specimen has a major influence on the weld profile formed and might have some influence on the properties of the weld.

Laser-hybrid welding can be used for the single-pass or multi-pass welding of thicker steel sections. The target is to reduce the number of welded passes to decrease the manufacturing costs. Instead of one welded pass, it is possible to use multi-pass welding technology to avoid weld defects. The usage of a second pass in welding can improve the weld quality by repairing a weld defect formed in the welding of the first pass (Farrokhi et al., 2017).

One interesting, new and special welding process is the laser beam submerged arc hybrid welding process. The submerged arc welding process is the predominant industrial welding process for joining various steel grades in the thickness range of about 40 mm. This new process variation could improve the weld quality and reduce the level of distortions (Reisgen et al., 2012; Reisgen et al., 2020). Studies have shown a reduction in the formation of porosity even when joining thicker steel sections (thickness  $\geq 12$  mm).

One of the latest innovations in laser welding is the dynamic manipulation of a laser beam. One example of this method is to utilize the wobble function of a two-dimensional welding scanner. The method is still relatively new, limiting the amount of results available. However, some positive effects on gap bridging capability have been reported; however, on the other hand, the formation of some weld imperfections has been identified (Kankala et al., 2021).

Other special technologies to improve weld quality in laser welding have been developed. The use of magnets in laser welding has also shown some positive effects on weld quality (Bachmann et al., 2015).

The advantages and disadvantage of laser welding and laser-hybrid welding against conventional arc welding as regards the welding process and economic aspects have been identified. Most of these have been verified by the end-users of laser welding technology, see Table 2.1.

Table 2.1: Comparison of advantages and disadvantages of laser and laser-hybrid welding.

<i>Advantages</i>	<i>Disadvantages</i>
Laser welding	
Capable of making a deep weld (a high width/depth ratio of joint)	Precise preparation of work piece, exact joint fit-up
Low heat input with minor distortion	High investment cost
Non-contact process, no tool wear	High level of know-how needed
Freedom in welding position	More complex weld defects
Possible to join advanced materials	
No consumables (shielding gas, filler material)	
Precise control of welding parameters = possible to influence weld properties	
Laser-hybrid welding	
Greater tolerance to joint gaps and better gap bridging capability	Increased number of welding parameters
Possible to control weld properties by the usage of additional filler material	Higher operation costs (equipment, maintenance, filler, shielding gas)
Higher welding speed than in conventional arc welding	



## 2.2 Laser welding parameters

It is important to know the main laser welding parameters and their influence on weld process and quality. The main parameters influencing laser welding can be listed in many ways. The list of the main laser and laser-hybrid welding parameters included in this section and presented in Table 2.2 has been collected from several sources and modified to fit the purpose. One way of categorizing is to divide the parameters into optical and welding set-up parameters. The optical parameters are typically constant, whereas the welding set-up parameters change according to the welding case. The material properties, such as chemical composition, thickness and surface quality together with the physical properties of the material (reflectivity of laser beam, thermal diffusivity, surface tension) have a great influence on welding. The groove preparation of the material before welding typically refers to the variables: angle of edges, the air gap between them. The correct selection of the above is important for achieving good weld quality and avoiding weld imperfections.

Some changes in the naming of laser welding parameters have occurred since fibre lasers came on the market, almost displacing CO<sub>2</sub> lasers. The optical parameters of a laser welding system have a great influence on the weld quality achieved and the total productivity of a welding system. For example, research made on fibre lasers has shown that optics with a wider focus depth produce better weld results than optics with a shorter depth of focus. A focus depth change from 2 mm to 4 mm produced a sound weld without imperfections such as underfill, undercut, humps or porosity; this was especially valid when a lower welding speed was applied (Matsumoto et al., 2017). The above results were explained by the excessive laser heat input at a lower welding speed caused by a higher peak power density with a small spot diameter of 200 µm in contrast to a lower peak power density with a spot size of 270 µm. X-ray analysis showed that the melt flow was unstable with optics that had a smaller focus diameter and depth.

Table 2.2: Main laser, arc and combined welding parameters (modified from Lawrence et al., 2001; Fellman, 2008; Steen, 2003; Dyley, 1998).

<b>Laser parameters</b>	<b>Arc parameters (hybrid)</b>
Laser power	Current
Laser wavelength	Voltage
Laser beam quality	Filler wire type and diameter
Focal length	Filler wire stick-out
Focal point position and diameter	Pulse parameters <ul style="list-style-type: none"> <li>- Frequency</li> <li>- Duration</li> <li>- Current</li> <li>- Base current</li> <li>- Pulse shape</li> </ul>
Alignment of laser beam	Torch angle and direction
Laser beam angle of incidence	
<b>Combined parameters of laser and arc</b>	
Welding speed	
Distance between welding processes	
Ordering of processes (leading / trailing laser)	
Shielding gas composition and flow rate	

The use of laser-hybrid welding has increased the number of parameters. The change from a CO<sub>2</sub> laser to a shorter wavelength fibre and disk laser simplified the laser-arc hybrid process. Guiding the beam is easier with a fibre and the control and plasma plume formation are different in fibre laser welding. This is because of the different absorption mechanism between the welded material and the laser beam when a fibre laser is applied in joining. In CO<sub>2</sub>-laser welding, controlling the plasma plume is extremely important and is done by selecting the correct shielding gas and gas flow in welding.

It should be noticed that some parameters are more critical than others for welding. For instance, a deeply penetrating weld can be produced by fibre laser welding with high laser powers even if argon is used as a shielding gas. In the case of CO<sub>2</sub>-laser welding, just a small addition of argon to helium, which is normally used as a shielding gas, decreases the penetration depth (Lawrence et al., 2010). In fibre-laser welding of press-hardened steels used in automotive applications, the usage of argon as a shielding gas instead of no gas (air atmosphere) showed no difference in mechanical properties or hardness of the welded joints. However, some amount of oxygen diffused in the weld metal (Sun et al., 2018). The orientation of the gas shielding pipe influences laser welding perhaps more than has been realized. The angle change of a shielding gas pipe from 30 degrees to 45 and 60 degrees can stabilize the welding process and increase the depth of penetration of welds as well. The new positioning of a gas flow enlarges and deepens the keyhole opening, making it easier for a laser beam to enter inside the keyhole, which produces a deeper weld. The penetration depth of a weld can also be increased by the use of a side gas jet but, in that case, the maximum gas flow is reduced to ensure a stable welding process (Zhang et al., 2008).

Laser power and welding speed are used to determine the rate of energy input to a workpiece. The energy input (rate) is named welding energy (E) or heat input (Q) and for laser welding it is calculated by using Equation 1. The only difference to the calculation of heat input is the efficiency ( $\eta$ ) factor, which is added to the calculation (Equation 2). In the case of laser-hybrid welding, the total welding energy or heat input is the sum of the heat inputs of the laser and arc processes (Equation 3):

$$E_l = \frac{P_l \times 60}{v} \quad (1)$$

$$Q_l = \eta_l \times E_l \quad (2)$$

$$Q_{total} = Q_l + Q_{arc} = \frac{\eta_l \times P_l \times 60}{v} + \frac{\eta_{arc} \times U \times I \times 60}{v} \quad (3)$$

where:

$E_l$  = laser welding energy [J/mm]

$P_l$  = laser power [W]

$v$  = welding speed or travel speed [mm/min]

$\eta_l, \eta_{arc}$  = efficiency factor

$Q_{laser}$  = laser heat input [J/mm]

$Q_{total}$  = total heat input [J/mm]

$I$  = current (A)

$U$  = voltage (V)

The efficiency factor depends on the welding process used. An efficiency factor of 0.8 is used in arc welding. The efficiency factors for conventional welding methods are quite accurate but the efficiency factor used for laser welding (1.0) is quite theoretical since the absorption of a laser beam has a great effect on the conduction of heat to the material. There are several factors influencing absorption:

- Welded material
  - o Reflectivity
  - o Surface roughness
- Laser wavelength (shorter wavelength = better absorption)
- Temperature in welding (absorption increases when the welded material is heated)
- Positioning of a laser beam (90 degree angle = highest absorption).

There are other equations to calculate some of the basic laser material interaction parameters, such as power density, interaction time, specific point energy and joining efficiency. The power density defines the ratio of laser power per area of laser beam. The interaction time defines the time in which a certain point on the surface of material is exposed to the laser beam. The specific point energy, defining the level of energy at a

certain point at a certain time, can be calculated by utilizing the values of welding speed and laser power joining efficiency and illustrates the amount of energy per area:

- (Average) power density,  $q_p$  [W/m<sup>2</sup>] (Equation 4)

$$q_p = \frac{P_l}{A_s} \quad (4)$$

- Interaction time,  $\tau_i$  [s] (Equation 5)

$$\tau_i = \frac{d}{v} \quad (5)$$

- Specific point energy,  $E_{SP}$  [J] (Equation 6)

$$E_{SP} = q_p \times \tau_i \times A_s = P \times \tau_i \quad (6)$$

- Joining efficiency,  $JE$  [mm<sup>2</sup>/kJ] (Equation 7).

$$JE = \frac{v \times d}{P_l} \quad (7)$$

where:

$A_s$  = area of laser spot on the surface [mm<sup>2</sup>]

$d$  = laser beam diameter [mm]

$P_l$  = laser Power [W]

$v$  = welding speed [m/s].

The significance of the previous equations is greatly dependent on the type of laser welding process. Energy in conduction laser welding has to be transferred to the material via conduction, which is a relatively slow process. Depth of penetration in laser welding is strongly dependent on the interaction time and the power density has to be high enough to ensure melting of the material (Ayoola et al., 2017). In keyhole laser welding, the role of laser power density is even more critical. The depth of penetration is mainly controlled by two parameters: power density and specific point energy. Decreasing the laser power does not provide a greater penetration depth if the specific point energy is insufficient (Suder et al., 2012). Figure 2.2 depicts the affiliation between the interaction time and the laser power density needed for different laser-based processes.

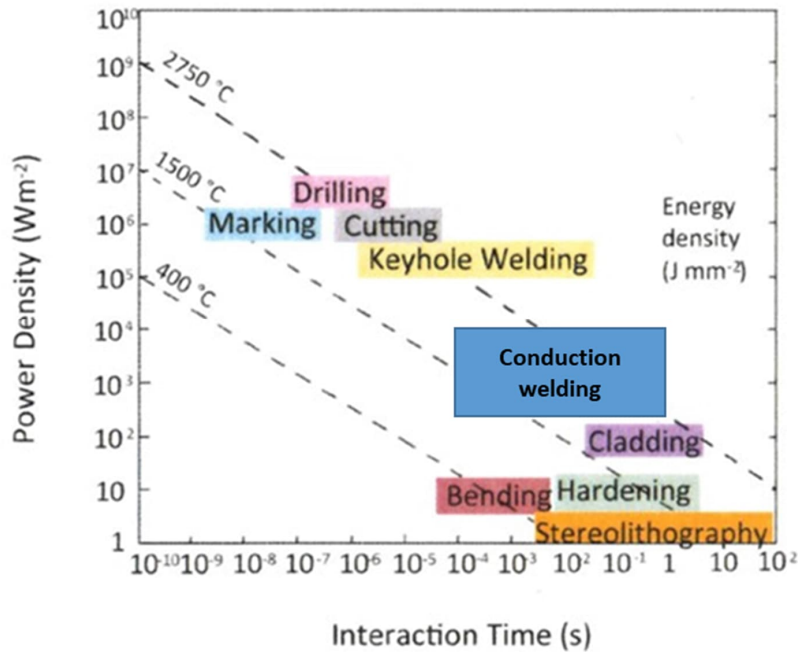


Figure 2.2: Processing map based on power density and interaction time (modified from Suder et al., 2012).

### 2.3 Laser weld quality, laser weld defects and imperfections

It is possible to produce a high-quality welded joint by both laser welding and laser-hybrid welding processes. However, as with all welding processes, some weld defects or imperfections might still appear in welding. ISO standards 13919-1 (laser welding) and 12932 (laser-arc hybrid welding) deal with weld imperfections and the allowed limits for different weld classes termed B, C and D. The accepted maximum values for each imperfection are specified under these classes. Quality level B corresponds to the highest requirement for the finished weld.

The probability of a weld defect forming is dependent on many variables. It is more challenging to weld a greater steel thickness than a thinner one. There are also some other factors influencing the formation of a possible weld defect: the welding parameters, joined materials, joint type, edge preparation method and quality of edges before welding and performance of welding. Performance of welding means for instance if the welding loop is made in the wrong way and an end crater might be formed in the weld. This end crater can provoke the formation of other weld imperfections, such as pores, cracks, root excess weld metal and shrinkage cavities (Gook et al., 2020). Luckily, it is possible to prevent these imperfections through the selection of correct laser welding parameters and planning of the welding loop.

Standard ISO 13919-1 clearly presents the typical weld imperfections in laser welding. Some welded defects or imperfections are more likely to form in laser welding. Figure 2.3 illustrates some weld imperfections of laser welding. The list is not complete but presents the most common imperfections.









Defect	Explanation
 Cracks	Hot crack in the fusion zone or cold in HAZ
 Porosity and gas pores	Voids in the material Spherical = gas bubbles Irregular = impurities
 Incomplete penetration	Not deep enough penetration
 Linear misalignment	The two parts centerlines do not coincide
 Lack of fusion	The two parts are not welded throughout the entire weldzone
 Undercut Root sagging	Lack of material in upper weldzone Too much material in lower weldzone
 Reinforcement Root cavity	Too much material in upper weldzone Not enough material in lower weldzone
 Blowout	Crater formation on top surface

Figure 2.3: Typical weld imperfections for laser and laser-hybrid welding (Frostevarg, 2014).

Controlling the weld quality in laser and laser-arc hybrid welding can be demanding. One advantage of laser welding and laser-arc hybrid welding compared to traditional welding processes, e.g. gas-metal-arc welding, is a higher welding speed. However, there is a limit for the welding speed. Too high a speed can disturb the laser welding process or the existence of a stable keyhole in the case of deep penetration welding.

The decreasing in welding or travelling speed can lead to the forming of serious weld defects, such as solidification cracking or undercut (Frostevarg, 2014). The groove preparation methods and the quality of the edges have a major effect on the weld quality achieved if laser and laser-hybrid welding are utilized. It is beneficial to use thermal cutting methods, such as laser and plasma cutting as a groove preparation method, diverging from the early instructions for edge preparation that preferred machining. When pressed together, the laser-cut edges guarantee the forming of a natural air gap between the parts and have a positive influence on the laser and laser-hybrid welding quality (Sokolov, 2015; Farrokhi, 2018). The butt joint was the main joint configuration studied in the above publications. However, a laser-cut edge can also be used in the case of a fillet weld (T-joint), which is a typical joint type used in shipbuilding (Unt, 2018). It is possible

to have a stable bead formation despite using a larger air gap between laser-cut edges when a CO<sub>2</sub> laser or fibre laser-arc hybrid welding are applied (Fellman, 2008; Eriksson et al., 2013). The following sections focus on some of most common weld defects or imperfections observed in keyhole laser or laser-hybrid welding and the actual appearance has been recognized in the welding tests made by the author of this dissertation. There are standards (ISO 13919-1, ISO 12932) available both for the laser and laser-arc hybrid welding of steel giving the quality requirements for weld classes. Product-specific standards and guidelines for laser welding have also been published. The previous standards mainly focused on the laser welding of automotive parts and components or in shipbuilding (SEP 1220-3, EN 10359, Lloyd's Register, DNVGL-CG-0287). There are some standards (ISO 1011-6, ISO 15609-3, ISO 15609-6) specifically for laser and laser-hybrid welding processes and the making of a welding procedure specification (WPS, WPQR). Another standard worthy of mention is the thermal cutting standard ISO 9013, which classifies the cut quality for different thermal cutting methods.

### 2.3.1 Porosity

Porosity is an often observed weld defect in laser welding of different steels and also in aluminium. The form of porosity varies and can be a localized single pore or linear and in addition it can extend to a different depth in a weld. Fortunately, porosity can be considered a less serious weld defect as long as its quantity or volume remains at a low enough level. The location of the porosity can indicate the root cause of its formation and may give a hint how to prevent it. The edge preparation of welded specimens also influences the probability of porosity formation. The possible oxides on the surface of the welded edges might affect the weld quality and formation of pores if the thickness of steel is 12 mm or more (Engström et al., 2002).

In multi-pass laser-hybrid welding, porosity typically forms in the welding of fill or cap passes. The most effective approach was found to be welding the highest possible root face with laser-hybrid welding and filling the remaining groove with a GMAW process (Grünenwald, 2019). Welding results confirm that bubbles are generated from a keyhole tip to form porosity at low welding speeds but are not formed at high welding speeds. The keyhole will collapse if a slow welding speed is used, making the formation of porosity possible (Katayama et al., 2009; Lawrence, 2010). The trapped bubbles turn into pores. The above-mentioned mechanism of porosity formation is illustrated in Figure 2.4. The use of an increased air gap in laser-hybrid welding seems to have a similar effect as the welding speed in the formation of pores (Bunaziv et al., 2019). The use of a partial penetration weld depth instead of a full penetration in laser welding can lead to the forming of pores in the root side of the weld (Figure 2.5).

There are some techniques available to prevent the formation of bubbles, which might lead to the forming of pores (Lawrence et al., 2010):

- Full penetration welding
- Proper pulse modulation
- Forwardly tilted laser
- Twin-spot laser welding
- Use of a tornado nozzle
- Laser-hybrid welding with laser and TIG or MIG at high arc current
- Higher speed welding.

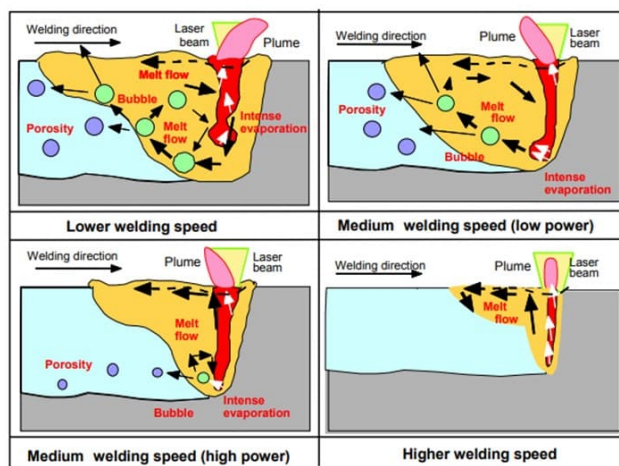


Figure 2.4: Schematic presentation of molten pool, keyhole, bubble, porosity and melt flows depending upon welding conditions (Katayama et al., 2009).

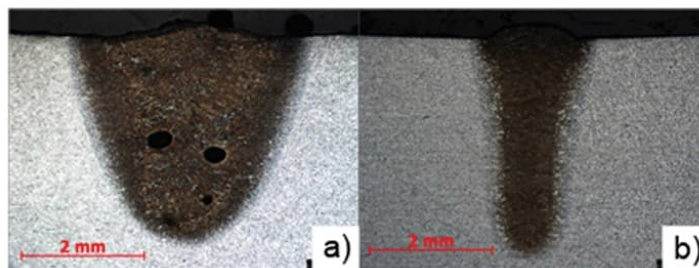


Figure 2.5: Porosity (left) in laser weld and free of porosity weld (right) (Suder et al., 2012).



### 2.3.2 Cracking

Cracking types are categorized according to the crack type and forming mechanism. Hot cracking (or solidification cracking) has been the crack defect connected to laser or laser-arc hybrid welding especially when welding thicker materials. Hot cracking mainly occurs if the width/depth ratio of a welded joint is unfavourable, causing a crack to form. The forming mechanism of hot cracking has been widely researched and three factors, namely thermal cycles, mechanical loading and local microstructure, have been identified as decisive for the determination of cracking behaviour in a welded part (Artinov et al., 2020; Bakir et al., 2020). It is possible to affect the forming of a weld defect by the usage of optimized welding parameters. In the case of laser-hybrid welding and if a partial penetration welding is applied, forming of solidification cracking is greatly dependent on the welding parameters used. The focal position and laser beam quality have a significant influence on crack formation (Bakir et al., 2019). It has been demonstrated in some preliminary laser welding trials that the number of hot cracks can be reduced by a modulation of laser power (Schaefer et al., 2017). A more common way to reduce the forming of solidification cracks is to reduce the travelling speed in a laser or a laser-arc hybrid welding in order to affect the orientation of grains in a solidified weld pool (Bunaziv et al., 2019; Karhu, 2019). Columnar and equiaxed solidification modes are usually developed in the welding of low carbon low alloy steel welding. Equiaxed orientation in the microstructure of laser welds is preferable to prevent solidification cracking from happening (Bunaziv et al., 2019).

Welds with full penetration should be preferred in order to avoid the formation of a solidification crack (Farrokhi, 2018). The change from single-pass welding to multi-pass welding can also reduce or prevent solidification cracking. It is possible to achieve a wider weld fusion zone and the tolerances of welding are increased by using an oscillated laser beam. This process might have a positive influence on cracking behaviour (Grünenwald, 2019). Solidification cracking has also been observed in the laser welding of pipes with a thick wall thickness. Typically, a crack initiates at the bottom of an end crater located at the end of a joint or in the welding of a pipe or tube when the weld is closed and some overlapping occurs in the weld start and end position when the welding stops (Üstündag et al., 2020).

Cold cracking or delayed cracking or hydrogen cracking is a relatively unusual weld defect in laser or laser-hybrid welding. Although the same weld defect has many names, basically it means a defect which forms shortly after welding or even some time after the welding itself. The increased usage of ultra-high strength steels with complex microstructures and high strength levels are showing increased cold cracking behaviour when joined by laser beam welding, especially if short weld lengths are used. The phenomenon of cold cracking in a laser weld is not yet fully understood but probably it will attract more interest in future.

Liquid metal embrittlement (LME) has been identified in the welding of cold-rolled high-strength steels with complex microstructures and those that have metallic coatings such

as a zinc coating. The LME is very serious weld defect. The LME phenomenon in resistance spot welding (RSW) has been widely researched. The WorldAutoSteel organization has recently completed a project focusing on LME in RSW, and a report of the project has been published (<https://www.worldautosteel.org/projects/liquid-metal-embrittlement/>). The report describes the mechanism of LME and gives some welding recommendations for avoiding LME as well as acceptance criteria of welds and some proposals for weld testing. The increased usage of laser welding in the joining of car body parts requires actions to prevent LME in laser welding, in the same way as for resistance spot welding. The different types of cracks in laser welding are depicted in Figure 2.6.

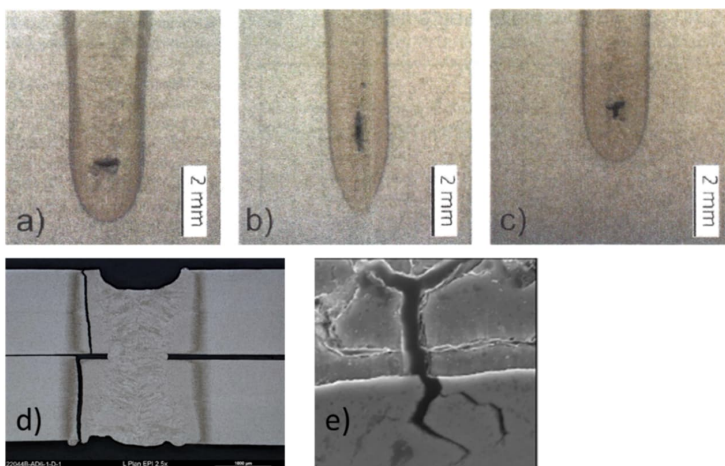


Figure 2.6: Different types of cracks formed in laser welding: hot cracking - a) horizontal direction, b) vertical direction, c) cross-shaped (Bakir et al., 2020), and d) cold cracking and e) LME cracking (Razmpoosh et al., 2018).

### 2.3.3 Undercut

Undercuts are usually an imperfection in welding that form either continuously or sporadically, especially when welding at high speed (Frostevarg, 2014). Frostevarg has identified many kinds of undercuts in laser, gas-metal arc and laser-hybrid welding. The types of undercut can be divided into continuous and irregular formation mechanism; the condition (mill scale or not) of the steel surface also influences the formation of an undercut. For example, in the laser-hybrid welding of mild steel with mill scale on the surface a sharp, angled undercut was formed and when the mill scale was removed the formed undercut had a more rounded geometry and was smaller in size (Figure 2.7). However, when a CO<sub>2</sub> laser is applied to welding, it is beneficial to use steel with mill scale on the surface because the reflectivity is reduced by approximately 30% (Xie et al., 1999).

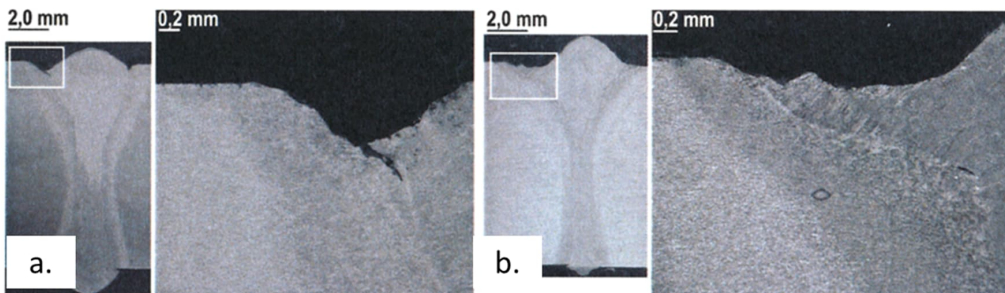


Figure 2.7: Weld cross-sections from a laser-hybrid weld and different types of undercut: a) steel with mill scale, b) mill scale removed (Frostevang, 2019).

Preventing of the undercut might require the reduction of the welding speed, leading to a loss of productivity when laser beam or gas-metal arc welding is applied. By the use of two combined welding processes, e.g. laser-hybrid welding instead of one process, a higher welding speed with increased productivity can be achieved. Productivity plays a key role when calculating the payback period for a new investment or making a decision on investment.

#### 2.3.4 Lack of fusion

The weld defect known as lack of fusion in laser or hybrid-laser welding is mainly related to the joining of thicker steel sections and is a relatively unusual weld defect in the above-mentioned welding processes. Lack of fusion occurs if the edge preparation before welding is not correctly made, if there are some impurities between the edges or too big an air gap between the edges (Figure 2.8). In some cases and for some reason the laser beam changes its route in welding and a small unwelded area forms.

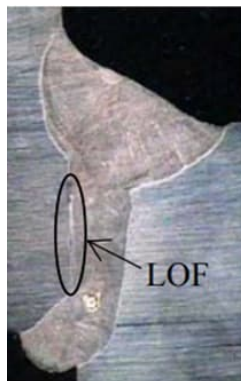


Figure 2.8: Lack of fusion (LOF) in a laser-hybrid welded joint (Alam et al., 2009).

### 2.3.5 Solidification flaw

Solidification flaws are mainly connected to a weld defect in laser welding. The forming of this defect has been attributed to the steel composition, heat input and plate thickness (Gerritsen, 2005). Solidification flaws are mainly observed in the upper limit of the thickness range welded by laser-assisted processes. The size of the flaw is relatively small, with isolated imperfections occurring with a certain regularity along a weld (Flemming et al., 2009). Detection of solidification flaws in inspections of laser welds can be relatively demanding. It is not possible to use visual examination for the inspection of solidification flaws because they are not open on the surface and radiographic inspection (RT) can be demanding due to the small volume of the flaw. Cases have been reported in which cracking in a final product was observed that was caused originally by a solidification flaw and despite large-scale NDT inspection, the flaw was not detected leading to the critical failure of the product.

### 2.3.6 Spatter

Spatter is considered a less critical weld defect and the acceptance level depends on the application. However, spatter formation on a joint indicates the presence of more critical weld defects, such as undercut, crater or blowout, and therefore the controlling of spatter formation is important (Kaplan et al., 2011). Heavy spatter formation is observed at high welding speeds, especially if a laser with a good beam quality is used (Weberpals et al., 2008). Spatter formation depends strongly on the laser welding parameters used. Operating with a one-micron laser at high power can offer a high welding speed for the joining of steels. However, the combination of a high laser power and welding speed can lead to different types of spatter formation, as depicted in Figure 2.9. The reason for this behaviour might be an unstable keyhole and the incorrect combination of welding parameters. In addition, the type of welded joint (BOP, I-joint, lap joint) and the penetration depth affects the amount of spatters formed. Studies have shown that spatter-free welds can be produced with full penetration laser welding (Vänskä, 2014). The laser welding of metal-coated steels is a typical example of heavy spatter formation. The vaporization of the coating is not controlled and in the case of overlap welding, a proper air gap is not used to prevent spatter formation.

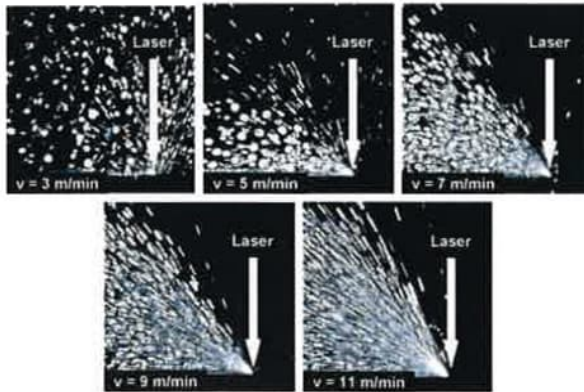


Figure 2.9: Spattering at different welding speeds and a constant 6 kW laser power (Weberpals et al., 2008).

## 2.4 Laser and laser-hybrid welding of high-strength steel

The development of high-strength structural steels has been very fast. Modern and advanced steel processing technology together with unique alloying possibilities has made it possible to development high-strength steels with good workshop processing properties for cutting, forming and joining. The current definition of structural steels defines steels having a yield strength higher than 700 MPa as ultra-high-strength steels (UHSS). These ultra-high-strength steels belong to the family of advanced high-strength steels (AHSS) and vice versa. The previous naming of steels according of their strength is flexible and changes all the time because of the fast development of steels. Standard CEN ISO/TR 15608 categorizes steels according to their alloying and strength level. Steels can have complex multiphase microstructures resulting in a good combination of strength and formability. Modern thermomechanical processing of steel utilizes rolling, tempering and quenching processes in a unique way (Figure 2.10).

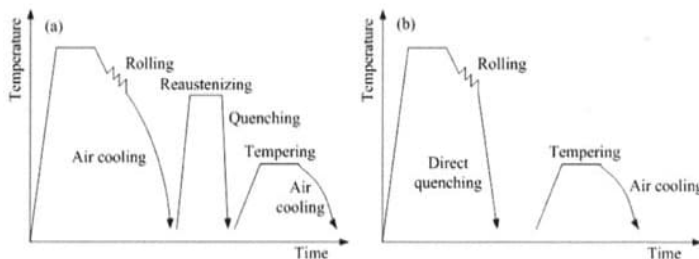


Figure 2.10: Schematic representation of different heat-treatment processes: (a) RQ+T, (b) DQ+T (Song et al., 2013).

The general trend in steel development is moving towards even higher strength steel with good toughness and weldability (Suikkanen, 2009). Good bendability or formability are often required as well, and from the steel development point of view, the previous factors of functionality can exclude each other if only a single element of those is developed at a time. The improved strength and toughness properties of modern high-strength structural steels are obtained by reducing the carbon content, by utilizing quenching and tempering technologies, and by optimization of alloying elements (Suikkanen, 2009).

The modern UHSS are often rolled in a steel mill using rapid water cooling and a relative mild alloying in steel can be used. Direct quenching (DQ) is a very cost-effective process for producing steels with unique properties. Direct quenching can be combined with a tempering process (DQ+T). One example of a direct quenched steel without tempering is S960 HSLA (HSLA = high-strength low-alloyed). The microstructure of the direct quenched S960 HSLA is a mixture of tempered martensite and bainite and the carbon equivalent (CE) is close to 0.5, indicating the limited weldability of the steel with conventional welding processes.

Other ultra-high-strength structural steel with the same nominal strength is S960QL. The mill processing of QL steel includes quenching and then tempering. The traditional and conventional method to make QL steels is to use reheated quenching and tempering and the process is marked as DQ+T.

In the arc welding of high-strength structural steels, the microstructure and mechanical properties of welded joints are determined by the chemical composition of the base material and filler material used, and by the cooling rate of welding; especially the cooling rate in the heat-affected zone matters (Pirinen et al., 2015).

The laser-based joining process can be favourable for joining high-strength steels, such as those described above, because of the possibility to adjust the processing parameters precisely in terms of weld quality and mechanical properties and to avoid preheating, which is needed in conventional welding if there is a risk of cracking.

The chemical composition of a steel influences the general weldability and quality of a welded joint. There exist several equations to predict the weldability of steel based on the main alloying elements of steel. As an example, the carbon content of steel is important because it indicates the hardness in the final welded joint. This depends mainly on the formation of martensite. The carbon content of the steel used in a laser or laser-welded application should be reduced to a maximum value of 0.12% in order to avoid the aggressive hardening of the welded joint, so that it does not exceed 380 HV, which is the upper limit set by the classification authorities (Nielsen, 2015). In laser-hybrid welding, the addition of filler material combined with heat input control are the key tools for controlling the defect level and mechanical properties of welds (Nielsen, 2015). However, obviously it is difficult or even impossible to avoid the forming of weld defects or imperfections totally. A wrongly adjusted welding speed can cause weld defects to form,

too high a welding speed can cause undercut and too low a welding speed can cause porosity.

#### 2.4.1 Microstructure of laser and laser-hybrid welded joint

Modern high- and ultra-high-strength structural steels combine good strength, hardness, toughness and ductility. These properties can be retained after welding. The manufacturing processes and alloying of steel influence the microstructure and mechanical properties of the steel. The original microstructure of the steel together with alloying elements “create” for example the strength of a steel. The target is a precisely controlled refinement of the microstructure. The yield strength of high-strength structural steels (HSS) is typically between 500 and 900 MPa and the microstructure of the base material is either ferritic-bainitic, ferritic-martensitic or fully bainitic. The yield strength of ultra-high-strength steels exceed the above strength levels extending up to 1300 MPa and even higher levels are targeted. The microstructures of UHSS consist of fully martensitic or bainitic-martensitic microstructures. In addition, UHSS can have small sporadic islands of retained austenite arranged along the prior austenite grain boundaries (Afkhani et al., 2022). In welding, the microstructural changes in the steel greatly depend on the heating and cooling rates being a function of welding speed, laser weld energy and thermal efficiency (Guo et al., 2015; Poorhaydari et al., 2005).

Advanced high-strength steels (AHSS) developed for the automotive industry follow the structural steels (HSS and UHSS) regarding strength properties and base material microstructures. In addition, more attention is paid to the forming properties in the steels and their behaviour in a crash situation. It is relatively demanding to combine good weldability and formability properties in the same steel. The steels used in automotive applications might have some metallic coating, making the joining of the steel even more challenging.

In a welded joint, the area between the base material and the fusion zone is called the heat-affected zone (HAZ) and the main metallurgical changes occur in that area. The area is divided into sub-zones often named the sub-critical heat-affected zone (SCHAZ), inter-critical heat-affected zone (ICHAZ), fine-grained heat-affected zone (FGHAZ) and coarse-grained heat-affected zone (CGHAZ). The areas differ in shape, width and microstructure, as well as in mechanical properties (Figure 2.11). The cooling time and maximum temperature reached vary in the welded joint area, affecting the formed zones (orientation and dimension) and the microstructures in those zones.

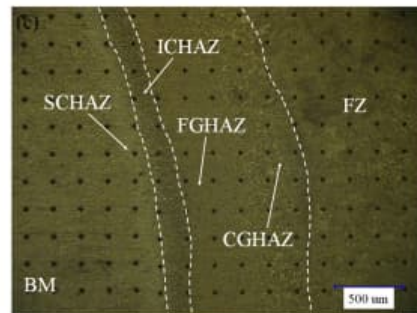


Figure 2.11: Different zones of a laser weld (Guo et al., 2015).

#### 2.4.2 Hardness of laser and laser-hybrid welded joint

The mechanical properties of a welded joint when utilizing high- and ultra-high-strength steels are strongly dependent on the welding parameters used. Through the usage of optimal welding parameter combinations it is possible to control the hardness values in an HAZ (Hesse et al., 2019). In their research Hesse et al. showed that the ultimate hardness of a laser welded joint is mainly determined by the carbon content of the steel. The welding test made by a conventional arc welding method showed a connection between the heat input used in welding and carbide formation in the coarse-grained heat-affected zone (CGHAZ) influencing the hardness and strength of the welded joints (Bayock et al., 2022). The above phenomenon can be observed with thermo-mechanically rolled (TMCP) and direct-quenched (QC) steels having different chemistries and processing in a steel mill. The different types of steel mill processing together with different alloying in steels lead to different microstructures and different mechanical properties in the steel. In joining of steel an increase in welding energy generated a wider softening region in the HAZ and lower tensile strength results, although with decreased welding energy a wider coarse-grained region in HAZ was formed and the toughness properties of a welded joint were altered in a negative direction (Skriko, 2018; Hesse, 2019). In the laser welding of low carbon structural steel (LSS) and ultra-high-strength steel using the same welding parameters, intensive hardening occurred in the weld area of the LSS whereas the hardness in the weld area of UHSS was close to the hardness of the base material. However, a narrow, softened zone was formed in the SCHAZ of UHSS due to the tempering of the base material (Figure 2.12 a.). It should be noticed that in this case the steel was direct quenched (DQ) and the microstructure fully martensitic or martensitic-bainitic. Another observation worthy of mention is the point of the highest hardness, located in the FGHAZ. Some differences can be found from the test results when compared to a quenched and tempered steel (QL) with the same strength level as the laser-welded. The highest value of hardness is measured in the FGHAZ as in the previous case but no softened area is formed in the SCHAZ or the drop of hardness is barely visible (Figure 2.12 b). There are remarkable differences in the heat inputs of



welding between case a (0.04 kJ/mm) and b. (0.20 kJ/mm) which might affect the hardness values and width of the weld zones. The phenomenon is real but the values of hardness might differ if a different heat input is applied in welding.

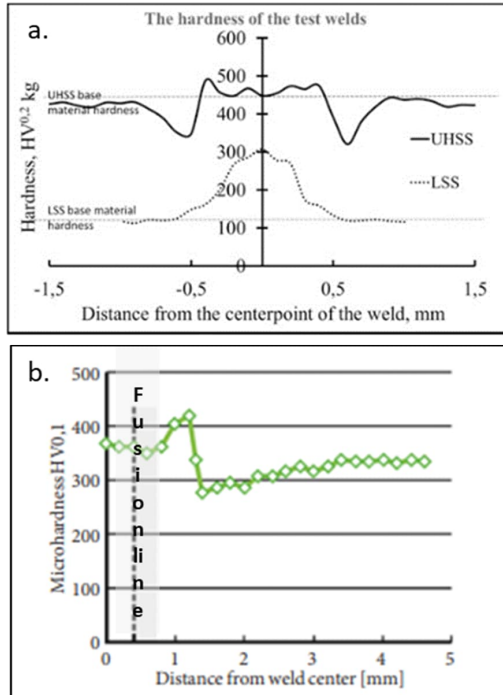


Figure 2.12: a. Hardness profiles of LSS and UHSS (Keskitalo et al., 2019). b. Hardness of laser welded S960QL steel (Ślęzak et al., 2017).

### 2.4.3 Strength properties of laser and laser-hybrid welded joint

It is a well-known fact that a weld is the weakest link of a welded joint. Welding never improves the mechanical properties of the joined material. In some places the strength properties of the material can be improved locally; however, when an HAZ is included in the observations the previous statement holds true. When a sound weld is produced with minor or no weld imperfections, weld strength is usually not an issue. A similar conclusion can also be made for the laser and laser-hybrid welding of high- or ultra-high-strength steels as long as the recommendations given by the steel suppliers are followed. The laser and laser-hybrid welding results of high-strength steels collected from the reference literature showed a high degree of deviation between the measured strengths and the place of fracture. Gao et al. reported matching strength to the base material (BM) for laser-welded S960MC (QC) and that the place of fracture was in the BM, whereas Kurc-Lisiecka et al. reported similar behaviour in strength in the laser welding of S1100

MC (QC) steel but that the place of fracture was in the weld metal (WM). Urbanczyk et al. published their laser-hybrid welding results for S960 QL where they achieved good strength properties corresponding to BM properties but in that case the place of fracture was in the HAZ. The above-mentioned welding test was made using under-matching filler material G79 5 M21 Mn4Ni1.5CrMo (EN ISO 16834-A) with (minimum) 790 MPa yield strength. Sumi et al. predicted from the measured hardness (HV 310) that the weld metal would meet the required 980 MPa strength level. They showed increased hardness values in welds according to the carbon content (C: 0.06-0.16%) of steels. It is possible to make a hypothesis that the ultimate tensile strength of a laser welded joint changes according to the hardness of the weld.

#### 2.4.4 Toughness and ductility of laser and laser-hybrid welded joint

Modern high-strength structural steels have been developed to perform and maintain their unique properties under the most extreme conditions, even under sub-zero temperatures. However, the steel strength has no direct influence on the resulting toughness of the laser-welded joint. It is more affected by the microstructure formed in the weld, which is dependent on the heat input (Q) during welding and cooling conditions ( $t_{8/5}$ ). These parameters influence the microstructure as well as grain sizes, which determine the toughness of a welded joint (Hesse et al., 2019). The toughness of laser-welded high-strength steels is greatly affected by the carbon content of the steel. Higher carbon content makes the microstructure become more martensitic instead of bainitic in structure, resulting in lower toughness values for the weld metal (Sumi et al., 2015). The influence of an individual alloying element on the toughness properties of weldments mainly depends on its influence on the microstructure of the steel matrix and M and A constituents. It also depends on the other alloying elements and the weld cooling rate as earlier pointed out (Laitinen, 2006).

Alloying elements such as nitrogen, boron, niobium, vanadium, molybdenum and chromium influence the formation of constituents resulting in the formation of hard and brittle microstructure in the HAZ of the weld. The effect of manganese, nickel and copper is less significant (Laitinen, 2006).

The formation of martensite in the fusion zone and HAZ of the weld strengthens the laser-welded joint but also increases the brittleness of the joint, which has a negative influence on the toughness of the weld (Guo et al., 2015). Many researchers have reported that the laser welding process may present difficulties for toughness testing because of the narrow weld (width/depth ratio) and its zones (FL, HAZ, WM), together with the high strength of the weld. Positioning the notches can be challenging, as the fusion line is not perfectly straight and in actual testing the fracture can turn spread/from the fusion zone in the direction of the base material, leading to incorrect toughness results. An evaluation of impact toughness (Charpy) of the weld metal for laser beam welds can in some cases be almost impossible due to the occurrence of this phenomenon, known officially as fracture

path deviation (FPD) from the weld metal into base steel. It is even recommended to use some more suitable testing methods (side grooved, oversized and longitudinal specimens) to determine the toughness of laser welds instead of Charpy testing (Laitinen, 2006).

The thickness range of automotive steels is such that toughness is not measured by the same methods as for thicker steel sections. However, often good ductility is required of the welded structures in automotive components. The standard Erichsen cupping test can be used to study the formability of laser-welded joints. The presence of martensite indicates the location of the fracture quite clearly. Laser welding tests made on QP980 (ultra-high-strength quenched and partitioned steels) and DP980 (ultra-high-strength dual-phase steel) showed the influence of microstructure on crack formation. QP in a base material contains RA, which is beneficial for delaying crack propagation and increasing the forming property. The Erichsen value for QP steel is 10.6 mm and 9.87 mm for DP steel. In a welded condition, both steel grades contain a brittle martensitic microstructure in the weld area, which initiates the formation of a crack in that area. Therefore, the Erichsen value for a dissimilar laser-welded joint (QP-DP) decreased to 5.92 mm (Xue et al., 2021). Fundamentally, the strength of a steel does not automatically indicate its behaviour in the Erichsen cupping test; however, if the microstructure is also known the location of cracking can be identified.

## 2.5 Laser welding applications

Scanning through the laser technology market as a whole gives a good start when mapping the applications that utilize laser processing. Understanding the general market situation helps to identify possible new areas and applications for laser technology. It is appropriate to start geographically from China, as an extremely good example of the state of the art of laser technology market and envisaging the development of technology and applications. The Covid pandemic caused, and partly continues to cause a global shortage shock in all areas of economics. However, in China, the influence of the pandemic as a whole on the industry was marginal. In 2020, the laser technology industry of China achieved 10% growth, exceeding expectations. The overall size of the laser equipment market in China increased by 18.3% year-on-year in 2021, reaching an all-time record in monetary value of 12.91 billion USD (Laser Focus World, 2022). In China, laser technology is one of the key technologies in industry that improves the quality of products and reduces costs. Considering the laser technology market as a sector and in percentage values, laser cutting accounts for the major share (40%), followed by laser welding (13%), laser marking (13%), semi-conductor/display (12%), precision machining (9%), non-metal processing (7%) and the rest (6%) (Laser Focus World, 2022).

China is the largest market for fibre lasers with a share of 63 per cent; high-power fibre lasers are used in many industrial applications. It is worth mentioning that in China lasers with a power of 10 kW can be as the new standard level in laser cutting (Laser Focus World, 2022).

This can be compared with what happened during the same time period in Germany. Germany is a dominant manufacturer of laser technology and a major user as well. The production and export of laser systems fell by 18 per cent in 2019 compared with the previous year. Despite the drop, it seems that the Germany economy is recovering and some growth is predicted (VDW, 2020). The latest statistics for 2022 show that the laser technology business is back on track and that its growth continues. However, the situation in Europe is still very sensitive because of the pandemic and the war in Ukraine and the higher price of energy will make the situation very challenging and turbulent. It is clear that if the global economy starts to suffer, eventually it will affect the laser technology market.

Laser technology is used in many industrial sectors and applications:

- Aerospace
- Automotive
- Biomedical
- Construction
- Domestic goods
- Electrical and electronics
- Machinery
- Petrochemical
- Power generation
- Shipbuilding.

Laser-arc hybrid welding (abbreviations: LAHW, LHW or HLAW) was developed after conventional laser welding. It was widely recognized as a potential joining method in the 21st century and the utilization of the process has been relatively fast since then. Industrial applications utilizing the process can be found in many different industrial sectors. The automotive and shipbuilding industries are often named as the pioneers in utilizing laser-hybrid welding (Olsen et al., 2009). The automotive components and parts such as gears and tailored steel blanks are typical examples of laser-welded or laser-hybrid welded products (Duley, 1998; Steen, 2003). The laser-welded tailored blank is one of the few laser-welded applications that has its own European level product standard (EN 10359-11, 2021). Laser-welded tailored blanks (LWTB) are used in car bodies, door rings, bumpers, roof rails and tunnels. Modern high-strength steels with and without a metallic coating are used in automotive applications and can be press-hardened to obtain good crash performance in the structure. The press-hardened steels (PH steels) can be laser-welded before or after the hardening process. PH steels can have a metallic coating, such as AlSi, Zn, ZnFe or ZnAl. The strength of laser-welded PH steel with a metallic coating is dependent on the fraction of ferrite phase formation. The hardness decreases as a result of the coating mixing and leads to failure either across a fusion zone or at a fusion boundary, depending on the condition of the PH steel in welding: welded before or after press hardening (Saha et al., 2016).

The automotive industry is targeting higher productivity and quality in their processes. Increased usage of advanced high-strength steels (AHSS) in motor vehicles can reduce their weight by up to 25% and cut the lifetime CO<sub>2</sub> emissions of a vehicle by up to 15%, which is more than any other material used in the automotive industry (Stahl, 2021). In addition, the strength level of steels used in the automotive industry has increased. They can have a very complex microstructure and versatile alloying based on the desired properties, and finally steel can have a metallic coating such as zinc, zinc-iron, aluminium-silicon or magnesium to protect against corrosion (Figure 2.13). The usage of high-strength steels will dramatically increase in the automotive industry. Today about 70 per cent of impact bars in bumpers are made from steel and changed requirements (strength/mass ratio) will lead to the increased usage of steel (Stahl, 2021).

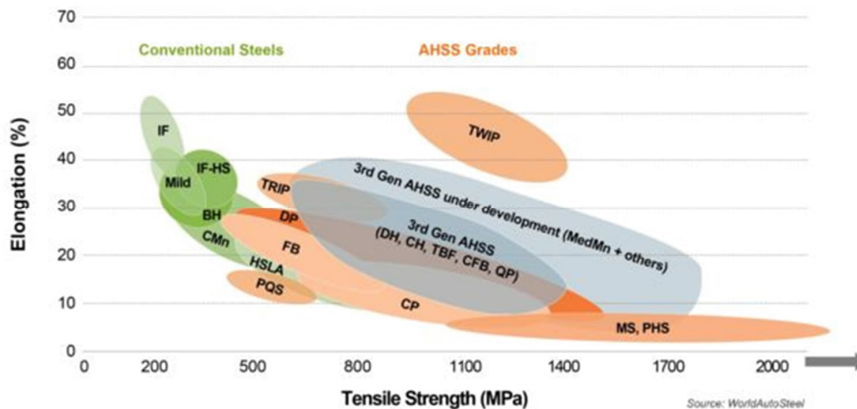


Figure 2.13: The Global Formability Diagram comparing strength and elongation of current and emerging steel grades (World AutoSteel, 2022, <https://www.worldautosteel.org/steel-basics/automotive-advanced-high-strength-steel-ahss-definitions/>).

The shipbuilding industry was the other pioneer to use laser and laser-hybrid welding in large-scale production. Laser-welded steel sandwich panels were the first laser-welded products utilized in shipbuilding with the US Navy the first to adapt them in hull structures (Kujala, 2005). The target was to decrease the weight of upper structures such as the antenna platform. The experience from that relatively small-scale experiment was positive and later laser-welded steel sandwich panels were installed in some civilian ships as well. Research on lasers in shipbuilding started as early as in 1992 when the European shipbuilding industry initiated work to look at the use of CO<sub>2</sub> lasers in the steel structures of ships. Already at that time, the main focus was on panel lines using both butt and fillet joint configurations (Gerritsen et al., 2005). The concrete result of the intensive research was the published guidelines for approval of CO<sub>2</sub> laser welding for ship construction by the European ship classification societies in 1996.

---

The German shipyard Meyer-Werf was one of the first to adopt laser welding in the production of cruise ships. They have separate laser welding lines for steel-sandwich panels (butt joint) and for the welding stiffeners for panels (Churiaque et al., 2019; Unt, 2018). The thickness of a stiffener can vary but the LHW process is relatively flexible, making it possible to weld either one-side or double-side fillet welds.

The main interest in investing in laser-based welding technology is the high productivity and efficiency of such production and the higher and consistent quality of the final product. The time reserved for rework in shipbuilding can be reduced by up to 30% through the utilization of laser technology in welding (Laser Systems Europe, 2020). Laser-based joining technology is among one of the manufacturing processes also used in vessel fabrication, pipe welding, and the energy and aerospace sectors (Kah, 2011). However, it is difficult to obtain any actual figures or volumes to estimate the size of such laser-assisted production.

The development of laser-based solutions and applications has not always been plain sailing. There are some good examples showing the importance of knowing the pros and cons of a new technology. One failed laser system investment was an early production line for the laser welding of steel sandwich panels. The line was installed at a time when the running costs were extremely high and the price of the final product was higher than the price of a product manufactured by conventional technology. Nor was the much better flatness of laser-welded panel seen as favourable enough to encourage further development of laser-based production. However, at the moment, there are several active laser welding lines operating in European shipyards. Shipyards such as Blohm+Voss, Fincantieri, Chantiers de l'Atlantique, Meyer Werf Pappenburg/Turku, Navantia, Nordic Yards Warnemünde and Odense Steel Shipyard are using or have used laser welding in the production of ships or cruisers (Gerritsen et al., 2005; Unt, 2018).

The usage of laser welding has increased in offshore applications and thick wall pipe welding (Kristiansen et al., 2017; Miranda et al., 2010; Üstündag et al., 2020). The driving force has been cost reduction. Utilizing laser technology in welding has made it possible to reduce the number of weld passes compared to gas metal and submerged arc welding. The time needed for groove preparation and welding is significantly shorter than in conventional welding. A big saving also comes from the cost of the filler material. The wall thickness of these applications is often 15 mm and above. The steels used in the structures are very basic ones, having a relatively high low strength and a simple chemistry making them easy to weld. One challenge in welding is demanding welding positions and the number of them: flat position and orientation, vertically up and down. In addition, butt and fillet joints are used as the joint configurations. One advantage of laser-based welding is that no groove bevelling is needed (Kristiansen et al., 2017).

Researchers in Fraunhofer IWS, Germany, have developed a new laser welding process that increases the efficiency of joining compared to submerged arc welding. The new process is called laser multi-pass narrow-gap welding (laser MPNG welding) and it consumes up to 80% less energy, up to 85% less filler material and takes 50-70% less

time than conventional arc welding. Researchers have also reported the reduced need for post-weld straightening for the welded structure (Laser Systems Europe, 2022). The existence of some serious weld imperfections and defects have delayed the use of laser welding in the joining of thicker wall thicknesses. Crack formation and insufficient dilution between filler and base material are often mentioned as causing some challenges and issues to the laser or laser-hybrid welding of thicker steel sections (Karhu, 2019; Grünenwald, 2019; Farrokhi, 2018).

The trend in pipe welding (oil and gas) and offshore structures (wind turbine) is to use higher strength structural steels. The development in steel grades for pipeline applications has led to new high-strength steel grades, such as X100 (yield strength min. 690 MPa) and X80 (yield strength min. 550 MPa) steels. Higher strength steel enables usage of thinner walled pipe with greater operating pressures and reduced overall costs (Miranda et al., 2009). A low carbon content together with the other alloying elements improves the general weldability. The use of modern laser or laser-hybrid welding technology makes it possible to achieve high weld penetration depths by a single pass while still achieving good mechanical properties in the welded joint. Steel thicknesses of up to 15 mm can be welded by a single pass; above that thickness, multi-pass welding is recommended to use and in addition preheating should be considered to prevent weld defects such as cracking. The use of preheating enables usage of higher welding speeds. It is possible to achieve a welding speed of 2.5 m/min without preheating although with heating ( $T=180^{\circ}\text{C}$ ) the welding speed increased to 3 m/min (Turichin et al., 2018). Industrial applications can face demanding conditions in use. A laser-hybrid welding process can be used in these applications to guarantee good quality in welds, e.g. excellent toughness properties in applications that work in sub-zero temperatures.

The production of lifting equipment, such as a mobile lift boom, is a good example in utilizing laser technology in production. Typically, most of the welds in a boom are rectilinear and the length of the weld is relatively long. The same laser can be used in welding and cutting. The final product has good accuracy with minor deformation. The trend in boom manufacturing is to use steels with an extremely high yield strength and the sector is often the first to utilize new steel grades. A large number of companies use a laser-based joining method in the production (welding and cutting) of boom profiles. The Austrian company, Manitowoc Cranes, started to use their laser-hybrid welding line in 2014 (Manitowoc, 2022). In Belgium, Vlassenroot followed them some years later. Vlassenroot's laser-hybrid welding system can be used to join up to 19.5-metre-long boom profiles (Vlassenroot, 2022). They use continuous laser welding without filler material if applicable. As early as 2006, Finnish steel mill Ruukki was aiming to start a laser-hybrid welding system in boom manufacturing in one of their units. The plan was to use the line for joining heavy mobile booms. Unfortunately, the timing of the project was wrong and it was utilized by other companies later as described. This is very typical when implementing new technology in production. Someone has to make the mistakes before the technology is ready for economically profitable production.

### 3 Research methodology

The key research findings of this dissertation are presented in five research publications published in scientific journals and conference proceedings. All publications include some amount of experimental study. The author of the dissertation has had the major role in doing the research for every publications, excluding Publication IV in which the role was more like an advisor. The approach in the study is very practical. The reason for this is the fact that the research was initiated by the needs of the company where the author was or is working. The doctoral dissertation provides information for understanding the laser welding and laser-hybrid welding of high-strength structural steels. Typically, these steels are used in demanding applications and loading conditions. In addition, detailed information is provided for the laser welding of zinc-iron coated boron steel according to the welding guidelines (SEP 1220-3) published by VDA.

#### 3.1 Materials and methods

The author contributed to the welding tests described in the publications, excluding Publication II. The author summarized the welding tests made on Optim 960 QC steel by other researchers in Publication II. The strength level of the tested steels is ultra-high but lower strength and automotive steel are included in the studies. Detailed information on the steels can be found in each publication. Overall, the research studies include a wide spectrum of testing for weld joints by non-destructive and destructive testing methods, in accordance with suitable standards if applicable. All concrete welding tests were made using one-micron lasers and the standards to make welding procedure specifications and to test the welded specimens were followed when practicable. The standards utilized in welding were as follows:

- ISO 15609: Specification and qualification of welding procedures for metallic materials. Welding procedure specification
  - Part 1: Arc welding
  - Part 4: Laser-beam welding
  - Part 6: Laser-arc hybrid welding
- ISO 15614: Specification and qualification of welding procedures for metallic materials. Welding procedure test
  - Part 1: Arc and gas welding of steels and arc welding of nickel and nickel alloys
  - Part 11: Electron and laser-beam welding
  - Part 14: Laser-arc hybrid welding of steels, nickel and nickel alloys
- ISO 12932: Quality levels for imperfections. Laser-arc hybrid welding of steels, nickel and nickel alloys



- ISO 13919-1: Requirements and recommendations on quality levels for imperfections. Electron and laser-beam welded joints. Part 1: Steel, nickel, titanium and their alloys
- ISO 5817: Quality levels for imperfections. Fusion-welded joints in steel, nickel, titanium and their alloys.

The applicable standards are listed in Table 3.1 together with the key information on the welding experiments made in the publications.

Table 3.1: Overview of key parameters applied and information on the welding experiments of the publications.

	Publication I	Publication II	Publication III	Publication IV	Publication V
<b>MATERIAL</b>					
Steel grade	SSAB Domex 355 MCD	Ruukki Optim 960 QC	S960 MC	Ruukki Optim 960 QC	22MnB5 Iron-zinc coating Furnace times [s]: 300 and 740
Standard designation	EN 10149-2	EN 10025-6	EN 10025-6	EN 10025-6	ISO 683-2
Typical application or industry for steel	versatile structural steel	heavy mobile cranes, transportation	heavy mobile cranes, transportation	heavy mobile cranes, transportation	automotive hot formed parts
Thickness [mm]	3, 4, 6	6	6	8	1.5
<b>JOINT CONFIGURATION</b>					
Joint type	bead on plate (BOP)	I-butt joint	I-butt joint	I-butt joint	I-butt joint lap-joint
Groove preparation	as delivered	laser cut, machined	machined	laser cut and shot blasted	as delivered
<b>WELDING</b>					
Welding method	laser welding	Laser-hybrid welding	laser welding laser-hybrid welding gas metal arc welding	laser welding	laser welding
Laser source	Trumpf disk laser 12 kW	CO <sub>2</sub> -laser Fibre laser Disk laser	Trumpf disk laser 12 kW	Fibre laser IPG Photonics YLS-10000	Trumpf disk laser 12 kW
Wavelength [nm]	1030	n/a	1030	1070	1030
Fibre diameter [µm]	400	n/a	400	200	400
Beam parameter product [mm mrad]	16	n/a	16	11.5	16
Collimator [mm]	200	n/a	200	150	200
Focal length [mm]	300	n/a	300	300	300
Focal point diameter [µm]	600	n/a	600	620	600
Rayleigh length [mm]	n/a	n/a	n/a	8.5	n/a
Welding optics	Trumpf	n/a	Trumpf	Precitec YW50	Trumpf
Shielding gas	-	n/a	92%Ar8%CO <sub>2</sub>	Argon	-

<b>Arc source</b>	-	Esab, Gloos, Kemppi, Fronius	Fronius Time 5000	-	-
<b>Filler material</b>	-	Union X96 Esab OK12.50	Union X96 Esab OK 12.51	-	-
<b>Movement/guidance</b>	Industrial robot KUKA KR30HA	n/a	Industrial robot KUKA KR30HA	Gantry	Industrial robot KUKA KR30HA
<b>Standards applied in welding and acceptance of welded joints</b>	-	ISO 15614-11 ISO 13919-1	ISO 15614-1 ISO 15614-11 ISO 15614-14 ISO 15609-1 ISO 15609-4 ISO 15609-6 ISO 13919-1 ISO 12932 ISO 5817	ISO 15614-11 ISO 13919-1 ISO 15609-4	SEP 1220-3
<b>TESTING</b>					
<b>Methods</b>	DT	NDT, DT	DT	NDT, DT	NDT, DT
<b>More specific information</b>	metallography, hardness, transversal tensile strength, weld dimensions	VT, RT, transversal tensile strength, hardness, Charpy-V impact test, transversal bend test	metallography, transversal tensile strength, bend test, hardness, Charpy-V impact test, fatigue testing	VT, RT metallography, hardness, transversal tensile strength, Charpy-V impact test	VT, RT, metallography, microstructure, hardness, shear tensile strength

### 3.2 Research limitations

The limitations of the research are mainly connected to the passing of time during the research, to the daily work of the author and to the remarkably fast development both in structural steels and laser welding technology. The limitations are listed in more detail below:

- The publications of the doctoral dissertation were made on very different topics, which might mean that the thread of the doctoral dissertation is lost.
- The development of ultra-high-strength steels has been rapid and is continuing. The doctoral dissertation focuses on the strength level of 960 MPa. Currently, structural steels at a strength level of 1300 MPa are available. Unfortunately, the dissertation does not provide information on laser welding of that strength level.
- The limited number of welding tests carried out reduces the general statistical reliability of the experimental research. The reasons for the above include the following:
  - it is time-consuming to perform extensive welding tests

- welding tests were mainly made with the help of outsourced services increasing the costs
- if standardised welding procedure specifications are followed in welding trials they include a relatively low number of welding tests
- testing of welded specimens faces the same challenges as welding, for example performing fatigue testing is time-consuming and increases the cost of research considerably.
- The information provided on the laser welding system and welding set-up used is not complete, which might make it difficult to compare the results with similar scientific work or research made by other authors.
- Some of the publications have a limited number of supporting references for the reason that the research studies were made as a part of normal daily work and the missing references were not considered a problem. The author has tried to amend this issue in the state of the art chapter by linking a decent amount of references.
- The analysis and characterization of the microstructures of welded specimens was not made on a very deep level, just a basic study according to the instructions of the applicable welding standard. The microstructural analysis of the welds is relatively cursory and the conclusions made for those are supported by publications made by other authors.

## 4 Summary of the publications

This chapter presents the objectives, key findings and contributions of the five publications as the second part of the thesis. The key research findings of all five publications are summarized here.

### 4.1 Publication I

#### Influence of welding parameters on the mechanical properties of a laser-welded joint

##### *Objective*

The objective set for the study was relatively simple, i.e. in what way does laser welding energy influence the properties of a welded joint and if that welding energy ( $E$ ) is kept constant but formed from the two variable main welding parameters (laser power and welding speed) used for the calculation of welding energy. The rest of the welding parameters were kept constant. The laser welding speeds used with different laser powers and base material thicknesses are presented in Table 4.1. Medium-strength structural steel of three thicknesses (3, 4 and 6 mm) was used as the test material. The bead on plate (BOP) joint configuration was used in welding to ensure constant welding conditions.

Table 4.1: Laser welding parameters used in Publication I.

Welding energy [kJ/mm]	3 mm	4 mm	6 mm
	0.069	0.092	0.20
Laser power 4 kW	3.5 m/min	2.6 m/min	1.2 m/min
Laser power 6 kW	5.25 m/min	3.9 m/min	1.8 m/min
Laser power 8 kW	7.0 m/min	5.3 m/min	2.4 m/min

The properties of the welded joints were evaluated by means of destructive testing including measurement of hardness, transversal tensile strength and impact toughness. In addition, weld cross sections were prepared to use in the measuring of weld dimensions. Spatter formation during welding was documented as well.

##### *Results*

It was evident that the selection of welding parameters had a huge influence on the weld quality as seen in the cross-sections of weld and spatter formation. However, it was surprising that the influence of weld quality on the measured mechanical properties was minor. In other words, poor weld quality does not automatically indicate poor mechanical properties in a laser weld. As an example, despite poor weld quality, cracking was mostly located in the base material in the transversal tensile strength specimens.

The hardness values of the laser welds showed some deviations between different combinations of welding parameters. It seems that the combination of high laser power and welding speed produced the highest hardness. The weld geometry dimensions were also measured. The width of the weld was measured from top, middle and bottom. The values showed that the welds were wider from the top and bottom than from the middle. It can be concluded that the role of welding parameters is significant on the weld quality and that the parameters should be optimized for each steel grade and thickness.

#### *Contribution to the whole*

Paper I focused on the laser weld results of a structural steel with several thicknesses. The paper gives an overall picture of laser weldability. The results show the behaviour of lower strength structural steel in laser welding and the results achieved complement the content of the doctoral dissertation.

## **4.2 Publication II**

### **Laser and laser gas-metal-arc welding of 960 MPa direct quenched structural steel in a butt joint configuration**

#### *Objective*

The objective of the study was to summarize the laser and laser-hybrid welding results of 960 MPa direct-quenched structural steel made between year 2007 and 2014.

#### *Results*

The publication summarized the results of laser and laser-hybrid welding tests made over a relatively long time period and therefore they might not be totally comparable with each other, as some changes may have happened in the steel manufacturing and its alloying. The studied steel has low alloying but minor changes are possible. The direct quenching process might have undergone some changes as well. Development of laser welding technology has been fast and the first steps in high-power fibre lasers were being taken during the publishing of some of the results. Some of the welding tests are very preliminary, gathering knowledge from laser welding with one-micron wavelength lasers. The steel supplier recommends using a cooling time of 4-15 seconds to achieve the desired properties in a welded joint. The calculated (not measured) cooling times given in the reference literature are even shorter than the recommended minimum four seconds of cooling time. The included gas-metal-arc welding tests were made using a single pass or multi-pass welding. Filler materials with matching and under-matching strength from several suppliers were used in the studies. The summarized publications include other variables, such as bevel angle, groove preparation method and treatment. Some modifications were made to the published results in order to make them comparable.

---

Some information was not complete and some of the presented test results are calculated as average values given in the references.

The transversal tensile strength of laser-welded specimens was matched with the nominal strength of the base material, i.e. between 954 MPa and 1090 MPa. In the case of laser-hybrid welding and with a matching filler material, yield strengths were close to the yield strength of laser welds. Use of under-matching filler material led to a higher deviation in strength values. The achieved yield strength of joints welded with gas-metal-arc welding and by using the matching filler was below the nominal yield strength of the base material ( $R_{p0.2}$ : min. 806 MPa and max. 964 MPa). The under-matching filler material did not bring any improvement to the joint strength ( $R_{p0.2}$ : min: 720 MPa and max. 810 MPa). The hardness values showed clear softening in the heat-affected zone, more precisely in the ICHAZ. The minimum values of hardness were below 300 HV and the maximum values were above 400 HV. The highest hardness was measured for laser welds and the lowest values for gas-metal-arc welding. The results show that the type of filler material has only a minor influence on the minimum hardness value and a much greater influence on the maximum hardness value.

The impact toughness testing of welds was carried out at several testing temperatures. The main interest in the publication was in sub-zero temperatures. Typically, there are several locations to place a notch in the fusion zone of a weld but only the results in a fusion line are observed in the publication. The values of impact toughness showed a large deviation in the values. The root cause for these deviations could be the weld quality and a defect or the impact testing of specimens if the place of the notch is not accurate enough. No clear correlation was observed between impact toughness and the cooling times used.

The transversal bend test was made by using a mandrel with a diameter of 80 mm. The available results are very discouraging, showing the complete passing of a bend test to be challenging or even impossible. Therefore, it is strongly recommended to use the longitudinal direction in a bend test instead of the transversal if applicable.

#### *Contribution to the whole*

The publication acts as an introduction to the laser and laser-hybrid welding of ultra-high-strength steels and supports the later studies made by the author of doctoral dissertation. It compares results of previous examinations made of 960 MPa direct-quenched steel, observing welding from many directions and despite some limitations provides information and complements the content of the doctoral dissertation.

### 4.3 Publication III

#### **Effect of welding process and filler material on the fatigue behaviour of 960 MPa structural steel at a butt joint configuration**

##### *Objective*

The objective of the study was to determine whether the fatigue results of welded ultra-high strength steel were in line with the recommendations of IIW and the influence of the welding method or filler material on the fatigue properties of a welded butt joint.

##### *Results*

One of the key findings of the study was the importance of the weld geometry on fatigue behaviour in a welded joint. In addition, the weld properties were tested by different destructive testing methods. The cross-sections of welds showed good performance by all three tested welding processes (laser, laser-hybrid and gas-metal-arc welding). The results of the transversal tensile strength tests were in line with the previous results presented by the author of the thesis. The tensile testing showed the place of fracture to be in the HAZ and more precisely in the softened area in the ICHAZ. In a tensile strength test all of the plasticity is concentrated in that area. The strength of the base material was not reached in any of the tensile strength test specimens. However, the laser-welded specimens reached the closest values to the base material. The relatively low values of elongation are worth mentioning.

The transversal bend test has been relatively difficult to pass fully with the tested base material if a laser-based joining process is applied. Surprisingly, in the study, laser-welded joints passed the test both in the face and root side directions. It is strongly recommended to use a longitudinal direction instead of transversal direction in a bend test if allowed. The possible softened zone of a weld does not affect testing if the longitudinal test direction is used.

The hardness curves illustrate softening in the HAZ of welds with all tested welding processes. The filler material used influences the hardness curves. With the under-matching filler material the formed area of weld was softer in the middle. With the matching filler material such softening in the middle of the weld was not observed. Overall that softened area is very narrow in the case of laser-GMA hybrid and laser welding. The differences in minimum and maximum hardness values in the weld area is independent of the weld method. The impact toughness of welded joints was tested using the Charpy V notch test. The toughness was tested from the weld and fusion line. For the tested steel the guaranteed impact toughness is 34 J/cm<sup>2</sup> (-40 °C). All tested specimens exceeded the guaranteed nominal impact toughness value of the base material.

The fatigue properties were defined using a constant amplitude cyclic loading where the stress ratio was kept constant ( $R=0.1$ ) but the applied stress range ( $\sigma$ ) was varied between

the different specimens. The slope ( $m=3$ ) is fairly suitable for most of the S-N curves but in the case of laser-hybrid welding a gentle slope might be a better choice. The following observation can be made regarding the cracked specimens. The cracks initiated mostly from the root side of the tested specimens, except for the laser-hybrid welded specimens joined with under-matching filler material where the fatigue crack propagated from the weld face side. The reason for this behaviour can be found from differences in the global and local geometries of the welded specimens.

The testing showed that the fatigue resistance of welds joined by three different welding processes (gas-metal-arc, laser-hybrid and laser welding) was close to the recommendation given by the International Institute of Welding (IIW). Surprisingly, the laser welds showed the highest FAT values compared to the GMA and LHW welds. The fatigue performance of the welded joint is highly dependent on the geometrical weld quality (weld profile), which typically requires usage of an automated and mechanized welding process. Laser welding and laser-hybrid welding always meet this requirement and modern gas-metal-arc welding should fill it if high-quality welding is targeted.

#### *Overall contribution*

The publication focuses on the fatigue behaviour of laser, laser-hybrid and gas-metal-arc welded joints. The publication includes other types of destructive testing as well. The publication gives valuable information about the weld properties and deepens the information on the welding of ultra-high-strength steels.

## 4.4 Publication IV

### **Fiber laser welding of direct quenched ultra-high strength steels: Evaluation of hardness, tensile strength, and toughness properties at subzero temperatures**

#### *Objective*

The study focused on the weldability of a high-strength structural steel under demanding conditions. The steel had a yield strength of 960 MPa and its thickness was 8 mm. A fibre laser with 10 kW maximum laser power was used. The joint configuration was a butt joint without a bevel. The mechanical properties of the laser-welded joints were tested with destructive testing including hardness, transversal tensile strength and toughness tests at sub-zero temperatures. Non-destructive testing was also included in the study. In addition, less standardized but very valuable information about weld quality was included, such as weld dimensions, visual outlook and identified weld defects.



### *Results*

One of the main conclusions of the publication is the relatively narrow welding parameter window when a high-power fibre laser is utilized in joining. It was observed that the welding speed and laser power must be above the critical limit to avoid problems in weld quality, such as insufficient penetration. It was observed that a relatively high laser power (above 9 kW) was needed for good weld quality and the welding speed achieved was considerable, i.e. in the range of 3 m/min.

NDT examinations of laser-welded specimens did not show any critical weld defects, apart from minor porosity. The specimens were also free of cracks. In welding, the calculated cooling times ( $t_{8/5}$ ) were below the specified 5 seconds for the steel grade. One of the joints was welded by a laser power of 9.5 kW and the welding speed used was 0.6 m/min, where the calculated cooling time was 7.85 seconds. That specific weld was found to have some weld defects such as a root concavity.

The edge preparation of test specimens was made by laser cutting. The edges were shot-blasted and cleaned and finally the surface roughness was measured. The roughness of the laser cut edge was 7.5  $\mu\text{m}$ . The depth of the hardened zone of laser cut edges was also examined and was approximately 0.5 mm. The width of the weld was much wider, approximately 2.6 mm, and thus the area affected in laser cutting melted totally in welding.

The phenomenon observed in some of the previous studies was also observed in this study. Direct-quenched steels (DQ) are sensitive to softening in the HAZ of a weld. The welding energy mainly affects the width of the weld area. The softened zone is very narrow being almost independent of the welding energy.

The transversal tensile strength of the laser welds was higher than the guaranteed minimum tensile strength for the base material. Values of elongation were close to the guaranteed value of the base material (7%). Increased heat input had a negative effect on the tensile strength and the value fell from 1130 MPa to 1030 MPa.

The fine-grained base material showed very good impact toughness properties at temperatures of 40 °C and -60 °C. Unfortunately, when welded this property suffered. The HAZ showed a relatively high toughness value but the weld area did not. Despite the higher impact toughness values of the HAZ, the impact energy absorbed was significantly lower in the weld metal and brittle fractures occurred either in the weld metal or the HAZ of the samples. The required impact toughness value of 22 J was reached in temperatures of -40 °C and -60 °C but only with the highest heat input.

Welding with a high-power fibre laser was found to be a suitable thermal joining method for joining direct-quenched high-strength steels. The welded joints showed good or moderate strength properties with all the welding parameter combinations used.

---

*Contribution to the whole*

The publication improves the content of the doctoral dissertation by adding information on laser welding when a high laser power is applied. The publication clearly increased the amount of testing results included in the doctoral dissertation. The publication has a wide range of results, starting from groove preparation up to testing results of the laser-welded joints.

## 4.5 Publication V

### **Laser welding of coated press-hardened steel 22MnB5**

#### *Objective*

The study focused on the laser welding of iron-zinc coated press-hardened automotive steel. The test material was heated up using a constant temperature of 900°C and two different furnace times (= austenitising times) were used. Shot blasting was used to remove the oxide layer from the surface of specimens before welding. These were compared to specimens with an oxide layer. The laser welding followed the automotive testing guidelines (SEP 1220-3).

#### *Results*

Some tests were performed on heated and press-hardened steel sheets. The specimens were prepared by metallography to examine the oxide layer thickness and its microstructure. The zinc content in the coating decreased from 32% to 25% when the furnace time was increased from 300 seconds to 740 seconds. Shot blasting of the test material flattened the oxide layer but some amount remained on the surface.

Lap and butt joints were used as joint types. A fixed 16 mm overlapping was used between the sheets before welding in the lap joint configuration. According to visual inspection and proved by examining the cross-section of welds, both of the joint configurations generated good weld quality. However, some quite harmless weld defects were present, such as an incompletely filled groove and root concavity. Radiographic examination of the laser-welded joints revealed some porosity, which is quite a typical finding when welding zinc-coated steels. However, no cracking of any kind was evident in the welds. The microstructure was analysed based on the above-mentioned welding test made by the main author of the publication. The microstructure of the weld area consisted of martensite, tempered martensite, ferrite and probably some bainite as well. A softened zone in the hardness curves was found in the butt and lap joints. The furnace time or surface conditions (shot-blasted or not) made no major difference to the hardness. The shear tensile strength of the lap joint was tested. All of the tested welds were fractured from the HAZ as expected.

#### Contribution to the whole

Laser technology is widely utilized in the automotive industry in many processes. Laser welding is used to join car body parts, such as A- and B-pillars and roof rails. The paper presents results of laser welding tests made on a new steel developed for the automotive industry. The zinc-iron-coated press-hardened steel 22MnB5 achieved high strength when hardened. The publication increases the knowledge of laser-welded high-strength steel used in the automotive industry.

## 5 Results and discussion

This chapter presents the results and discussions on the experiments made in the publications. Continuous laser and laser-hybrid welding with different filler materials were studied. The weld quality was inspected by the selected non-destructive and destructive testing methods including mainly static testing, with a fatigue testing made to a minor extent as well. The role of welding parameters on the resulting weld quality is essential and therefore the parameters are analysed in more depth in the publications. The tested steel grades in the publications were from both thin and thick steel as the thickness had various strength levels but the main focus was on ultra-high strength structural steel, including press-hardened 22MnB5 steel used in automotive applications which is often named a high-strength steel.

### 5.1 Role of welding parameters

The number of welding parameters in laser welding is high and increases when laser-hybrid welding is applied to joining. Nowadays, one micron laser is mainly used in laser welding and has replaced the traditional CO<sub>2</sub> lasers. A well-known fact related to one micron lasers which has been proved in many research studies is the narrow optimal welding parameter window. If laser welding is done outside that parameter window, the mechanical properties of the weld suffer and some weld defects, such as pores and spatter, are formed. In the welding of special steels, such as a high strength steel, some limits might be set for the heat input and cooling time in welding. The previous values are calculated from the laser power and travelling speed of welding. However, the great amount of welding variables are not included in the equation of heat input or cooling time and that should be kept in mind when comparing welding results collected from different sources. The values of heat inputs (efficiency factor not taken into calculation) in the publications varied, being between 0.07 and 0.95 kJ/mm for laser welding, 0.3 - 0.35 kJ/mm for laser-hybrid welding and 0.45 - 0.6 kJ/mm for conventional MAG welding. Cooling time  $t_{8/5}$  is also an important value because the most important metallurgical changes occur in that temperature range, having a strong influence on the mechanical properties of the welded joint. Cooling times vary between welding processes and are typically around one second for laser welding and much longer for laser-hybrid (1.5 – 3.0 seconds) and MAG welding (2 – 6 seconds). The values in brackets were collected from the publications of the thesis. The welding parameters were selected based on the thickness of material to be joined instead of a steel grade. It is possible to affect general weld quality to some extent by varying the welding parameters (Figure 5.1) in laser welding and by selection of filler material to a great extent. The figure shows weld profiles of typical lower strength structural steel of 4 mm thickness welded with the same welding energies but with different welding parameter combinations (laser power and travelling speed). Figure 5.2 depicts some of the welding parameters used in the welding tests for all three tested thicknesses of steels (3, 4 and 6 mm). A greater thickness requires increased welding energy but it is obvious that there is an upper limit for utilization of

laser power without forming weld defects, such as sagging (weld defect no. 509 acc. to ISO 13919-1) or an incompletely filled groove (weld defect no 511 acc. to ISO 13919-1).

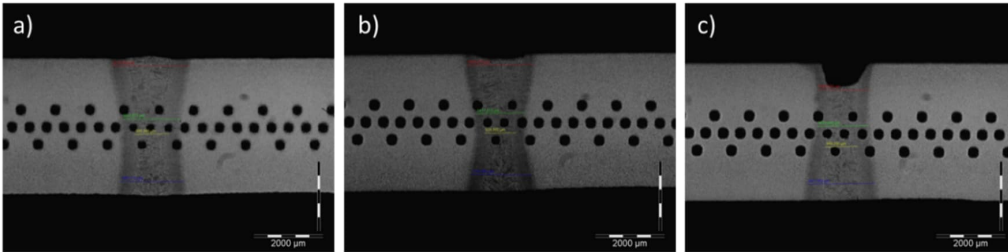


Figure 5.1: Cross-sections of laser welded 4 mm structural steel. a) 2.6 m/min 4kW, b) 3.9 m/min 6 kW and c) 5.3 m/min 8 kW.

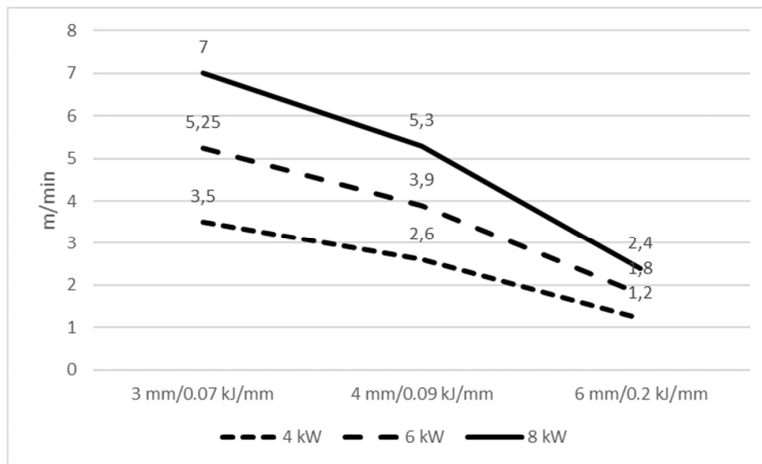


Figure 5.2: Laser welding speeds and laser powers for welding of steel S355 MC from Publication I.

Figure 5.3 illustrates the importance of the welding speed when a high power fibre laser is utilized in welding. The shape and dimensions of a weld are greatly influenced by the welding speed when laser power is kept constant. The welding speed has a minimum value below which the keyhole becomes unstable; in addition, the volume of molten steel increases dramatically and causes the formation of a root concavity or the formation of an incompletely filled root (= surface side concavity), as depicted earlier in Figure 5.1.

A similar effect on the weld geometry is possible with a variation of the laser power (Guo et al., 2015). The maximum value for suitable laser power was discovered to be 6.5 kW; when this value is exceeded, the keyhole becomes unstable, resulting in a face side concavity in the weld. Controlling the keyhole laser welding process becomes difficult when a high laser power is utilized. With the use of 10 kW of laser power, controlling the welding process is difficult and the weld may have weld imperfections, such as a

concavity on the face side but then some excessive penetration on the root side (Zhang et al., 2022). However, with precise selected welding parameters, high laser power can produce a good quality weld. With an optimized combination of process fibre diameter, focal point position, laser power and welding speed, it is possible to achieve good quality welds (Salminen et al., 2016).

With the use of a welding filler material, the above phenomenon can be avoided and use of the filler can also stabilize the welding process. Table 5.1 shows some values from the laser welding tests made for the thesis publications and other tested welding methods are excluded from the table. The thickness of steel is a dominant factor in the calculation of heat input (kJ/mm). Despite the very different welding set-ups and laser systems used in the welding trials and even though the joint type was not the same, the heat input values show only minor differences.

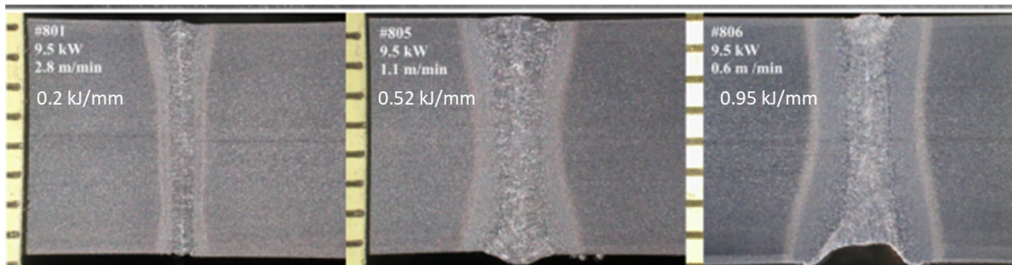


Figure 5.3: Cross-sections of laser welded S960 steel ( $t=8$  mm).

Table 5.1: Welding energies of laser welding tests made in publications.

	Publication I			Publication II	Publication III	Publication IV	Publication V	
<b>Steel grade</b>	S355 MC			S960 MC	S960 MC	S960 MC	22MnB5	
<b>Thickness [mm]</b>	3	4	6	6	6	8	1.5	3.0
<b>Joint type</b>	BOP	BOP	BOP	I	I	I	I	Lap
<b>Welding energy [kJ/mm]</b>	0.07	0.09	0.2	0.1 - 0.15	0.23	0.2 - 0.38	0.02	0.07

Conventional arc and laser-hybrid welding show very different weld profiles in cross-section. Typically, a groove angle is needed in arc welding and it is also recommended for use in some cases in laser-hybrid welding. Figure 5.4 presents the groove angle used in the welding tests of Publication II. The groove angle also gives a relatively good overview of the final shape of the weld.

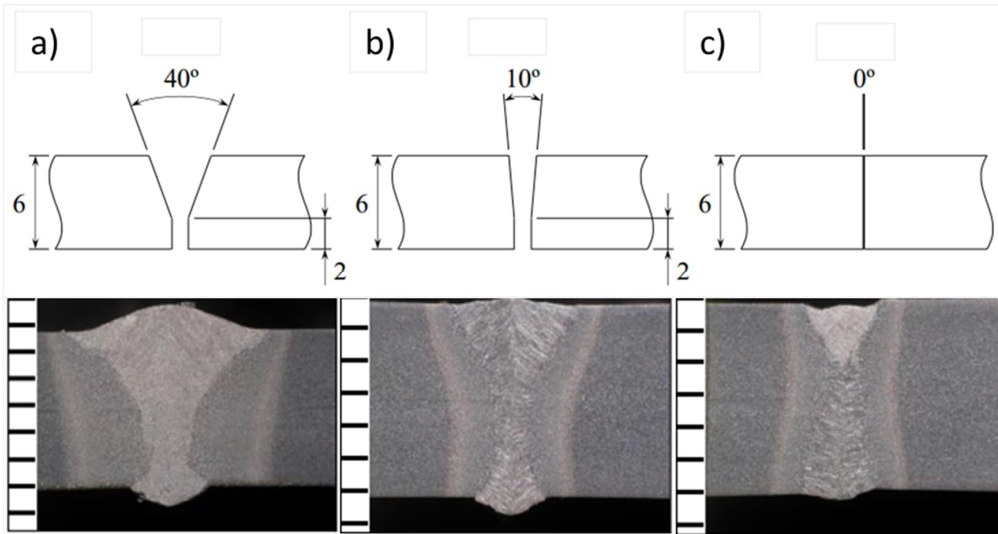


Figure 5.4: Groove shape and dimensions of a) GMA-welding, b) laser-hybrid welding and c) laser welding. All dimensions and scales in mm.

## 5.2 Importance of steel grade

The thesis publications are mainly focused on the joining of high strength structural steel with 960 MPa yield strength. The tested steel is a thermo-mechanically rolled and direct quenched, commercially available steel. Some welding tests were made with other steel grades such as lower strength structural steel (thermo-mechanically rolled S355 MC) and typically used press hardened automotive steel (22MnB5). The welding tests described in the publications show that the use of laser welding is not limited by the grade or thickness of the steel. It can be used either to join lower or higher strength structural steels without any limitations of strength level or joint type. However, it is recommended to follow the instructions from the steel supplier for the minimum and maximum heat input and cooling time. The gap bridging capability of laser welding can be improved if laser-hybrid welding is used instead. The chemical compositions and mechanical properties of steels included in the thesis are presented in Tables 5.2 and 5.3. According to standard CEN ISO/TR 15608 S960, MC steel is classified as a QT steel and belongs to the material group 3.2 and S355 MC steel belongs to the material group 1.2. The 22MnB5 steel is not included in the previous standard but, with some reservations, it can be placed in delivered condition (soft) in group 1.3 and hardened in group 3.2.

Table 5.2: Chemical composition and carbon equivalent (wt.%) of test materials.  
 $CEV = (C+Mn/6+Cr+Mo+V/5+Ni+Cu/5)$ .

Steel	C	Si	Mn	P+S	Cr	Ti	B	Mo	V	Al	Nb	CEV
<b>22MnB5</b>	0.2-0.25	0.4	1.1-1.4		0.1-0.3	-	0.0008-0.005	-	-	-	-	N/A
<b>S960 MC</b>	0.11	0.25	1.2	0.03	-	0.07	-	-	-	-	-	0.52
<b>S355 MC</b>	0.055-0.061	0.16-0.18	1.18-1.23	-	-	-	-	0.002-0.007	0.078-0.083	0.032-0.039	0.041-0.042	0.28-0.30

Table 5.3: Nominal mechanical properties of test materials.

Steel	$R_{p0.2}$ (MPa)	$R_m$ (MPa)	A (%)	Toughness (J)
<b>22MnB5 rolled</b>	400	600	22	
<b>22MnB5 hardened</b>	1200	1600	11	
<b>S960 MC</b>	960	1000	7	27 (-40°C)
<b>S355 MC</b>	355	430-550	23	40 (-20°C)

### 5.3 Testing of weld quality

The weld quality of the tested specimens was evaluated with numerous testing methods. Inspection and evaluation of welded specimens included the following testing: cross-section, microstructure, hardness, tensile strength, bend test and fatigue. Each publication contains a different scope of testing based on the set research targets. Each study is linked to the daily work of the author.

#### 5.3.1 Visual quality of welds

The welded joints were evaluated at least visually before further destructive testing to avoid testing specimens with some weld defects. The testing methods were selected in each publication separately to find answers for the specific research topic that was active at the time. The use of radiographic inspection was very limited and was only used for the valuation of welded specimens in Publication IV. The welded specimens in that specific case were found by radiographic inspection to be free of weld defects such as porosity or cracking.



### 5.3.2 Weld cross-section, dimensions and microstructure

The effect of different welding heat inputs and welding processes can be observed from the weld cross-sections. The cross-section can also give valuable information for further testing or even some hints about the results of those tests. In general, it can be said that the width of a weld increases as the welding speed decreases, since with higher welding energy more steel is melted in the joint. However, a change of width in welded joints does not exactly proceed linearly with a change in welding energy. After a certain maximum value of welding energy, the width of the weld can remain unchanged but show some weld defects. The root side of the weld opens more than joints welded with a lower welding energy. The previous phenomenon can be observed in Figure 5.3. The incompletely filled groove was formed with a high welding energy. The spatter formation was also higher with higher welding speeds. The same observation was made in a laser welding study of a lower strength structural steel ( $R_{p0.2} = 355$  MPa); however, in that study, the reason was the increased laser power from 4 kW up to 8 kW rather than the welding energy or heat input which was kept constant. Figure 5.5 depicts the correlation between the amount of spattering and laser weld quality. At lower laser power (4 kW) and welding speed (2.6 m/min), better process stability was achieved with a low level of spattering resulting in good weld quality. The use of higher laser power (8 kW) and welding speed (5.2 m/min) results in high spatter formation and the weld quality suffers. The calculated welding energies were equal, at 0.07 kJ/mm in both of the above cases.

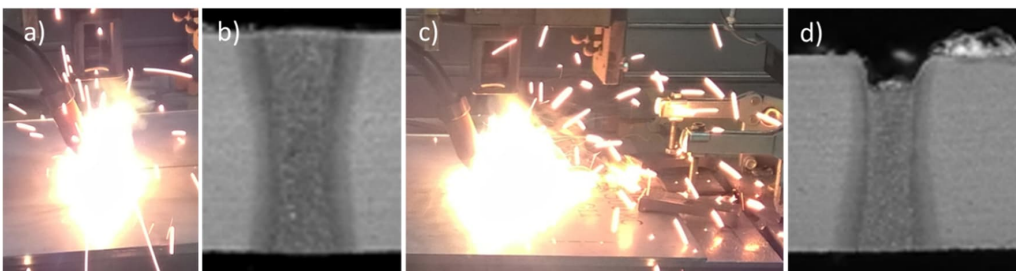


Figure 5.5: Laser welding of structural steel ( $t = 3$  mm). Higher welding values: a) spatter formation, b) cross-section of laser weld; lower welding values: c) spattering and d) cross-section of laser weld.

The microstructures of welded joints were evaluated to some extent but the evaluation was not done methodically or scientifically precisely enough. For this reason, only a few assessments of the final microstructures are made here.

When welded, direct quenched steels are more susceptible to softening compared to quenched and tempered steels. Direct quenched steels have a lower level of alloying although they still achieve good strength properties, making them very attractive to use in applications under heavy load conditions. However, the formation of a softened zone located in SCHAZ and ICHAZ should be taken into account when joining direct quenched

steels. The peak temperature and cooling rate are the most important factors in determining the microstructural evolution within each zone of the welded joint. The tested ultra-high strength ( $R_{p0.2} = 960$  MPa) steel has a martensitic-bainitic microstructure when non-welded, while the lower strength thermo-mechanically rolled structural steel ( $R_{p0.2} = 355$  MPa) has a ferritic-pearlitic microstructure. The third tested steel grade 22MnB5 can also be called ultra-high strength steel after press hardening. It then has a fully martensitic microstructure and when delivered its microstructure is similar to the microstructure of a S355 MC steel, i.e. ferritic-pearlitic. When welded, a martensitic base material stays martensitic in the fusion zone but some softening occurs there in the HAZ area. The same phenomenon is discovered in some studies made by other authors as well (Amraei et al., 2019; Guo et al., 2015; Keränen et al., 2022). Lower strength structural steel S355 MC shows some hardening in the fusion zone (= weld area), being martensitic. All of the tested steels also show some mixed microstructures with different grain sizes and ratios in HAZ areas.

### 5.3.3 Hardness

The effects of different welding methods and heat inputs used can be observed from weld hardness profiles. A hardness profile can also indicate the origin and type of steel in some level. The hardness profiles of laser-welded S355 MC structural steel are depicted in Figure 5.6. The microstructure of the above steel when non-welded consisted of ferrite and pearlite. It should be observed that the specimens were welded with the same welding energy but using different laser powers and welding speeds. Nevertheless, the hardness profiles were different although the same welding method was used.

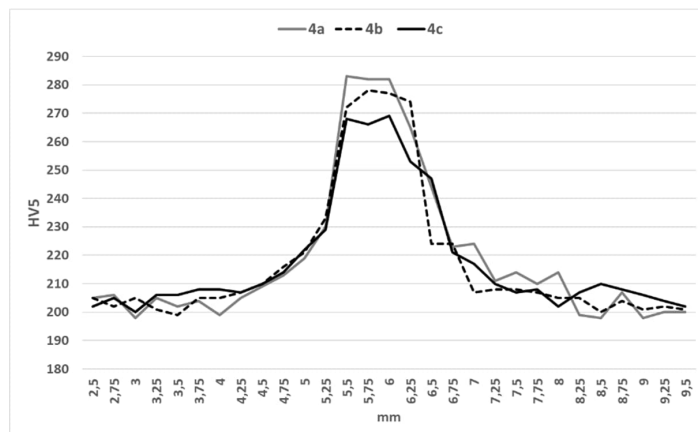


Figure 5.6: Vickers hardness (HV5) of laser-welded S355 MC steel (thickness 4 mm). Constant welding energy applied, i.e. 0.1 kJ/mm. 4a)  $P_1 = 4$  kW,  $v = 2.6$  m/min, 4b)  $P_1 = 6$  kW,  $v = 3.9$  m/min, c)  $P_1 = 8$  kW,  $v = 5.2$  m/min.

The laser-welded ultra-high strength steel S960 MC shows a totally different hardness profile than the above-mentioned lower strength steel S355 MC (Figure 5.7). The maximum hardness achieved for the S960 MC steel is almost double compared to the hardness of the S355 MC steel. The microstructure of the S960 MC steel consisted of martensite and bainite. In laser welds, the maximum value of hardness was observed in the middle of the weld metal and the minimum in the tempered base material, which may also be called the subcritical HAZ (SCHAZ). For the laser-welded specimens in Publication III, the maximum and minimum values were 368 and 264 HV, respectively, where the maximum value was measured in the weld metal and the minimum in the tempered base material (SCHAZ). For the laser-welded specimens in Publication IV, the maximum and minimum hardness values in the weld area were 330 and 410 HV, respectively, and with a higher welding energy the values for minimum and maximum hardness were 300 and 400 HV, respectively. The above-mentioned hardness values were evaluated from the hardness curves in Figure 5.8 since no actual numerical values were available. All of the tested steels have a martensitic microstructure in welds when laser-welded. The difference in the maximum hardnesses can be explained by their different carbon content. The use of a filler material influences the hardness in welds. Continuous laser welding produced the highest hardness of welds in all of the welding tests performed; in contrast, welding processes utilizing some welding filler material produced a softer weld.

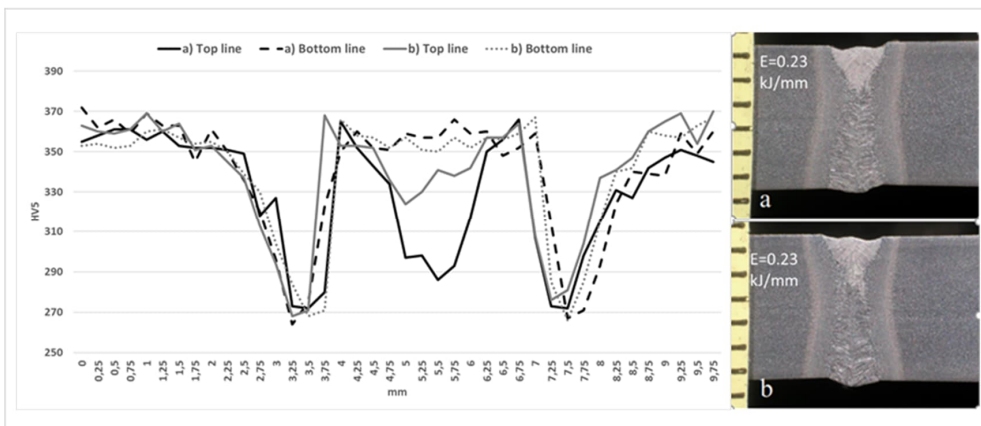


Figure 5.7: Hardness of laser-welded joints of S960 MC steel ( $t = 6$  mm).

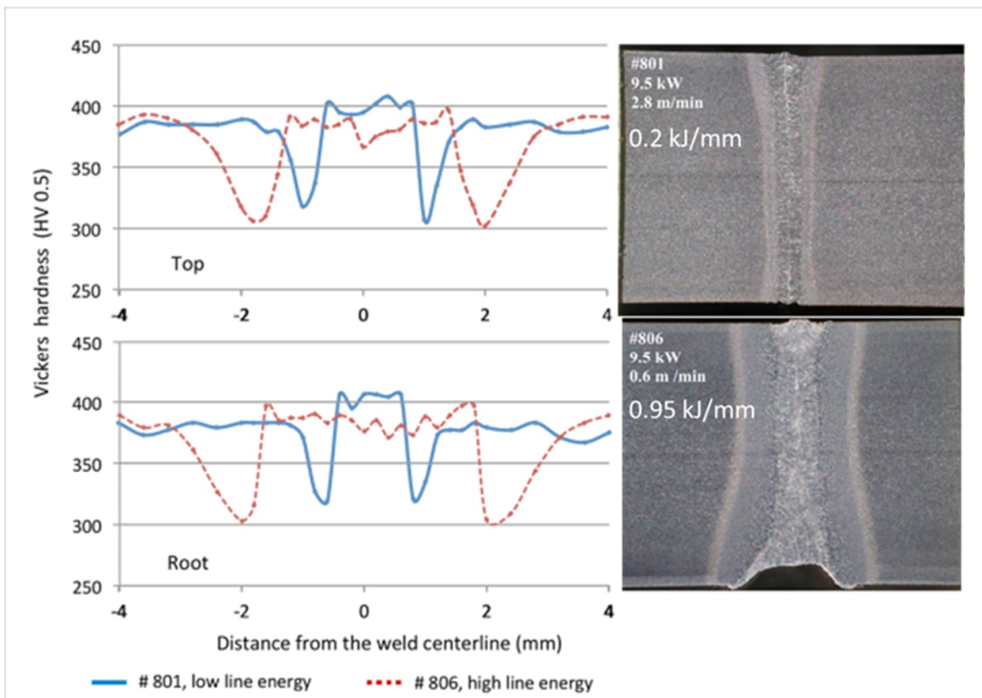


Figure 5.8: Hardness of laser-welded joints of S960 MC steel ( $t = 8$  mm) with different welding energies: low line energy = 0.2 kJ/mm and high line energy = 0.95 kJ/mm.

It is worth mentioning that, regarding HAZ softening, this phenomenon is characterized by two measurements: the width of the soft zone and the minimum hardness of the soft zone. It has been shown by numerical finite element simulations and experimental tests that both of the previous factors are responsible for a decrease in overall strength and especially a decrease in the ductility of laser and laser-hybrid welded joints. The above-mentioned softening phenomenon in the HAZ area is well-known. (Guo et al., 2015; Keränen et al., 2022; Kurc-Lisiecka et al., 2017; Salminen et al., 2016).

However, in the case of laser-hybrid welding it is possible to influence to some extent the strength and ductility of a welded joint by using a welding filler material. Figure 5.9 shows the effect of welding filler material on hardness, strength and elongation. With the use of an undermatching filler ( $R_{p0.2} = 470$  MPa) instead of a matching filler ( $R_{p0.2} = 930$  MPa) in laser-hybrid welding, the strength properties of a welded joint are maintained at an acceptable level for many applications and, in addition, elongation (ductility) is slightly improved despite hardness shows some softening in the weld centreline.

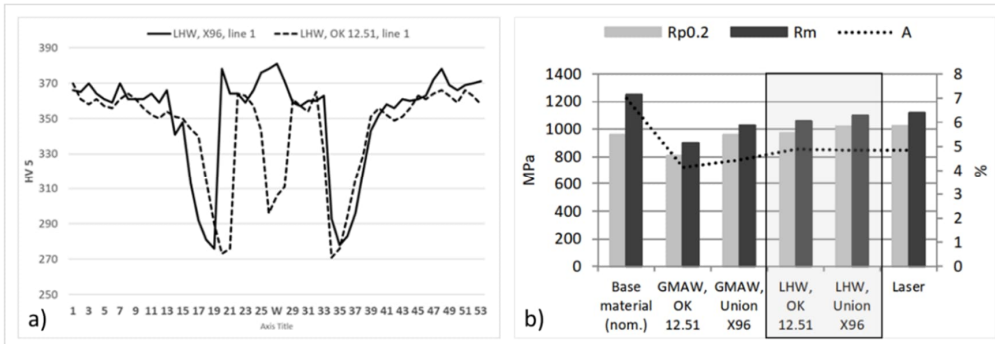


Figure 5.9: Hardness (a) and strength values (b) of welded S960 MC steel. Hardness line 1 located 1 mm below the surface of the plate.

The laser welding of the press-hardened 22MnB5 steel used mainly by the automotive industry shows the same phenomenon of SCHAZ softening as the laser welding of S960MC structural steel (Figure 5.10). Martensite is the dominating element in the microstructure of the above-mentioned steels and therefore the behaviour is similar in laser welding and some softening occurs. The test steel 22MnB5 had a zinc coating, different furnace times (= austenitising times) were used and, in addition, the steel was subjected to different surface treatment before laser welding, being welded as press-hardened and as shot- blasted after press hardening. The influence of the above variables on the properties of the welded joint was minor. With the selection of quenching process variables it is possible to affect the mechanical properties of 22MnB5-steel. As an example, it is possible to increase the elongation with correctly selected quenching parameters (Çavuşoğlu et al., 2020).

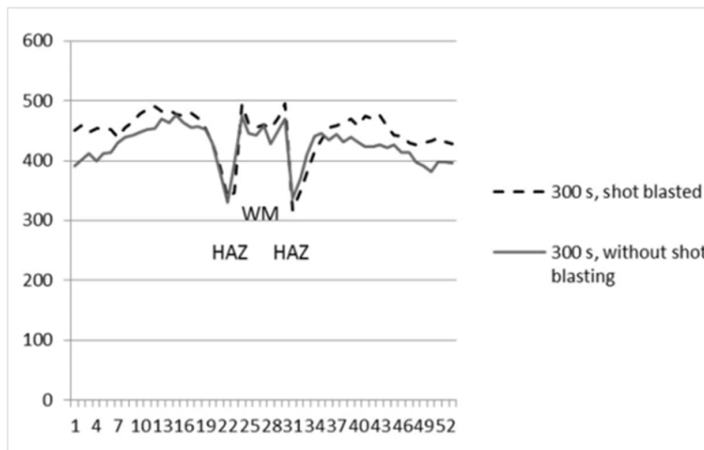


Figure 5.10: Hardness (HV1) of laser-welded 22MnB5 steel. The steel was laser-welded after press hardening. WM = weld metal, HAZ = Heat affected zone and s = second.

### 5.3.4 Tensile strength

The welding parameters used affected the overall weld quality of the welded joint. However, it was surprising that the influence of that quality on the measured mechanical properties was only minor, apart from elongation. In other words, poor weld quality does not automatically correlate with the mechanical properties of a welded joint. The poor weld quality can be seen from the cross-sections of the welds (Figure 5.11). The figure shows an incompletely filled groove and some spatter formation visible in specimen 4c. This poor weld quality decreased the value of elongation and the location of failure in tensile test specimens changed from the base material to the fusion zone or HAZ area. The same phenomenon was observed with the other two tested thicknesses (3 and 6 mm).

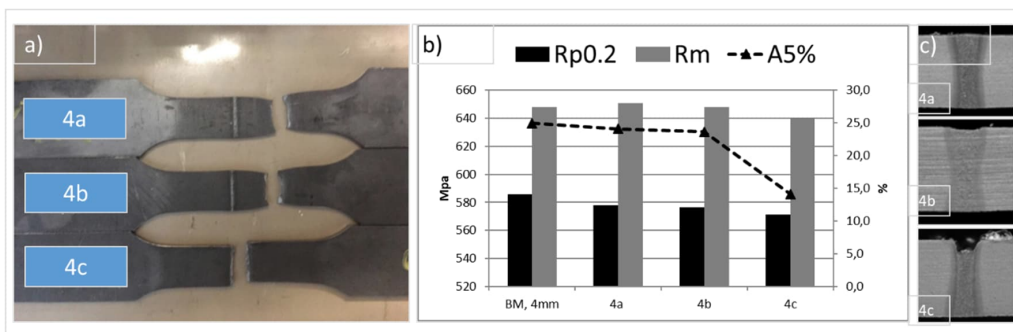


Figure 5.11: Laser-welded steel S355 MC (thickness = 4 mm). a) transversal tensile specimens after testing, b) transversal tensile strength test results, c) cross-sections of laser-welded specimens.

When the steel type and strength level change from thermo-mechanically rolled S355 MC to direct quenched S960 MC some differences are to be expected in the final weldments as well. The tested direct quenched steel as a base material mainly consisted of a martensitic microstructure. After welding, some softening is known to happen in a HAZ area or more precisely in a subcritical HAZ, which is typically the softest area of a welded joint (Guo et al., 2015; Keränen et al., 2022; Kurc-Lisiecka et al., 2017; Salminen et al., 2016).

The transversal test results show some differences in the results depending on the publication (Table 5.4). In particular, the elongation values show a clear difference, which can be explained by the differences in the welding set-up, despite the calculated welding energy being the same. For example, absorption was not taken into account and also the groove preparation was done with different methods: machined (Publication III) vs. laser-cut (Publication IV). The cross-sections of the weld profiles show some differences, which affects the mechanical properties and particularly the elongation values might differ. However, the biggest difference is found in the hardness profiles (weld dimensions and hardness values), which may also partially explain the differences in mechanical properties and especially in the above-mentioned elongation value. The ratio between the minimum and maximum hardness values is 0.72 for the laser welds in Publication III and

the same ratio for laser welds in Publication IV is around 0.8 with a low welding energy (0.20 kJ/mm) and significantly lower 0.73 with a high welding energy (0.95 kJ/mm). This calculated value of ratio indicates the change of hardness in the weld area. In addition, the laser welds with lower elongations showed some weld defects visible in the cross-sections of those specific welds.

Table 5.4: Strength properties of welded S960 MC steel.

Publication and test id.	Thickness (mm)	Welding process	Heat input (kJ/mm)	Yield strength (MPa)	Tensile strength (MPa)	Elongation %
Base mat Publication III	6			1030 (tested)	1139 (tested)	11 (tested)
Base mat Publication IV	8			960 (nominal)	1000 (nominal)	7 (nominal)
GMAW OK 12.51	6	GMAW	0.52	810	902	4.2
GMAW X 96	6	GMAW	0.51	961	1031	4.5
LHW OK 12.51	6	LHW	0.31	974	1061	4.9
LHW X96	6	LHW	0.31	1024	1100	4.9
Laser	6	Laser	0.23	1020	1091	3.9
#801	8	Laser	0.20	1080	1127	7.4
#802	8	Laser	0.23	1090	1130	6.5
#803	8	Laser	0.28	1050	1113	7.6
#804	8	Laser	0.38	1055	1104	6.8
#805	8	Laser	0.52	1034	1091	6.7
#806	8	Laser	0.95	1008	1027	4.3

### 5.3.5 Bend tests

The bend test results show that it can be demanding for conventional GMAW or laser-hybrid welded joints to pass the test (Table 5.5). A laser-welded joint is an exception and the test was passed both by the face and root side. The problem of a direct quenched high strength steel joined by a conventional welding or laser-assisted process passing the standardized bend test has also been recognized in many previous studies made by other authors (Kupiec et al., 2022; Kurc-Lisiecka et al., 2017). A smooth radius for bent specimens is difficult to achieve, as can be seen in Figure 5.12. The bend curve does not follow a smooth radius but instead has an almost acute angle in the weld or HAZ area. Some other authors have produced the opposite result and researched acceptable transversal bend test results both for the face and root sides (Guo et al., 2015; Urbańczyk et al., 2021). However, it is unclear if the bend test standard (ISO 5173) was followed precisely. The diameters of the former and roller used are either missing or unclear.

The results of bend tests in the publications are such that it is highly recommended to use a longitudinal bend test instead of a transversal bend test if the testing procedure allows. The transversal bend test is used to determine the ductility of the welded specimen. In the case of the transversal bend test, the narrowness of a laser weld, normally seen as an advantage becomes a disadvantage when all of the ductility on bending centralizes in the weld or HAZ area with a less elongation, and naturally thus becomes a place of fracture. With the use of the longitudinal bend test, the focus of the test is more on weld quality assurance. Bending in the longitudinal direction can help ensure that the welds are of good quality and free from defects such as cracks, undercut or pores.

Table 5.5: Bend test results welded with different welding processes and filler materials.

Process	Filler material	Bend side	Publication II	Publication III	Summary Passed/Tested
			Result	Result	
GMAW	OK 12.51 / OK 12.50 (G42 4 M20 3Si1)	face	passed	passed	face side 4/4 root side 0/4
		face	passed	passed	
		root	rejected	rejected	
		root	rejected	rejected	
GMAW	Union X96 (G89 5 M21 Mn4Ni2.5CrMo)	face	rejected	rejected	face side 0/4 root side 1/4
		face	rejected	rejected	
		root	rejected	passed	
		root	rejected	rejected	
LHW	OK 12.51 (G42 4 M20 3Si1)	face	rejected	rejected	face side 0/4 root side 3/4
		face	rejected	rejected	
		root	passed	passed	
		root	rejected	passed	
LHW	Union X96 (G89 5 M21 Mn4Ni2.5CrMo)	face	rejected	rejected	face side 1/4 root side 2/4
		face	rejected	passed	
		root	rejected	passed	
		root	rejected	passed	
Laser		face	passed	passed	face side 4/4 root side 4/4
		face	passed	passed	
		root	passed	passed	
		root	passed	passed	





Figure 5.12: Bend test specimen welded with laser-hybrid welding.

### 5.3.6 Toughness properties

The thesis included impact toughness testing (CVN) of 960 MPa ultra-high strength structural steel. The absorbed energy during fracture was measured. This steel offers good toughness properties if the welding recommendations are followed and welded joints serve well at sub-zero temperatures, even below  $-60\text{ }^{\circ}\text{C}$ .

The place of the notch on the impact toughness specimen varied depending on the welding method. For conventional arc and laser-hybrid welding the notch was placed at the weld, at the fusion line, the fusion line + 1 mm and the fusion line + 3 mm, and for laser welding the notch was placed at the weld and the fusion line. The sub-dimension impact test piece was used instead of the standard size specimen. The guaranteed value of toughness for S960 MC steel is  $34\text{ J/cm}^2$  at a temperature of  $-40\text{ }^{\circ}\text{C}$  tested with a standard size specimen.

It has been demonstrated in impact toughness tests of laser-welded joints that a Charpy V-notch (CVN) impact toughness test is not the best method for toughness testing. The correct placing of the notch can be challenging and the location may vary because of the narrow fusion zones, together with a higher degree of strength overmatching of the welded joint (Guo et al., 2015; Takashima et al., 2014). Therefore, tested values can show a high level of deviation. If a notch is placed in the middle of the weld, the strain is concentrated on the narrow soft zone in the HAZ and can influence the toughness values measured when the wrong place is actually measured. In laser-hybrid welding, the choice of a welding filler material has a great impact on the toughness of welded joints. The laser-hybrid welding tests showed that the best impact toughness was achieved with the use of a non- or low-alloyed undermatching filler material, and it can be recommended to use this instead of matching high-alloyed filler materials, provided that the design of the structure permits this and that the desired strength level is reached. A hard and brittle,

non-tempered, martensitic-bainitic microstructure is formed in the weld and HAZ area if more alloyed welding filler material is used. The impact toughness of a hard martensitic or bainitic microstructure is not as good as the impact toughness of the acicular ferrite microstructure formed when a low-alloyed and undermatching filler material is used.

Figure 5.13 shows some selected values of the CVN impact test results of butt joints welded with different welding processes and filler materials. The complete results can be found from each publication of the doctoral thesis. The impact toughness values are expressed in the unit of J. Based on the 27 J toughness requirements for a full-thickness specimen, the test results were assessed based on 22 J requirements with a correction factor of 5/6 for 7.5x10 mm subsize specimens and 18 J requirements with a correction factor of 2/3 for 5x10 mm subsize specimens. 18 and 22 J lines are marked in the chart. The welding energy or heat input used can be found on the y-axis on the right-hand side.

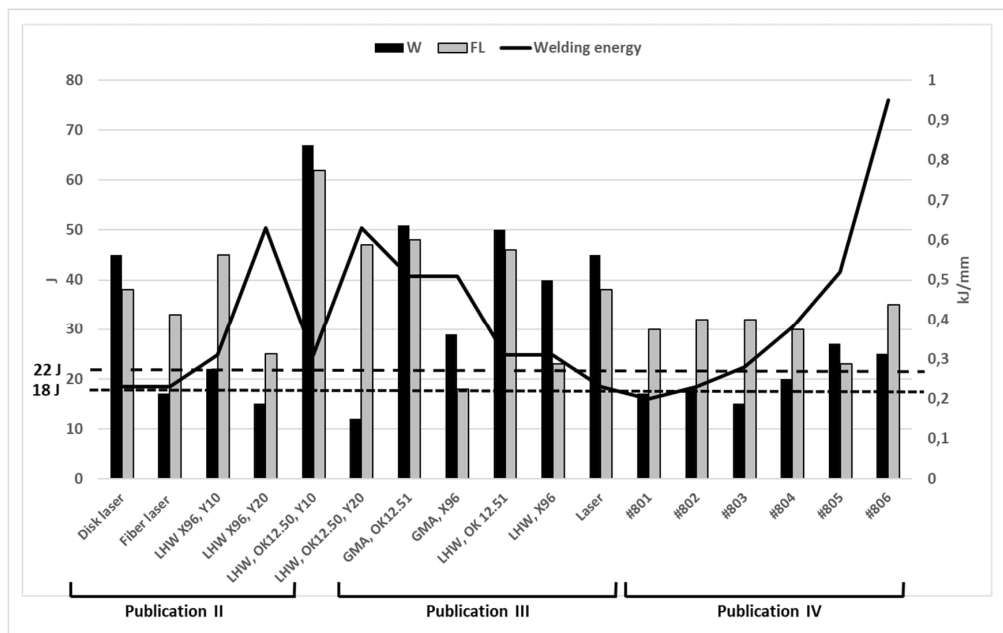


Figure 5.13: CVN impact test results of butt joints welded with different welding processes and welding filler materials collected from Publication II, III and IV. ( $T = -40^{\circ}\text{C}$ ). W = weld, FL=fusion line, Y10 =  $10^{\circ}$  groove angle, Y20 =  $20^{\circ}$  groove angle.

The results of impact toughness are in line with the findings of other authors showing the importance of the weld quality and selection of the correct welding filler material in the case of laser-hybrid welding.

### 5.3.7 Fatigue

The fatigue properties of welded joints were studied in Publication II. The fatigue properties of the butt-welded joints for S960 MC were defined using a constant amplitude cyclic loading where the stress ratio was kept constant ( $R = 0.1$ ) but the applied stress range ( $\Delta\sigma$ ) was varied between different test specimens. According to the recommendations of the International Institute of Welding (IIW), mean and characteristic S-N curves were determined for the different welding processes.

The fatigue test results indicated minor differences between the characteristic fatigue resistance (FAT) values of different welding processes. All of the results are close to the IIW recommendations where the fatigue resistance against structural hot spot stress for butt-welded joints is stated to be 100 MPa. However, the effect of the weld cross-section, the heat input used in the welding or possible weld defects formed in the joints cannot be specified but some approximate conclusions can be made. The mean and characteristic FAT values for different welding processes and welding filler materials are presented in Table 5.6.

Table 5.6: Mean and characteristic FAT values of different welding processes and filler materials.

FAT value	GMA OK	GMA X96	LHW OK	LHW X96	Laser
FAT <sub>mean</sub>	125	139	133	151	149
FAT <sub>char</sub> ( $m = 3$ )	103	81	101	96	115
FAT <sub>char</sub> ( $m = 3$ )	109	97	108	106	122

Laser-welded joints showed slightly better FAT values and less deviation compared to the gas metal arc (GMA) and laser-hybrid welds (LHW). In 2005 Laitinen et al. reported a lower fatigue strength for laser and laser-hybrid welds than for GMA-welded joints. They used a slightly under-matching welding filler material that had a yield strength of 850 MPa. The results are not completely comparable because of the different weld quality being the dominant factor for the fatigue performance of a welded joint; in addition, the welding set-up and system were different.

It should be stated that the S-N curves of GMA welded joints are not completely reliable due to the limited number of data points and thus more test results are needed from the high-cycle fatigue region in order to define more precise S-N curves for both undermatching and matching welding filler materials. The S-N curves are presented in the actual publication and are omitted from this chapter.

The fixed slope  $m = 3$  seems to be suitable for most S-N curves but when using matching filler material in GMA and laser-GMA hybrid welding, a less steep slope might fit better. However, more experimental tests and analyses will be needed to confirm this and, based on the results from this study, the filler material does not have a direct effect on the fatigue

strength of butt joints. Geometrical factors, such as weld toe radius, angular distortion and misalignment, have a major influence on fatigue resistance.

Fatigue cracks initiated mostly from the root side of welded joints, apart from the laser-hybrid welds with undermatching filler material where the fatigue crack propagated almost invariably from the face side of the weld. The reason for this behaviour can be explained by the differences in the global and local geometries of the welded joints. In gas metal arc welds, the angular distortion was detrimental to the face side but the local geometry on the root side was more abrupt compared to the face side so the root side became critical.

The laser welds had a weld defect (incompletely filled groove) located on the face side and excessive penetration on the root side. In addition, the angular distortion was detrimental to the root side as opposed to other welding processes, so the root side fatigue fracture was expected in the case of laser welding. In laser-hybrid welds, the filler material does not necessarily explain why the welds with undermatching filler material failed from the face side and the welds with matching filler material failed from the root side. The angular distortion was detrimental to the face side in both variations. In laser-hybrid welds with undermatching filler material, weld defects such as undercut or incomplete filled grooves were also common on the face side; therefore the face side was more sensitive to fatigue. In contrast, in laser-hybrid welds with the matching filler material, the face side was filled better with a good shape of weld bead and the weld toe geometry was very smooth which can lead to root side fatigue, despite the angular distortion. The cross-sections of welded joints (two from the same weldment) are presented in Figure 5.14.

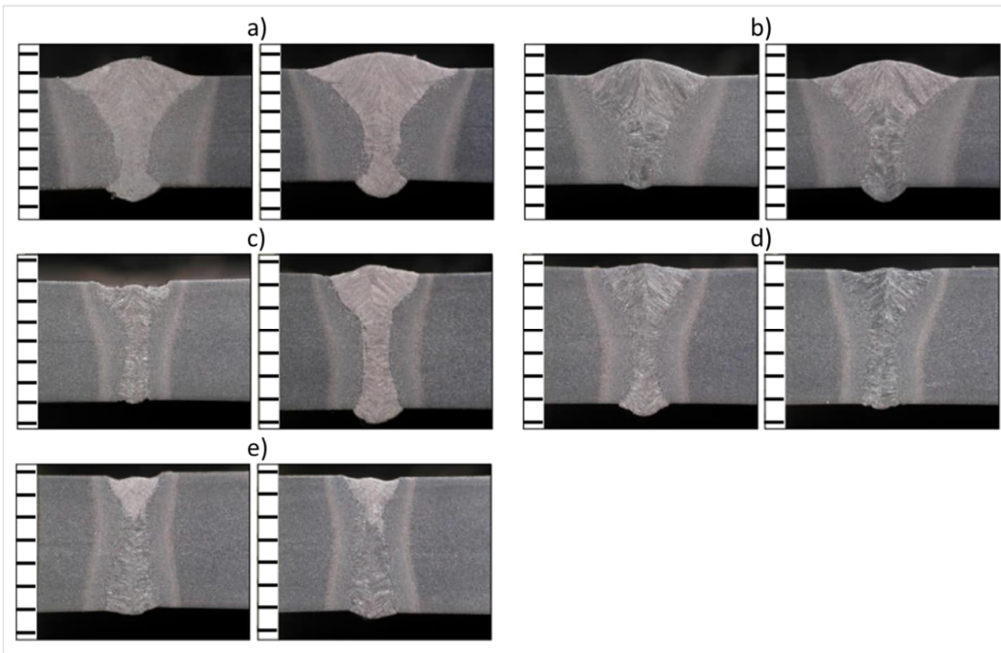


Figure 5.14: Cross-sections of butt joints: a) GMA weld with filler metal OK 12.51 (G42 4 M20 3Si1), b) GMA weld with filler metal X96 (G89 5 M21 Mn4Ni2.5CrMo), c) laser- hybrid weld with filler metal OK 12.51 (G42 4 M20 3Si1), d) laser-hybrid weld with filler metal X96 (G89 5 M21 Mn4Ni2.5CrMo), e) laser weld. The scales are in 1 mm increments.

## 6 Conclusions

Many aspects of the laser welding of structural steels have been studied in this doctoral dissertation. The list of welding tests made is comprehensive and covers the steels used in heavy engineering applications as well as steels used in the automotive industry. The research studies show that laser and laser-hybrid welding are potential joining methods for use in industrial applications. The main findings of the doctoral dissertation are listed as follows:

- It is possible to produce high-quality welds with high-power lasers. The main interest here was in one-micron lasers. The laser itself is a very callous tool making it easy to utilize in the joining of modern structural steels. The overall weld quality achieved is good provided that the recommendations given by steel suppliers are followed.
- Good weld quality can be achieved by laser and laser-hybrid welding. However, weld imperfections were identified, such as incompletely filled grooves, root concavity and porosity. Surprisingly, no cracking of any kind was observed in the studies carried out. The lack of cracks could be explained by the joint type, weld length and penetration depths used. The joint type was mainly a butt joint and welded with full penetration; in addition, the weld was long enough to prevent the stress from increasing to a critical level which might lead to the formation of pipe cracking. The weld depth/width ratio was at such a level that there was no risk of hot cracking.
- A wide spectrum of destructive testing, such as hardness, transversal tensile strength, bend test and impact toughness were included in the publications.
  - Laser and laser-hybrid welded joints of direct-quenched steel showed softening of the HAZ. It was demonstrated that the influence of the formed softened zone on the mechanical properties of joints was minor and, in addition, it is possible to affect the width of the softened zone by changing the welding parameters.
  - The presence of correlation between the width of the softened zone and the achieved strength properties of the welded joint was proved in the studies, i.e. the formed softened zone has a major influence on resistance to bending.
  - The toughness testing presented in the publications reveals a problem in the toughness testing procedure. A laser weld is typically very narrow. Placing a notch for Charpy-V testing can be very demanding. Furthermore, the place can vary unintentionally and can result in unexpected crack propagation occurring in the weld, causing some deviation in the results.
- The optimal welding parameter window for high-power fibre lasers is narrow and the selected parameters in that window affect the mechanical properties of the weld. With

a small heat input, the strength properties of welded joints can be superior but with the use of a higher heat input the impact toughness of the welded joint is improved.

The findings can be implemented in welding production if considering the use of lasers as a tool in welding and if the aim is to utilize higher strength structural steel in welded structures.

## 7 Future work

The research work of the author was strongly guided by daily needs. Currently, the focus is on laser welding of high-strength steels for the automotive industry including dual phase and martensitic steels. The strength level of these steels is from 1000 up to 2000 MPa. Microstructures and alloying of steels can fluctuate a great deal, which should be taken into account in welding. In addition, steels are often coated. New types of phenomena in laser welding have been observed and a limited amount of research results are available. The author would also like to emphasize the need to characterize the equations used for calculations in laser welding (heat input, welding energy, joining efficiency, specific point energy, interaction time etc.).





## References

- Afkhami, S., Javaheri, V., Amraei, M., Skriko, T., Piili, H., Zhao, X-L., Björk, T. (2022). Thermomechanical simulation of the heat-affected zones in welded ultra-high strength steels: Microstructure and mechanical properties. *Materials and Design*. 213. <https://doi.org/10.1016/j.matdes.2021.110336>.
- Alam, M.M, Barsoum, Z., Jonsén, P, Häggblad, H-Å, Kaplan, A. (2009). The effects of surface topography and lack of fusion on the fatigue strength of laser-hybrid welds. *Proceedings of 28<sup>th</sup> International Congress on Applications of Lasers and Electro-Optics*. pp. 38-46.
- Amada weld tech. Laser welding modes: Conduction, transition, & keyhole welding, <https://amadaweldtech.com/blog/laser-welding-modes-conduction-transition-keyhole-welding/>.
- Amraei, M., Ahola, A., Afkhami, S., Björk, T., Heidarpour, A., Zhao, X-L. (2019). Effects of heat input on the mechanical properties of butt-welded high and ultra-high strength steels. *Engineering Structures*, vol. 198, <https://doi.org/10.1016/j.engstruct.2019.109460>.
- Artinov, A., Bachmann, M., Meng, X., Karkhin, V., Rethmeier, M. (2020). On the relationship between the bulge effect and the hot cracking formation during deep penetration laser beam welding. *Procedia CTRP*, 94, pp. 5-10.
- Ayoola, W., Suder, W., Williams, S. (2017). Parameters controlling weld bead in conduction laser welding. *Journal of Materials Processing Tech*. 249. pp. 522-530.
- Bachman, M., Avilov, V., Gumenyuk, A., Rethmeier, M. (2015). Magnets improve quality of high-power laser beam. *Industrial Laser Solutions*. pp. 10-12.
- Bakir, N., Üstündag, Ö., Gumenyuk, A., Rethmeier, M. (2020). Experimental and numerical study on the influence of the laser-hybrid parameters in partial penetration welding on the solidification cracking in the weld root. *Welding in the World*, 64. pp. 501-511.
- Bakir, N., Gumenyuk, A., Pavlov, V., Volvenko, S., Retmeier, M. (2019). In situ determination of the critical straining condition for solidification cracking during laser beam welding. *Procedia CIRP*, 94, pp. 666-670.
- Bayock, F., Kibong, M., Timba, S., Che, N. (2022). Thermomechanical and microstructural constituents of dissimilar S700MC-S960QC high-strength steel welded joints using overmatched filler wire. *International Journal of Engineering and Technology* 11. pp. 1-9.

Bunaziv, I., Dørum, C., Nielsen, S.E., Suikkanen, P., Ren, X., Nyhus, B., Eriksson, M., Akselsen O.M. (2019). Laser-arc welding of 12- and 15-mm thick structural steel. *The International Journal of Advanced Manufacturing Technology*, 107. pp. 2649-2669.

Bunaziv, I., Frostevarg, J., Ren, X., Kaplan, A.F.H., Akselsen, O.M. (2019). Porosity and solidification cracking in welded 45 mm thick steel by fiber laser-MAG process. *Procedia Manufacturing* 36, pp. 101-111.

Çavuşoğlu, On., Çavuşoğlu, Ok., Yılmazoğlu, A.G., Aydın, U-Ü-H., Güral, A., Microstructural features and mechanical properties of 22MnB5 hot stamping steel in different heat treatment conditions, *Journal of Materials Research and Technology*, Vol. 9, No. 5, pp. 10901-10908, <https://doi.org/10.1016/j.jmrt.2020.07.043>.

CEN ISO/TR 15608. (2017). Welding. Guidelines for a metallic materials grouping system.

Charschan, S.S. (1993). Guide to laser materials processing. Laser Institute of America. ISBN 0-912035-11-0.

Churiaque, C., Chludzinski, M., Porrúa-Lara, M., Domiguenz-Abecia, A., Abad-Fraga, F., Sanchez-Amaya, J.M. (2018). Laser-hybrid welding of large thickness naval steel. *MDPI Metals Journal*, 9, 100, doi:10.3390/met9010100.

DNV-GL. (2015). Hybrid laser-arc welding. DNVGL-CG-0287.

Duley, W.W. (1998). Laser welding. John Wiley & Sons, Inc. ISBN 0-471-24679-4.

Engström, H., Nilsson, K., Flinkfeldt, J., Nilsson, T., Skirfors, A., & Gustavsson, B. (2001). Laser-hybrid welding of high strength steels. *International Congress on Applications of Lasers & Electro-Optics*, Vol. 2001, No. 1, pp. 125-134. Laser Institute of America.

Eriksson, I., Powell, J., Kaplan, A. (2013). Guidelines in the choice parameters for hybrid laser arc welding with fiber lasers. *Laser in Manufacturing Conference. Physics Procedia*, 41, pp. 119-127.

Farrokhi, F., Nielsen, S.E., Schmidt, R.H., Pedersen, S.S., Kristiansen, M. (2015). Effect of cut quality on hybrid laser arc welding of thick section steels. *Physics Procedia* 78, pp. 65-73.

Farrokhi, F., Larsen, R., M., Kristiansen, M. (2017). Single-pass hybrid laser welding of 25 mm thick steel. *Physics Procedia*, 89, pp. 49-57.

Farrokhi, F. (2018). Hybrid-laser welding of large steel structures. Doctoral dissertation. Aalborg University. ISBN: 978-87-7210-163-7.

- Fellman, A. (2008). The effects of some variable on CO<sub>2</sub>-laser-MAG hybrid welding. *Acta Universitatis Lappeenrantaensis* 306. ISBN 978-952-214-575 8.
- Frostevarg, J. (2014). The morphology of laser arc hybrid welding. Doctoral thesis. Luleå University of Technology. ISBN 978-91-7439-916-5.
- Gerritsen, C., Howarth, D. (2005). A review of the development and application of laser and laser-arc hybrid welding in European shipbuilding. 11<sup>th</sup> CF/DRDC International Meeting on Naval Applications of Materials Technology. 7-9<sup>th</sup> of June, Halifax, Canada.
- Gook, S., Üstündag, Ö., Gumenyuk, A., Rethmeier, M. (2020). Avoidance of end crater imperfections at high-power laser beam welding of closed circumferential welds. *Welding in the World*, 64, pp. 407-417.
- Grünenwald, S. (2019). High power fiber laser welding thick section materials- Process performance and weld properties. Doctoral dissertation. *Acta Universitatis Lappeenrantaensis* 877.
- Guo, W., Crowther, D., Francis, J.A., Thompson, A., Liu, Z., Li, L. (2015). Microstructure and mechanical properties of laser welded S960 high strength steel. *Materials and Design* 85. pp. 534-548.
- He, H., Forouzan, F., Volpp, J., Robertson, S.M., Vuorinen, E. (2021). Microstructure and mechanical properties of laser-welded DP steels used in the automotive industry. *Materials* 2021, 14, 456. <https://doi.org/10.3390/ma14020456>.
- Hesse, A-C., Nitschke-Pagel, T., Dilger, K. (2019). Investigations on the impact and fracture toughness of beam welded structural steels with yield strengths from 355 to 960 MPa. *Welding in the World*, 63, pp. 87-95.
- Hong, S-G., Lee, J-B. (2007). Effects of hybrid welding parameters on the toughness of weld metal in ship structural steel. *ICALEO conference proceedings*. pp. 935-939.
- Ion, J.C. (2005). *Laser processing of engineering materials*. Elsevier. ISBN 0-7506-6079 -1.
- ISO 683-2. (2018). Heat-treatable steels, alloy steels and free-cutting steels. Part 2: Alloy steels for quenching and tempering.
- ISO 13919-1. (2019). Electron and laser-beam welded joints. Requirements and recommendations on quality levels for imperfections - Part 1: Steel, nickel, titanium and their alloys.
- ISO 12932. (2013). *Welding - Laser-arc hybrid welding of steels, nickel and nickel alloys - Quality levels for imperfections*.

ISO 15609-1. (2019). Specification and qualification of welding procedures for metallic materials. Welding procedure specification. Part 1: Arc welding.

ISO 15609-4. (2004). Specification and qualification of welding procedures for metallic materials. Welding procedure specification. Part 4: Laser beam welding.

ISO 15609-6. (2013). Specification and qualification of welding procedures for metallic materials. Welding procedure specification. Part 6: Laser-arc hybrid welding.

ISO 15614-1. (2017). Specification and qualification of welding procedures for metallic materials. Welding procedure test. Part 1: Arc and gas welding of steels and arc welding of nickel and nickel alloys.

ISO 15614-11. (2002). Specification and qualification of welding procedures for metallic materials. Welding procedure test. Part 11: Electron and laser beam welding.

ISO 15614-14. (2013). Specification and qualification of welding procedures for metallic materials. Welding procedure test. Part 14: Laser-arc hybrid welding of steels, nickel and nickel alloys.

ISO 5173. (2023). Destructive tests on welds in metallic materials. Bend tests.

ISO 5817. (2014). Welding. Fusion-welded joints in steel, nickel, titanium and their alloys (beam welding excluded). Quality levels for imperfections.

ISO 9013. (2017). Thermal cutting. Classification of thermal cuts. Geometrical product specification and quality tolerances.

ISO 1011-6. (2018). Welding. Recommendation for welding of metallic materials. Part 6: Laser beam welding.

Kah, P. (2011). Usability of laser-arc welding processes in industrial applications. Doctoral dissertation. Acta Universitatis Lappeenrantaensis 434.

Kah, P. (2011). Overview of the exploration status of laser-arc hybrid welding processes. *Advanced Materials Science*. Vol. 30. pp. 112-132.

Kankala, T., Salminen, A. (2021). A study on use of wobble features in laser welding of low alloy steel with butt joint configuration. *IOP Conf. Series: Materials Science and Engineering*. 1135 012021. <https://doi:10.1088/1757-899X/1135/1/012021>.

Kaplan, A., F., H., Powell, J. (2011). Spatters in laser welding. *Journal of Laser Applications*, Vol. 23, No. 3, pp. 032005-1-7.

Karhu, M. (2019). On weldability of thick section austenitic stainless steel using laser processes. Doctoral dissertation. Acta Universitatis Lappeenrantaensis 869.

Katayama, S., Kawahito, Y. (2009). Elucidation of phenomena in high power fiber laser welding, and development of prevention procedures of welding defects. SPIE Proceedings Volume 7195, Fiber Lasers VI: Technology, Systems, and Applications; 71951R. <https://doi.org/10.1117/12.807211>.

Keränen, L., Nousiainen, O., Javaheri, V., Kaijalainen, A., Pokka, A.-P., Keskitalo, M., Niskanen, J., & Kurvinen, E. (2022). Mechanical properties of welded ultrahigh-strength S960 steel at low and elevated temperatures. *Journal of Constructional Steel Research*, 198, 107517. <https://doi.org/10.1016/j.jcsr.2022.107517>.

Keskitalo M., Hietala, M., Mäntyjärvi, K. (2019). The normal and shear strength properties of laser lap weld. *Procedia Manufacturing* 36, pp. 224-231.

Kristiansen, M., Farrokhi, F., Kristiansen, E., Villumsen, S. (2017). Application of hybrid laser arc welding for the joining of large offshore steel foundations. *Physics Procedia* 89, pp. 197-204.

Kujala, P., Klanac, A. (2005). Steel Sandwich Panels in Marine Applications. *Brodo Grandja* 56-4, pp. 305-314.

Kupiec, B., Urbańczyk, M., Radoń, M., Mróz, M. (2022). Problems of HLAW Hybrid Welding of S1300QL Steel. *Materials*, 15(16), 5756, [https://doi: 10.3390/ma15165756](https://doi.org/10.3390/ma15165756).

Kurc-Lisiecka, A., Piwnik, J., Lisiecki, A. (2017). Laser welding of new grade of advanced high strength steel Strenx 1100 MC. *Arch. Metall. Mater.* 62, 3, pp. 1651-1657.

Laitinen, R., Lehtinen, M., Fellman, A., Kujanpää, V. (2005). Influence of laser and hybrid laser-MAG hybrid welding on the strength and toughness of the weld HAZ of ultra high strength steel Optim QC. *Nordic Laser Materials Processing Conference*, Luleå, Sweden.

Laitinen, R. (2006). Improvement of weld HAZ toughness at low heat input by controlling the distribution of M-A constituents. *Acta Universitatis Ouluensis C Technica* 234.

Laser Focus World. (2022). <https://www.laserfocusworld.com/photonics-business/article/14234148/chinese-laser-market-under-the-emerging-new-order>.

Laser Systems Europe. (2020). *Lasers in action*. Autumn 2020. <https://content.yudu.com/web/tzly/0A441ad/LSEaut20/html/index.html?page=6&origin=reader>.

Lawrence, J., Pou, J., Low, D.K.Y, Toyserkani, E. (2010). *Advantages in laser materials processing: Technology, Research and Applications*. Woodhead Publishing series in mechanical engineering. ISBN 978-1-84569-474-6.

Lloyd's Register (2007). Marine Division Lloyd's Register of Shipping: Guideline for Approval of CO<sub>2</sub>-laser welding, March 1997.

Manitowoc (2022). <https://www.manitowoc.com/company/news/manitowocs-new-laser-welding-technology-adds-value-tecras-grove-gmk5095>.

Mahrle, A., Beyer, E. (2006). Hybrid laser welding- Classification, characteristics, and applications. *Journal of Laser Applications*, 18, pp. 169-180.

Matsumoto, N., Kawahito, Y., Nishimoto., K. (2017). Effects of laser focusing properties on weldability in high-power fiber laser welding of thick high-strength steel plate. *Journal of Laser Applications*, 29, pp. 012003-1-8. <http://doi.org/10.2351/1.4966258>.

Miranda, R.M, Quintino, L., Williams, S., Yapp, D. (2010). Welding with power fiber laser API5L-X100 pipeline steel. *Advanced Materials Forum V. Vols. 636-637*.

Nemecek, S., Muzik, T., Misek., M. (2012). Differences between laser and arc welding of HSS steels. *Physics Procedia*, 39, pp. 67-74.

Nielsen, S.E. (2015). High power laser-hybrid welding- Challenges and perspectives. *Physics Procedia*, 78, pp. 24-34.

Olsen, F. (2009). Hybrid laser-arc welding. Woodhead Publishing Ltd. ISBN 978-1-84569-370-1.

Pirinen, M., Martikainen, J., Lays, P.D, Karkhin, V.A., Ivanov, S.Y. (2015). Effect of heat input on the mechanical properties of welded joints in high strength steels. *Welding International*. <http://dx.doi.org/10.1080/09507116.2015.1036531>, pp. 14-17.

Poorhaydari, K., Patchett, B.M, Ivey, D.G. (2005). Estimation of cooling rate in the welding of plates with intermediate thickness. *Welding Journal*, 84, pp. 149-155.

Razmpoosh, M.J., Macvan, A., Biro, E., Chen, D.I., Peng, Y., Goodwin, F., Zhou, Y., (2018). Liquid metal embrittlement in laser beam welding of Zn-coated 22MnB5 steel. *Materials and Designs*, 155, pp. 375-383.

Ready, J., F., Farson, D., F (Eds.). (2001). *LIA Handbook of Laser Materials Processing*. Laser Institute of America, Orlando.

Reisgen, U., Olschok, S., Engels, O. (2020). Visualization of the molten pool of the laser beam submerged arc hybrid welding process. *Welding in the World*, 64, pp. 721-727.

Saha, C., Biro, E., Gerlich, A.P., Zhou, Y.N. (2016). Fiber laser welding of Al-Si-coated press-hardened steel. *Welding Journal*, 95, pp. 147-156.

---

Salminen, A., Farrokhi, F., Unt, A., Poutiainen, I. (2016). Effect of optical parameters on fiber laser welding of ultrahigh strength steels and weld mechanical properties at subzero temperatures. *Journal of Laser Applications*, Vol. 28, No. 2, pp. 022415-1-7.

SEP 1220-3. (2011-8). Testing and documentation guideline for the joinability of thin sheet of steel. Part 3: Laser beam welding. VDEh. Stahleisen.

Schaefer, M., Kessler, S., Scheible, P. (2017). Modulation of the laser power to prevent hot cracking during laser welding of tempered steel. *Journal of Laser Applications*, Vol. 29, No. 4, pp. 042008-1-4.

Skriko, T. (2018). Dependence of manufacturing parameters on the performance quality of welded joints made of direct quenched ultra-high-strength steel. Doctoral dissertation. *Acta Universitatis Lappeenrantaensis* 812.

Ślęzak, T., Sniezek, L. (2017). Properties of welded joints made in high strength steel using laser technology. *Bulletin of the Military University of Technology*, 66, pp. 55-66. Doi: 10.5604/01.3001.0009.9484.

Sokolov, M. (2015). Thick section laser beam welding of structural steels: Methods for improving welding efficiency. Doctoral dissertation. *Acta Universitatis Lappeenrantaensis* 655.

Song, H., Zhang, S., Lan, L., Li, C., Liu, H., Zhao, D., Wang, G. (2013). Effect of direct quenching on microstructure and mechanical properties of a wear resistant steel. *Acta Metallurgica Sinica*. Vol. 26, No. 4, pp. 390-398.

Stahl, J. (2021). Advanced materials in automobiles here to stay. <http://www.bodyshopbusiness.com/advanced-materials-in-automobiles-here-to-stay/>.

Steen, W.M. (2003). *Laser material processing*. Springer-Verlag London Limited. ISBN 1-85233-698-6.

Suder, W., Williams, S.W. (2012). Investigation of the effects of basic laser material interaction parameters in laser welding. *Journal of Laser Applications*. Vol. 24, No. 3. pp. 032009-1-10.

Suikkanen, P. (2009). Developing and processing of carbon bainitic steels. Doctoral dissertation. *Acta Universitatis Ouluensis C Technika* 340.

Sumi, H., Oi, K., Yasuda, K. (2015). Effect of chemical composition on microstructure and mechanical properties of laser weld metal of high-tensile-strength steel. *Welding in the World*, Vol. 59, pp. 173-178.



Sun, Q., Di, H-S., Wang, X-N., Chen, X-M., Qi, X-N., Li, J-P. (2018). A study of microstructure and properties of PHS fiber laser welded joints obtained in air atmospheres. *Materials*. Vol. 11, 1135, doi:10.3390/ma11071135.

Takashima, Y., Nishi, T., Shoji, H., Ohata, M., Minami, F. (2014). Evaluation method for Charpy impact toughness of laser welds based on lateral contraction analysis. *Welding in the World*, Vol. 58, No. 3, pp. 289-295. <https://doi.org/10.1007/s40194-014-0114-2>.

Turichin, G., Kuznetsov, M., Sokolov, M., Salminen, A. (2018). Hybrid laser arc welding of X80 steel: Influence of welding speed and preheating on the microstructure and mechanical properties. *Physics Procedia* 78, pp. 35-44.

Unt, A. (2018). Fiber laser and hybrid welding of T-joint in structural steels. Doctoral dissertation. *Acta Universitatis Lappeenrantaensis* 835.

Urbańczyk, M., Adamiec, J. (2021). Hybrid welding (laser-electric arc mag) of high yield point steel S960QL. *Materials*, 14, 5447, <https://doi.org/10.3390/ma14185447>.

Üstündag, Ö., Gook, S., Gumenyuk, A., Rethmeier, M. (2020). Hybrid laser-arc welding of thick-walled pipe segments with optimization of the end crater. *Procedia CIPR*, 94, pp. 676-679.

Üstündag, Ö., Bakir, N., Gook, S., Gumenyuk, A., Rethmeier, M. (2022). Hybrid laser-arc welding of laser- and plasma cut 20 mm thick structural steels. *Welding in the World*, Vol. 66, pp. 507-514.

VDW (2022). Palpable decline in Germany's 2019 production of laser systems. <https://vdw.de/en/palpable-decline-in-germanys-2019-production-of-laser-systems/>.

Vlassenroot (2022). Welding steel. Think long, thick and complex. <https://www.vlassenroot.be/welding-steel/>.

Vänskä, M. (2014). Defining the keyhole modes- The effects on the weld geometry and the molten pool behavior in high power laser welding of stainless steels. Doctoral dissertation. *Acta Universitatis Lappeenrantaensis* 625.

Wouters, M. (2005). Hybrid laser-MIG welding. An investigation of geometrical considerations. Licentiate thesis. Luleå University of Technology. ISSN 1402-1757; 2005:82.

Weberpals, J., Dausinger, F. (2008). Fundamental understanding of spatter behavior at laser welding of steel. *ICALEO conference proceedings*, pp. 364-373.

Xie, J., Kar, A. (1999). Laser welding of thin sheet steel with surface oxidation. *Welding Journal*. Vol 78. pp. 343-348.

---

Xue, J., Peng, P., Guo, W., Xia, M., Tan, C., Wan, Z., Zhang, H., Li, Y. (2021). HAZ Characterization and mechanical properties of QP980-DP980 laser welded joints. *Chinese Journal of Mechanical Engineering*, 34, 80, <https://doi.org/10.1186/s10033-021-00596-x>.

Zhang, X., Ashida, E., Katayama, S., Mizutani, M. (2008). Development of ultra deep penetration welding with 10 kW fiber laser. *ICALEO conference proceedings*. pp. 374-379.

Zhang, H., Meng, J., Xi, C., Lianfeng, W., Shizhong, W., Yumo, J., Nan, J., Zhiyuan, W., Zhenglong, L., Yanbin, C. (2022). Investigation of Weld Root Defects in High-Power Full-Penetration Laser Welding of High-Strength Steel. *Materials*. <https://doi:10.3390/ma15031095>.

World Autosteel. (2021). Advanced high-strength steel (AHSS) definitions, Today's AHSS for automotive, <https://www.worldautosteel.org/steel-basics/automotive-advanced-high-strength-steel-ahss-definitions/>.



## **Publication I**

Siltanen, J.

**Influence of welding parameters on the mechanical properties of a laser-welded joint**

Reprinted with permission from  
*Procedia Manufacturing*  
Vol. 36, pp. 232-239, 2019  
© 2019, Elsevier





Available online at [www.sciencedirect.com](http://www.sciencedirect.com)

**ScienceDirect**

Procedia Manufacturing 36 (2019) 232–239

**Procedia**  
MANUFACTURING

[www.elsevier.com/locate/procedia](http://www.elsevier.com/locate/procedia)

17th Nordic Laser Material Processing Conference (NOLAMP17), 27 – 29 August 2019

## Influence of Welding Parameters on the Mechanical Properties of a Laser-Welded Joint

Jukka Siltanen<sup>a,\*</sup>

<sup>a</sup> *SSAB Europe Oy, Harvialantie 420, FI-13300 Hämeenlinna, Finland*

---

### Abstract

Laser welding is a well-known and relatively widely-used joining process in the engineering industry. Laser welding is also a proven suitable welding method for the joining of modern, high-strength structural steels. Welding of these steels can be challenging when using traditional manual fusion welding, since limits are set for the minimum and maximum welding energy and the cooling time, to retain the original properties of the base material. In the laser welding process, constant welding parameters are used and the movement is performed mechanically, to achieve a high and even processing speed, so that the welding values set can be fulfilled. In the study, the mechanical properties of laser-welded joints were researched in respect of the welding energy used and the cooling time resulting from different combinations of laser power and travelling speed. Several welds with a variable laser power and travelling speed were joined. The thicknesses of the test materials were 3, 4 and 6 mm and the welding energies used for each thickness were 0.05, 0.07 and 0.15 kJ/mm, respectively. The test material was thermo-mechanically rolled structural steel with 500 MPa of yield strength. The joint configuration used was bead-on-plate. Various destructive testing was performed for welded joints. For example, the transversal tensile strength results only showed just minor differences between the values, whereas the hardness values showed clearer differences between the joints.

© 2019 The Authors. Published by Elsevier B.V.

Peer-review under responsibility of the scientific committee of the 17th Nordic Laser Material Processing Conference.

*Keywords:* SSAB Domex; Structural steel; Laser welding; Welding energy; Cooling time

---

---

\* Corresponding author. Tel.: +358-40-542-8214

*E-mail address:* [jukka.siltanen@ssab.com](mailto:jukka.siltanen@ssab.com)

## 1. Introduction

The joining of modern, high-strength steels can be challenging, and some knowledge is needed to be able to produce high-quality joints. Fortunately, steel suppliers often provide good information for the processing of special steels, such as welding recommendations. The recommendations are not limited to joining, since some aid for other manufacturing processes are given such as bending [1]. As a rule of thumb, it can be said that the higher the strength level of the steel, the lower the heat input required in welding. However, for very modern structural steels there are also limits for the minimum values. The low heat input naturally leads to a short cooling time, as the value  $t_{8/5}$ . The reason for these recommendations is the risk to lose some of the materials properties and formed unwanted structures like the softened zone in a HAZ area of weld [2, 3]. The heat input or welding energy used in laser welding is calculated from the welding speed and the laser power used [4]. The formula is identical to the one used for conventional welding, except that current and voltage values are replaced by a value for laser power. In conventional welding, the factor for thermal efficiency is also known and included in the formula, although not often in the case of laser welding. Despite the many efforts of the academic world to define the exact and right value for the laser beam absorption into a material like steel, this is still somewhat unknown, and the value of absorption varies from publication to publication. Therefore, in laser welding the term heat input is replaced by other characteristics describing the welding conditions, such as welding energy, line energy or specific point energy [5, 6]. These characteristics have a certain influence on the shape of the weld formed, as well as the depth of penetration. Laser welding as a modern, precisely controlled, joining process is highly suitable for the joining of steels with special welding requirements. Many previous studies have clearly proved the influence of laser welding parameters on the weld quality and the mechanical properties of a laser welded steel joint [7, 8, 9, 10]. The studies also included a wide variety of welding parameters, including special features such as the welding position. The key idea behind this conference paper was to research influence of a constant welding energy on the mechanical properties of welded joints. In other words, the welding parameters were selected in the way than the results were the equal welding energy. The timing of the study is perfect because, as described earlier, steel manufacturers provide recommendations for welding, and the use of laser welding is becoming more common in industry. In summary, the research aims to answer the question: is it enough to solely calculate the heat input and/or cooling time by using a specific welding parameter combination, or is there a need to perform larger-scale laser welding tests as a matrix for the variable combinations of welding parameters, in order to gain more information about the properties of laser-welded joints. There are only a few standards published especially for laser welding that can help to establish the welding procedure specification and welding procedure qualification record [11, 12, 13]. None of those have clear information to depict and calculate the welding energy used in laser welding.

## 2. Experimental set-up

### 2.1. Test materials

The test materials comprised the structural steel Domex 500 MC, with thicknesses of 3, 4 and 6 mm. Domex is the brand name for structural steels manufactured by steel maker SSAB which have yield strengths below 550 N/mm<sup>2</sup> [14]. SSAB Domex steel is available as a hot-rolled strip in the yield strength range of 240-550 N/mm<sup>2</sup> and as a hot-rolled plate in the yield strength range of 355-500 N/mm<sup>2</sup>. The Domex 500 MC used for the tests was a hot-rolled strip steel that exceeds the requirements of standard EN 10149-2. SSAB Domex hot-rolled strip steels do not need preheating in welding, since there is no risk of hydrogen cracking if welded surfaces are kept clean and fairly low hydrogen welding consumables ( $H \leq 10$  ml/100 g) are used. The dimensions of the welded test sample were 400 × 500 mm. The main chemical composition with the quantities of those and as well the mechanical properties of the base materials are presented in Tables 1 and 2.

Table 1. Chemical composition (wt. %) of the base material Domex 500 MC.  
 $t$  = thickness, CEV= Carbon equivalent ( $C+Mn/6+Cr+Mo+V/5+Ni+Cu/5$ )

t [mm]	C	Mn	Mo	V	Si	Al	Nb	CEV
3	0.061	1.23	0.007	0.080	0.16	0.035	0.042	0.30
4	0.055	1.21	0.002	0.078	0.18	0.032	0.041	0.28
6	0.061	1.18	0.005	0.083	0.18	0.039	0.042	0.29

Table 2. Mechanical properties of the base metal Domex 500 MC.  
 $t$  = thickness,  $R_{p0.2}$  = yield strength,  $R_m$  = tensile strength,  $A_5$  = elongation).

t [mm]	$R_{p0.2}$ [MPa]	$R_m$ [MPa]	$A_5$ [%]	Toughness [J, -20°C]
3	545	637	27	40 J (guarantee)
4	555	629	25	40 J (guarantee)
6	561	640	24	62 J (tested)

## 2.2. Welding of test pieces

The laser welding experiments were carried out by using a 12 kW Trumpf disc laser, the laser was equipped with a 400  $\mu\text{m}$  feeding fibre and the welding optics had a 200 mm collimator, while a focal length of 300 mm was used. The diameter of the focused laser beam on the surface was 0.6 mm. The diameter and place of the laser beam were tested before starting the welding test. The movement of the welding test was performed with a Kuka KR 30 HA-C industrial robot. A strong and rigid clamping device was used to fasten the test pieces, to avoid the distortions formed on welding. The aforementioned test set-up is typically in use at SSAB for laser welding tests performed for structural and automotive steels. The welding was performed as one pass for the welding processes and the welding position was a flat position (PA/1G) in all cases. No tack welding was used because the root configuration was the bead-on-plate (BOP), meaning that no actual joint was welded.

The main welding parameters are presented in Table 3 for all three material thicknesses. Columns a, b and c describe the three welding parameter combinations used in welding. The most important information is increased laser power in 2 kW steps; starting at 4 kW, then 6 kW and finally, 8 kW. The welding speed is fixed according to the laser power and material thickness used. No shielding gas was used in the tests. The coaxial cross-jet with a compressed air stream was used to protect the welding optics.

The cooling rate  $t_{8/5}$  was calculated for the welding processes by using Equations 1 and 2. The value of thermal efficiency for laser welding is 1 in the equation. Equation 1 is for the 2-dimensional heat conduction and equation 2 is for the 3-dimensional heat conduction [3].

$$t_{8/5} = (4300 - 4.3T_0) \times 10^5 \times \left(\frac{\eta \times E}{d}\right)^2 \times \left\{ \left[ \frac{1}{(500-T_0)^2} \right] - \left[ \frac{1}{(800-T_0)^2} \right] \right\} \times F_2 \quad (1)$$

$$t_{8/5} = (6700 - 5T_0) \times \eta \times E \times \left\{ \left[ \frac{1}{500-T_0} \right] - \left[ \frac{1}{800-T_0} \right] \right\} \times F_3 \quad (2)$$

Where,

$T_0 = 25^\circ\text{C}$ ,

$\eta$  = thermal efficiency,

$E$  = laser energy (kJ/mm),

$d$  = plate thickness (mm) and

$F_{2/3}$  = joint factor.

The recommended maximum heat inputs used for the tested steels are between 0.5 (3 mm) and 1.0 kJ/mm (6 mm). The welding parameter tables also show the values for the interaction times ( $T_i$ , ms). Interaction time was calculated using the following equation [5].



$$\tau_i = D_s \div v \quad (3)$$

Where,

$D_s$  = diameter of the spot exposed to the laser beam (m)

$v$  = welding speed (m/s).

The specific point energy ( $E_{SP}$ ) was calculated, in order to get more information about the welding conditions. The specific point energy was calculated using the following equation [5]:

$$E_{SP} = (P_l \times d) / v \quad (4)$$

Where,

$P_l$  = laser power (kW)

$d$  = beam diameter (mm)

$v$  = welding speed (m/min).

Table 3. Laser welding parameters: 3 mm material: 3a, 3b and 3c, 4 mm material: 4a, 4b and 4c, 6 mm material: 6a, 6b, and 6c.

Weld specimen id.	Value								
	3a	3b	3c	4a	4b	4c	6a	6b	6c
Welding speed, $v$ [m/min]	3.5	5.25	7.0	2.6	3.9	5.2	1.2	1.8	2.4
Laser power, $P_l$ [kW]	4.0	6.0	8.0	4.0	6.0	8.0	4.0	6.0	8.0
Welding energy, $E$ [kJ/mm]	0.069	0.069	0.069	0.092	0.092	0.092	0.20	0.20	0.20
Cooling time, $t_{s/s}$ [s]	0.6	0.6	0.6	0.6	0.6	0.6	1.30	1.30	1.30
Interaction time, $\tau_i$ [ms]	10.2	6.9	5.1	13.8	9.2	6.9	30	20	10
Specific point energy, $E_{SP}$ [J]	41.14	41.14	41.14	55.38	55.38	55.38	120.0	120.0	120.0

### 2.3. Testing of welded joints

Large-scale testing and inspections were performed for the welded joints, including the following cross –sections of joints, hardness measurement and transversal tensile strength testing. In addition, the weld appearance and joint profiles were analysed by measuring the width of weld from three locations, which were the top, middle and root sides of the weld.

#### Cross-sections of welded joints

The cross-sections of welded joints are depicted in Fig. 1. The scale visible in the figure is in millimetres, where the distance from line to line is exactly one millimetre of distance. The same scale is used in all photos. The quantity kW presents the used laser power in kilowatts.

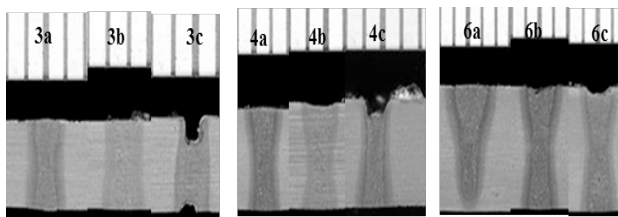


Fig. 1. Cross sections, 3, 4 and 6 mm material: (3a, 4a, 6a) 4 kW laser power; (3b, 4b, 6b) 6 kW laser power; (3c, 4c, 6c) 8 kW laser power. Scale above the figure is in millimeters.

The photos of cross sections clearly show that the changes in the laser welding parameters have a clear influence on the weld profiles, even though the calculated welding energy and cooling time for the previous parameters were the same and constant for all of the three welded joints with the same thickness. The cross sections also show that there is a limit to the maximum increase in the laser power and welding speed. The joints welded with laser power of 4 and 6 kW mostly show no visible incompletely filled groove or root concavity, while the use of even higher laser power, such as 8 kW lead to the presence of these weld defects. There may be several reasons for this, such as the massive melting of the material, the instability of the keyhole, the long interaction time between the laser beam and the material, and different heat conduction on welding. Especially the top side of the weld began to suffer as a consequence of this poor welding quality and an incompletely filled groove weld defect was formed.

#### Transversal tensile strength

The transversal tensile strength results are presented in Fig 2. The welded specimens were tested in welded condition, so that no welding reinforcement was removed before testing. The testing of each thickness formed from two tensile tests and the final value shown in the table are the average of two test results. The transversal tensile strength values are at a good level, despite some specimens of which the poor welding quality influences the joint strength properties. All specimens have the place of fracture in the base materials, except the material thicknesses of 3 and 4 mm welded with a laser power of 8 kW, where the place of fracture was either in the fusion or heat-affected zone.

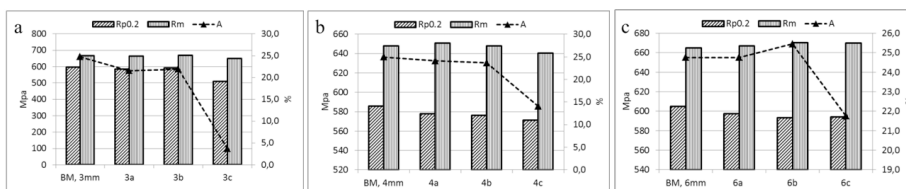


Fig. 2. Transversal tensile strength,  $R_{p0.2}$ =Yield strength,  $R_m$ =Tensile strength,  $A\%$ =Elongation. (a) 3 mm material; (b); 4 mm material; (c); 6 mm material.

#### Hardness

The hardness (HV5) values of welded samples were measured from the base material and weld area. The material thicknesses of 3 and 4 mm have one measuring line in the centre of material thickness, and the 6 mm material has two measuring lines. The first line being at a 1 mm distance from the material surface and the second line at a 1 mm distance from the root of weld. The distance between the measuring points was 0.25 mm. The hardness values are presented in graphic form in Fig 3 and 4. The quantity kW presents the used laser power in kilowatts. According to the results, there is no clear indication that changed welding power and speed has remarkable influence on the hardness values in the weld and HAZ areas. With a material thickness of 3 mm, the highest hardness value was achieved with the 3c parameter combination, in which the highest laser power and welding speed values were used. The next highest hardness was achieved with the specimen 3a and 3b respectively. The hardness profile growth from specimens 3a to 3c is not linear. With the material thicknesses of 4 and 6 mm, the differences between the hardness values were smaller than with a material thickness of 3 mm. The influence of different laser power and welding speed combinations on the hardness profile formation of 4 and 6 mm of material thickness does not follow any clear and systematic scale. In all cases, the highest value of hardness was measured from the fusion zone, which indicates hardening in that area and thereby the formation of a harder microstructure (martensite) than in a base material (fine-grained ferrite). The minimum and maximum values of hardness (weld and HAZ area) are depicted in Table 4. In the table the quantity kW presents the used laser power in kilowatts.

Table 4. Minimum and maximum values of hardness.  
3a, 4a, 6a = 4 kW laser power, 3b, 4b, 6b = 6 kW laser power, 3c, 4c, 6c = 8 kW laser power.

HV 5	3a	3b	3c	4a	4b	4c	6a (top)	6a (root)	6b (top)	6b (root)	6c (top)	6c (root)
Min	212	218	218	213	207	214	218	216	213	217	221	220
Max	295	274	314	295	278	269	260	275	275	272	290	293

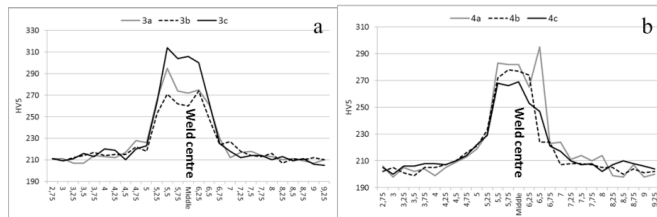


Fig. 3. Hardness profiles, (a) 3 mm material; (b) 4 mm material:  
3a, 4a= 4 kW laser power, 3b, 4b= 6kW laser power,  
3c, 4c= 8 kW laser power.

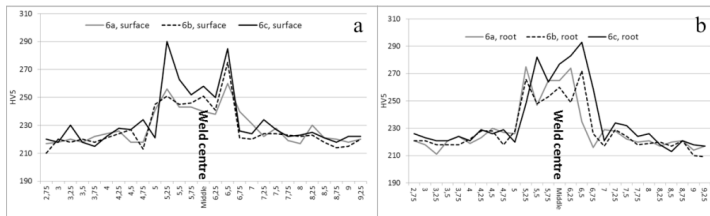


Fig. 4. Hardness profiles, 6 mm material: (a) Surface; (b) Root.  
6a = 4 kW laser power, 6b = 6kW laser power, 6c = 8 kW laser power.

*Measurement of the weld dimensions*

The weld dimensions were measured in order to obtain numerical data for the evaluation of the influence of different laser welding parameters, in particular on the shape of laser welds. Measurement was performed by placing three measurement lines on the welds: the first line, number, 1 was placed in the top part of the weld, the next line, number 2, was placed in the middle of the weld (waist of the weld) and the last line, number 3, was placed in the root side of the weld. These three lines were not located in absolutely the same place for all welds, because there were, for example, some weld defects in the joints that influenced the position of the lines. This leads to some uncertainty concerning the results, and possibly also deviation. The information is therefore more informative than scientifically reliable. The location of the measurement lines is presented in Fig. 5. There are three lines in the figure; top line, middle line and bottom line. The placing of these measuring lines on the cross sections can varied due to the fact that weld defects like incompletely might be present on measuring area forcing to change the place of measure.

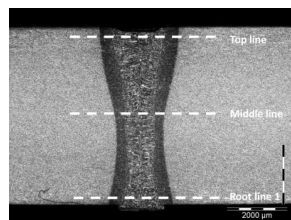


Fig. 5. The location of measurement lines over the laser weld.

Fig. 6 shows the resulting weld dimensions. Typically, for the fibre laser-welded joint the top and root sides of the weld are wider than the middle area of the weld. However, in the study there exists one exception to this, which is the joint for 6 mm of material thickness, welded with 4 kW of laser power and with a weld defect of incomplete penetration that leads to a narrower root side instead of the waist of the weld. Values of 3 mm of material thickness showed the decreasing dimension values when the laser power and welding speed were increased. The dimensions of material thicknesses 4 and 6 mm follow the same trend, but this was not as clear as in the case of 3 mm of material thickness.

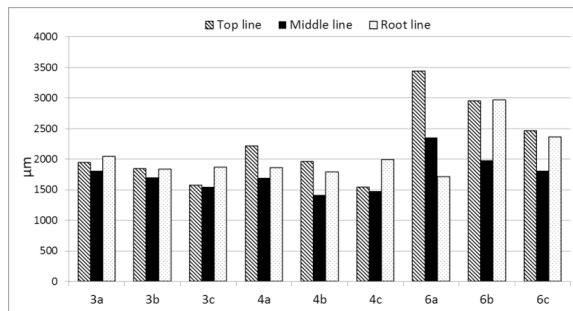


Fig. 6. Dimensions of the weld, 3 mm material: 3a, 3b and 3c; 4 mm material: 4a,4b and 4c; 6 mm material: 6a, 6b and 6c  
 Top: Measuring line close to the surface of material, Middle: Material thickness/2,  
 Root: Measuring line close to the lower surface of material.

### 3. Discussion

The focus of the paper is to study the influence of welding parameters on the mechanical properties of the laser-welded joint. The welding energy was kept constant irrespective of the laser power and welding speed. It was assumed that when the laser welding energy is unchangeable, there should not be any differences in the mechanical properties of welded joints, because the laser beam should interact in the same way with the material when this same welding energy is used. The cross sections taken from the welded joint showed some weld defects. The type of defect on the top side of the weld was an incompletely filled groove, and on the root side it was a root concavity. These defects were seen when the highest laser power of 8 kW was used, the interaction time was short and the heat had no time to conduct on the material. Some previous studies have found that, for the investigation of the laser process in welding, the terms power density and interaction time are insufficient to characterise the laser welding process and a third term, specific point energy, is needed in order to uniquely characterise the process. The influence of the previously used terms on the shape of the weld was described as follows: the weld's depth of penetration is mainly controlled by the laser power density and the specific point energy, while the weld width is controlled by the interaction time. This research is not in complete agreement with the previous research. For example, the interaction time has no clear connection with the weld width. In addition, the shape of the laser weld makes this type of study more difficult. According to this study, it is clear that there is a limit to the maximum laser power for each material thickness. If high laser power such as 8 kW is used in the study, more changes are needed to the welding parameters than just the fixing of the welding speed. The tensile strength results do not show major differences in the yield and tensile strength values, while the elongation values were relatively low for specimens welded with high laser power (8 kW). The hardness curves showed interesting values for a 3 mm thickness, whereby the greatest hardness in a weld area was measured when 8 kW of laser power was used, and the values were clearly lower for laser power of 4 and 6 kW. With other thickness ranges no such trend was visible and hardness values showed minor differences.

### 4. Conclusions

Based on the experimental elements and large-scale destructive testing of the laser-welded specimens, the conclusions are:

1. The assumption made at the beginning of the study that the use of the same welding energy does not lead to the absolutely same mechanical properties of the laser-welded joints was partly disproved. For example, there were no differences in the microstructures of the welded specimens joined with the same welding energy. The mechanical properties of welds achieved with laser power of 4 and 6 kW were very similar, but with 8 kW of laser power the quality of the welded joint suffered, which influenced the mechanical properties of the welded joint, but not the microstructures, as previously stated. The main differences were evident in a weld shape pool and its dimensions.

2. The welding parameters used should be optimised for each steel grade, in order to achieve a high-quality welded joint and also good mechanical properties. In the study, it was not possible to apply the highest laser power (8 kW) with the welding parameter combination used, so that the maximum welding efficiency was not achieved. In this case, the calculated interaction time was relatively short, which is probably a good indication of the success of laser welding. This poor weld quality when extremely high laser power is used is a situation that might change if more laser welding parameters, such as focus position or the alignment of the laser beam, are corrected.

3. The laser welding tests performed in a bead-on-plate (BOP) configuration do not unambiguously answer the question: How does the laser welding energy used influence the mechanical properties of the weld? Therefore, one element of the subsequent measures will be to perform a similar test matrix using a real joint configuration, such as a butt joint in this case.

### Acknowledgements

The author would like to acknowledge SSAB Europe Oy for the opportunity to publish this conference paper, and also appreciation of the support given by several specialists on preparing the conference paper.

### References

- [1] SSAB Design Handbook, Edition 1 (2012) 195-219.
- [2] F. Farrokhi, J. Siltanen, A. Salminen, Fiber laser welding of direct-quenched ultrahigh strength steels: Evaluation of hardness, tensile strength, and toughness properties at subzero temperatures, *Journal of Manufacturing Science and Engineering* 137 (2015) 061012-1.
- [3] D. Gery, H. Long, P. Maropoulos, Effects of welding speed, energy input and heat source distribution on temperature variations in butt joint welding, *Journal of Materials Processing Technology* 167 (2005) 393–401.
- [4] SSAB Welding Handbook, Edition 1 (2004) 13-18, 31-38.
- [5] S. Williams, W. Suder, Investigation of the effects of basic laser material interaction parameters in laser welding. *Journal of Laser Applications*, 24 (2012) p.032009
- [6] M. Hashemzadeh, W. Suder, S. Williams, J. Powell, A.F.H. Kaplan, K.T. Voisey, The application of specific point energy analysis to laser cutting with 1  $\mu\text{m}$  laser radiation, 8th International Conference on Photonic Technologies LANE (2014) 909-918.
- [7] M. Sokolov, A. Salminen, V. Somonov, A.F.H. Kaplan, Laser welding of structural steels: Influence of the edge roughness level, *Optics & Laser Technology* 44 (2012) 2064–2071.
- [8] A. Unt, A. Salminen, Effect of welding parameters and the heat input on weld bead profile of laser welded T-joint in structural steel, *Journal of Laser Applications*, 27 (2015) S29002.
- [9] J. Siltanen, T. Skriko, T. Björk, Effect of the welding process and filler material on the fatigue behaviour of 960 MPa structural steel at a butt joint configuration, *Journal of Laser Applications Journal of Laser Applications* 28 (2016) 022413.
- [10] W.W. Duley, *Laser welding* (1999) 114-136.
- [11] European standard EN ISO 13919-1, Welding. Electrons and laser beam welded joints. Guidance on quality levels for imperfections. Part 1: Steel (1996).
- [12] European standard EN ISO 15609-4, Specification and qualification of welding procedures for metallic materials. Welding procedure specification. Part 4: Laser beam welding (2009).
- [13] European standard EN ISO 15614-11, Specification and qualification of welding procedures for metallic materials. Welding procedure test. Part 11: Electron and laser beam welding (2002).
- [14] SSAB steel data, Domex - Optimized for you and structures, [www.ssab.com](http://www.ssab.com) (2018).

## **Publication II**

Siltanen, J., Tihinen, S., and Kömi, J.

**Laser and laser gas-metal-arc hybrid welding of 960 MPa direct-quenched structural steel in a butt joint configuration**

Reprinted with permission from  
*Journal of Laser Applications*  
Vol. 27 (S2), pp. S29007-1-8, 2015  
© 2015, Laser Institute of America



## Laser and laser gas-metal-arc hybrid welding of 960 MPa direct-quenched structural steel in a butt joint configuration

Jukka Siltanen

*Ruukki Metals Oy, Harvialantie 420, Hämeenlinna FI-13300, Finland*

Sakari Tihinen and Jukka Kömi

*Ruukki Metals Oy, Rautaruukintie 155, Raahе FI-92101, Finland*

(Received 5 January 2015; accepted for publication 12 January 2015; published 26 February 2015)

Welding trials have been carried out using direct-quenched 960 MPa ultrahigh-strength steel utilizing several welding processes: gas-metal-arc, laser, and laser gas-metal-arc hybrid welding. Laser power sources like the CO<sub>2</sub>-laser and the fiber-delivered solid state laser were used. In the trials, butt joints with various groove geometries were used and the thickness of the base material was a constant 6 mm. Welding filler materials varied from matching Union X96 (ISO 14341: G 89 5 M Mn4Ni2.5CrMo) to undermatching Esab OK 12.50 (G3Si1). The diameter of the filler wire varied from 1 to 1.2 mm. The highest hardness value, over 400 HV, was reached on laser welds. According to the results, the strength of the joints corresponded to the nominal strength of base materials (tensile strength of 960 MPa), regardless of the welding method and welding filler material used. As a whole, the results of transverse bend testing were poor as expected, especially when the face side of welds was under tension. The standardized bend and also the used impact toughness tests (Charpy-V) are not the best methods to evaluate the ductility or the toughness of a weld in direct-quenched steels. However, relatively good impact toughness values were achieved to the fusion line of the welds both with the continuous laser and laser hybrid welding process, reaching 57 J with the laser welding and 49 J with the laser hybrid welding when the matching filler material was used. © 2015 Laser Institute of America. [<http://dx.doi.org/10.2351/1.4906386>]

**Key words:** Laser welding, Laser gas-metal-arc welding, Direct-quenched-steel

### I. INTRODUCTION

The use of ultrahigh-strength steels (UHSS) is increasing in the engineering industry. Typical applications in heavy engineering where the use of UHSS brings clear benefits are in the structures of load handling and transportation vehicles and lifting equipment such as telescopic booms or cranes. The target is to decrease the weight of structures to safe fuel or make higher payloads possible. However, the welding of these special steels is more demanding because the smaller processing windows set limits on the heat input and cooling rate. Modern gas-metal-arc welding power sources with a versatile pulse mode and higher cost laser and laser hybrid welding processes have been proved to be good welding methods for UHSS, fulfilling the requirements set for the heat input and cooling times. QC-quality strip steels are made by modern hot strip rolling and direct-quenching processes which differ from the manufacturing process of QL-steels. QL-steels are made in the conventional way: hot rolling, reheating, quenching and finally tempering (Fig. 1).

From the metallurgical point of view, direct-quenching is a more versatile process than the conventional manufacturing process of QL-steels, offering more possibilities to control the microstructure of steel. Optim 960 QC is standardized as thermo-mechanically rolled steel corresponding the S960MC steel according to standard EN 10149-2: 2013. Optim 960 QC steel is not tempered and it has a lower level of alloying if

compared to the conventional quenched and tempered steels with the same yield strengths. The effect of this phenomenon has an impact on the mechanical properties of Optim 960 QC when it is welded, e.g., the hardness profile of QC-steel differs from QL-steel (Fig. 2).

Optim 960 QC steel has a wider and deeper soft zone when welded than S960 QL steels due to the softening of the intercritical/subcritical heat-affected zones (ICHAZ/SCHAZ) and the tempered zone in the peak temperature range of 450–850 °C. In addition, the hardness of the coarse-grained HAZ of Optim 960 QC steel is typically lower than QL steels. It is possible to reach the matching joint if laser and laser-hybrid welding or modern pulsed gas-metal-arc welding are utilized.<sup>1</sup> Laser welding and laser-gas-metal-arc hybrid welding as fully automated welding processes ensure the homogeneous welding quality, together with the relatively high processing speed. This study is a summary of the welding research carried out for Optim 960 QC steel. The focus is on destructive testing, e.g., tensile strength test, bend test, hardness, and toughness. The results of nondestructive-testing like visual or radiographic examinations are excluded from the study but normally good or even excellent welding quality is evident from nondestructive examination, corresponding typically to weld classes B (stringent) or C (moderate). The thickness of tested steel was 6 mm, representing the typical thickness of strip steel used in the engineering industry and in welded structures. In addition, a lot welding results were



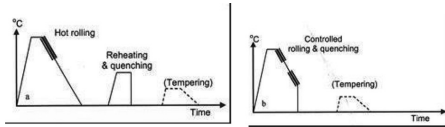


FIG. 1. Schematic presentation of UHSS steel manufacturing routes. Temperature diagrams showing the differences between the conventional manufacturing route (left) and direct-quenching (right) (Ref. 1).

available for this thickness level. The objective of the study was to investigate the effect of the welding method and the filler material to the mechanical properties of the weld, and especially the HAZ-area of welds is particularly interesting. The effect of the welding parameters and more precisely the effect of heat input on the mechanical properties of welds were observed.

## II. EXPERIMENT

The references include results of many welding tests carried out on Optim 960 QC between 2006 and 2014. The time period is relatively long and there has been progress both in laser technology and in conventional welding processes. In addition, Optim 960 QC steel has been modified in this time-span. This can have some influence on the tests results and thus they are not totally comparable, such as the study carried out in 2007, at a time that welding research with the modern 1  $\mu\text{m}$  lasers was just starting; therefore, the achieved results were poor, not because of the technology but because of the lack of experience. The aim of the study is not to put the lasers in order of superiority but to study the suitability of technology on a general level for the quality welding of ultrahigh-strength steel.

## III. MATERIALS

The examined material was Optim 960 QC steel with a thickness of 6 mm. The QC-steel is manufactured by Ruukki Metals in the modern direct-quenching steel-making process for strip steels. The typical chemical composition and mechanical properties of Optim 960 QC are given in Tables I and II.

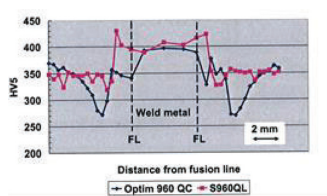


FIG. 2. Vickers hardness profiles of the gas-metal-arc welded butt joints in Optim 960 QC and S960QL steels. Heat input 0.46 kJ/mm and plate thickness 6 mm. The welding wire was Union X96 (Ref. 1).

TABLE I. Chemical composition of Optim 960 QC-steel (typical and maximum in wt. %).

Material	Optim 960 QC
t (mm)	6
C	0.11
Si	0.25
Mn	1.20
P	0.020
S	0.010
Ti	0.070
Other	Al, V, Cr, Mo, B
CEV, typical	0.52

## A. Welding

The steel manufacturer Ruukki provides detailed information on the welding of special steels. The maximum cooling rate value ( $t_{8/5}$ ) for Optim 960 QC steel is limited to 15 s in welding and if the matching weld is targeted, the cooling rate should be much shorter, at around 4 s. Some references recommend the use of differing minimum and maximum cooling rates to ensure weld quality: e.g., 2–11.7 s (Ref. 2) and 2–10 s (Ref. 3). Normally, achieving such short cooling rates of this short requires an automated and exactly controlled welding process, e.g., laser welding, laser hybrid welding, or modern pulsed gas-metal-arc welding. Special attention must be paid to the arc energies and heat inputs utilized in the welding of special steels.

Several welding processes and systems with different laser power sources ( $\text{CO}_2$ -laser, disk, and fiber laser) and arc sources were used (Table III). The references include test results of specimens welded with the laser, laser hybrid and gas-metal-arc welding processes. The gas-metal-arc welding was done with one or two passes. If the gas-metal-arc welding is made with one pass, there is a risk of weld defects forming and the limit set for the maximum heat input could be exceeded.

The size of welded specimens varied from the standard size specimen ( $300 \times 300$  mm) used for preparing of welding procedure specification, to larger welded specimens used to simulate production. This should be kept in mind when comparing results. The used filler materials varied from the matching Union X96 (G 89 5 M Mn4Ni2.5CrMo) to under-matching Esab OK 12.50/OK12.51 (G3Si1) filler material. The filler materials like Böhler X70-IG (G 69 5 M Mn3Ni1CrMo), Böhler X90-IG (G 89 6 M Mn4Ni2CrMo), Esab Aristorod 89 (G Mn4Ni2CrMo), Esab Coreweld 89 (T 89 4 Z M M 3 H5), and Esab OK 13.13 (GMn3NiCrMo) were also used in welding tests, but because of the very limited number of welding tests, those results are not included in

TABLE II. Mechanical properties (minimum) of Optim 960 QC-steel.

Material	t (mm)	$R_{p0.2}$ (N/mm <sup>2</sup> )	$R_m$ (N/mm <sup>2</sup> )	$A_5$ (%)	Charpy-V (J/cm <sup>2</sup> )
Optim 960 QC	6	960	1000	7	34 (–40 °C) <sup>a</sup>

<sup>a</sup>Corresponding to 27J, 10  $\times$  10 size specimen.

TABLE III. Welding equipment used in welding tests (L = laser, LHW = laser HYBRID welding, GMA = gas-metal-arc welding).

Reference	Welding process	Laser source	Arc source
1	LHW	Fiber laser, 10 kW	Esab Aristo
11	L, LHW	CO <sub>2</sub> -laser, 6 kW Fiber laser, 5 kW	Esab Aristo LUD 450
4	L	Disk laser, 4 kW	
7	GMA		Gloos quinto 603
8	GMA		Kemppi Pro 4200 Evolution
3,5	L	Fiber laser, 10 kW	
6	L, LHW, GMA	Disk laser, 12 kW	Fronius TIME 5000
9	LHW	CO <sub>2</sub> -laser, 10 kW Disk laser, 8 kW	Fronius

the study. The mechanical properties of the filler materials Union X96 and Esab Ok 12.50 are depicted in Table IV. The diameter of the used filler material varied from 1 to 1.2 mm.

The groove preparation of weld specimens varied from straight (90°) to bevelled edges (Table V). The choice of correct geometry was based on preliminary welding tests or was done according to the standards. It is important to select the correct groove geometry because it has a significant influence on the quality and properties of welds.<sup>1</sup> In the reference articles, two different groove preparation methods were applied: laser cutting and machining. In some references, the oxide layer was removed by the sand blasting process.<sup>2,5</sup> The removal of the oxide layer also makes the surfaces of the groove rougher and this can have an effect on the absorption and reflections of the laser beam especially if 1 μm laser is used.

Table VI presents the values of some key welding parameters collected directly from the articles or calculated if the value did not exist. The cooling rate has a significant effect on the strength properties of welded Optim 960 QC steel. Not all cooling rates values are presented in Table VI because of the limited information available. Online measuring of the cooling rate for laser and laser hybrid welded joints is demanding, the welding process is fast, and the formed weld area is very narrow and the placing of thermocouples is a demanding process.<sup>4</sup> Ion *et al.* have presented the equation (Eq. (1)) to calculate cooling rate  $t_{8/5}$  if the width of the HAZ is known.<sup>11</sup> The cooling rate  $t_{8/5}$  is not calculated in all cases because the information necessary for the calculation was not available

$$t_{8/5} = \left[ \frac{AP_l}{vd} \right]^2 * (4\pi\lambda\rho c)^{-1} * \left[ \frac{1}{(773 - T_0)} - \frac{1}{(1073 - T_0)} \right], \quad (1)$$

where A = fraction of incident energy absorbed by the workpiece, Pl = laser power (W), v = welding speed (m/s), d = thickness of material (m), X = thermal conductivity

TABLE IV. Mechanical properties of filler material.

Filler material	R <sub>p0.2</sub> (N/mm <sup>2</sup> )	R <sub>m</sub> (N/mm <sup>2</sup> )	A <sub>5</sub> (%)	Toughness (J)
Union X 96	930	980	14	47 (-50 °C)
Esab OK 12.50	470	560	26	70 (-30 °C)

(W/m/K); 30 for carbon manganese steels, ρ = density (kg/m<sup>3</sup>); 7860 for carbon manganese steels, c = heat capacity (J/kg/K); 680 for carbon manganese steels, and T<sub>0</sub> = initial temperature (K).

The cooling rate of gas-metal-arc welded joints can also be calculated by using Eqs. (2) and (3). Equation (2) is for the 2-dimensional heat conduction and Eq. (3) for the 3-dimensional heat conduction

$$t_{8/5} = (4300 - 4, 3T_0) \times 10^5 \times \left( \frac{\eta \times E}{d} \right) \times \left\{ \left[ \frac{1}{(500 - T_0)^2} - \frac{1}{(800 - T_0)^2} \right] \right\} \times F_2, \quad (2)$$

$$t_{8/5} = (6700 - 5T_0) \times \eta \times E \times \left\{ \left[ \frac{1}{500 - T_0} \right] - \left[ \frac{1}{500 - T_0} \right] \right\} \times F_3, \quad (3)$$

where T<sub>0</sub> = 25 °C, η = thermal efficiency, E = laser energy (kJ/mm), d = plate thickness (mm), and F<sub>2/3</sub> = joint factor.

#### IV. DESTRUCTIVE TESTING

The study includes the destructive testing (DT) results made for welded Optim 960 QC steel. Most of the welds were

TABLE V. Groove geometries of weld specimens (M = machined, L = laser cut, S = sand blasted).

Reference	Edge prep. method	Joint prep. method	Bevel (deg)	Depth of root face (mm)
1	M	V	10, 20	
11	L	I		
4	M	I		
7	M	V	50	1
8	M	V	45	1
3,5	M	I		
6	M	S		
		I <sup>a</sup>	—	2
		V <sup>b</sup>	10, 40	2
9	M	Single-bevel <sup>c</sup>	20, 30	
		I	—	—

<sup>a</sup>Laser: PA, PC, PE (welding position).

<sup>b</sup>LHW: PA, PE; MAG: PA, PE.

<sup>c</sup>LHW: PC and MAG: PC.

TABLE VI. Welding energies/heat inputs and cooling rates  $t_{8/5}$  (L = laser, LHW = laser hybrid welding, GMA = gas-metal-arc welding).

Reference	Welding process	Heat input (kJ/mm)	$t_{8/5}$ (s)
1	LHW	0.31	1.7
	LHW	0.63	7.2
11	L CO <sub>2</sub>	0.26–0.38	1.3–3.04
	L Fiber	0.10–0.15	0.18–0.46
	LHW CO <sub>2</sub>	0.35–0.39	2.16–2.65
	LHW Fiber	0.28–0.30	1.63–1.74
4	L	0.11–2.1	1.4–4.1
7	GMA	0.35–0.56	2.2–5.7
10	GMA	0.45–0.62	2.2–2.9
3,5	L	0.2–0.95	0.36–7.85
	L	0.23	
6	LHW	0.30–0.31	
	GMA	0.45–0.6	
9	LHW CO <sub>2</sub>	0.35	
	LHW Disk	0.25	

also evaluated by using nondestructive (NDT) testing methods like the visual and radiographic examinations fulfilling weld quality level B or C. The destructive testing was performed for welds that fulfilled the quality criteria evident in NDT. Test results are collected from a time period of almost ten years and some of the test standards are out of date and have now been replaced. However, the test results are presented and evaluated according to the standards that were valid at the testing time. The destructive testing included the following examination: tensile strength test, hardness examination, bend test, and impact toughness test. Macroscopic and microscopic examinations are not included to the study but the importance of metallurgy is noted, if applicable.

### A. Transversal tensile strength test

The tensile testing was performed according to standards EN 895 and ISO 4136. The results of tensile strength tests for each welding process are depicted in Figs. 3–7. The values of elongations are left out of the study because the elongation value based on the standardized transversal tensile test does not provide a proper picture of ductility of material being an intrinsic property of material.<sup>3</sup> It is typical for Optim 960 QC steel that there is a softened zone in the

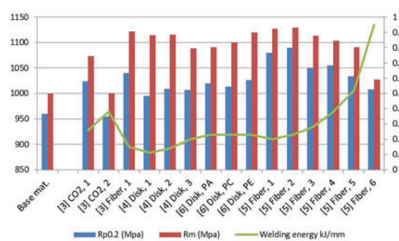
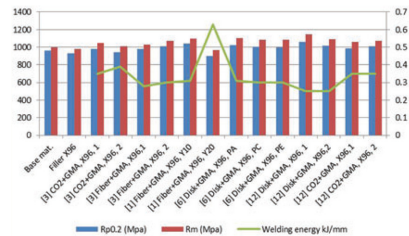
FIG. 3. Strength properties of laser-welded joints, [x] = reference, CO<sub>2</sub>, fiber, disk = type of laser resonator, 1/2 = number of the test, PA (flat position), PC (horizontal-vertical), PE (overhead) = welding position.

FIG. 4. Strength properties of laser hybrid welds, Filler: X96.

HAZ-area of the weld driving the place fracture point to the ICHAZ/SCHAZ-area (intercritical heat-affected zone/sub-critical-heat-affected zone). Figure 8 depicts a fractured tensile strength test specimen. The welding trials have also showed that in the welds joined with the undermatching filler material, the fracture point is on the welds, which are the weakest points of the welded sample. When the effect of welding process the strength levels is evaluated, it can be seen the tensile strength values of laser welds are stable and relatively even. The lowest yield strength value is 954 MPa and the highest 1090 MPa when the total number of tests was 15. The tests results of laser welds evidenced very clearly the effect of the welding energy to the strength properties: higher welding energy leads to lower strength and vice versa.<sup>5,6</sup> A similar effect can be seen in gas-metal-arc welding.<sup>6–8</sup> It is notable that special attention must also be paid for tack welding and its length. The use of overly long tack welds decrease tensile strength, but on the other hand it improves toughness.<sup>8</sup> The values collected from references are presented in the following charts (the values are named so that: first code = the reference number, second code = the welding process(es), third code = the type of filler material if used, fourth code = the welding position or the bevel angle if applicable, fifth code (or third code in some cases if other codes are missing) = number of test if similar specimens were tested).

The analysis of laser hybrid and gas-metal-arc welded specimens is more demanding because of the high number of variables. A total of 13 specimens were joined with laser hybrid welding and the matching filler material Union X96. The lowest measured value yield strength was 900 MPa and the highest value 1057 MPa. The yield strength of one specimen was below the nominal yield strength of 960 MPa set

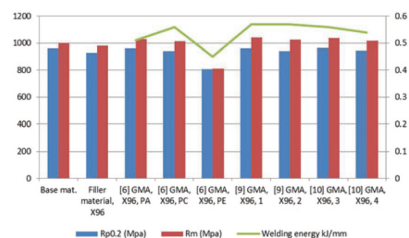


FIG. 5. Strength of gas-metal-arc welds, Filler: X96.

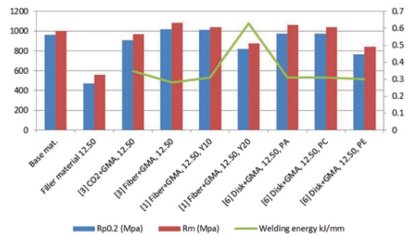


FIG. 6. Strength properties of laser hybrid welds, Filler: OK 12.50.

for the base material. With gas-metal-arc welding using matching filler material Union X96, a total of seven specimens were welded and the lowest yield strength value was 806 MPa and the highest being 964 MPa. The yield strength of three specimens was below 960 MPa. The joining of Optim 960 MPa steel with gas-metal-arc welding is quite a demanding process and special attention must be paid to the groove preparation, air gap, welding parameters, cooling rates, and interpass temperatures when multipass welding is applied. The welding instruction provided by steel manufacturers must be followed carefully.

When the undermatching filler material was used in the laser hybrid welding, the lowest yield strength value was 764 MPa and the highest 1020 MPa. The total number of tests was seven and four of the specimens passed the yield strength level of 960 MPa. With the gas-metal-arc welding, the total number of tests was six and none of them passed the yield strength value of 960 MPa. The lowest yield strength value was 720 MPa and the highest 810 MPa. The welding costs are higher if more alloyed filler materials are used, which are typically more expensive compared to a non-alloyed consumable like G3Si1-type filler material. This makes the use of lower cost filler material in laser hybrid welding tempting, which still guarantees a strength corresponding to the strength of the base material.

**B. Hardness test**

The hardness profiles are determined in the references according to standards EN 1043-1 or ISO 9015-1. A similar phenomenon was present in every hardness profiles: a softened area in the heat affected zones. This softening was depicted above in Fig. 2. The place, width, and min/max

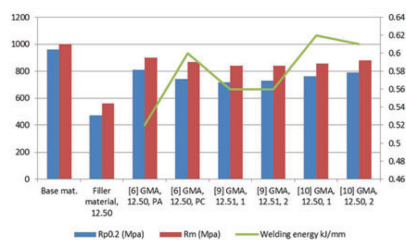


FIG. 7. Strength properties of gas-metal-arc welds, Filler: OK 12.50.

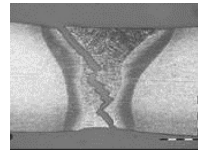


FIG. 8. Typical fracture form of laser hybrid welded specimen after tensile strength test (material Optim 960 QC, 6 mm) (Ref. 9).

values varied according to the welding process used, as well as the heat input, cooling rate, and filler material. With low heat input welding processes like laser and laser hybrid welding, the softening of hardness is placed at intercritical (ICHAZ) or subcritical HAZ (SCHAZ).<sup>1,11-14</sup> The hardness profiles of laser-welded joints and laser hybrid and gas-metal-arc welded joints welded with matching filler show a similar tendency: in the coarse grained HAZ (CGHAZ) area, hardness increases and in the intercritical-subcritical HAZ - area (IC/SCHAZ) the hardness decreases. The softened zone that is formed is relatively narrow, especially when laser or laser hybrid welding processes are used. However, it must be taken into account when designing the structure and the welding procedure. The minimum and maximum hardness values measured from the HAZ are presented in Table VII. Some of the hardness values are estimated from hardness profiles, causing some uncertainty in the values. Hardness has been measured mainly in two places: the surface and root side of the specimen, but in some cases is simply measured one line or just minimum values are given. The hardness values measured from the HAZ (=softened zone) have minor differences, regardless of which welding process or filler material is used. With the undermatching filler material, the weld area is of course much softer than the base material. In some cases there might be a limit for the maximum hardness value like 380 HV given in standards CR ISO 15608, nonheat treated, steel group 2 and ISO 15614-1 + A1 + A2, Specification and qualification of welding procedures for metallic materials, welding procedure test, Part 1: Arc and gas welding of steels and arc welding of nickel and nickel alloys. The hardness values above that hardness limit are marked in bold font in the table. The exceeding occurs in cases where the cooling rate has been very rapid, such as laser welding done with a fiber laser. However, the high hardness value has no or a minor effect on the other mechanical properties of the weld and with use of undermatching filler material hardening can be avoided. Another important point to note is the width of hardness profiles in the softened zones and the effect of the welding process; with a higher heat input, the softened zone gets wider, which has a negative effect on tensile strength but a positive effect on toughness.

**C. Bend test**

Bend tests were carried out according to standard EN 910. Lately, this standard has been replaced with the new ISO standard 5173. The diameter of the mandrel used in bend tests was 80mm. The amount of bend test results was relatively small (Table VIII). The reason for this might be

the test procedure itself; in order to get both the face and the root-side bend tests passed can be very demanding. Figure 9 illustrates what happens when the specimens joined by gas-metal-arc welding with undermatching and matching filler materials are bent.<sup>7</sup> In the specimen welded with the undermatching filler, all of the bent force is concentrated to the weld, which is the weakest point, which leads to breakage. In the specimen welded with the matching filler, the bending force is spread across a wider area, including to the base material forming a clear U-shaped bent sample. Figure 10 depicts a typical crack form and the location of the laser hybrid welded bend test specimen

#### D. Toughness (Charpy-V test)

The impact toughness of welded Optim 960 QC has been studied widely. Several testing temperatures have been

TABLE VII. Vickers hardness minimum and maximum values for face and root side.

Reference	Face		Root	
	Min	Max	Min	Max
Ref. 11, CO <sub>2</sub> , 1	280			
Ref. 11, CO <sub>2</sub> , 2	285			
Ref. 4, Disk, 1	280	<b>410</b>		
Ref. 4, Disk, 3	270	380		
Ref. 6, Disk, PA	268	365	264	360
Ref. 6, Disk, PC	271	369	268	366
Ref. 6, Disk, PE	280	369	274	373
Ref. 5, Fiber, 1	305	<b>410</b>	320	<b>410</b>
Ref. 5, Fiber, 6	300	<b>400</b>	300	<b>400</b>
Ref. 11, CO <sub>2</sub> + GMA, X96, 1	280			
Ref. 11, CO <sub>2</sub> + GMA, X96, 2	270			
Ref. 11, Fiber + GMA, X96, 1	295			
Ref. 11, FiberGMA, X96, 2	275			
Ref. 1, Fiber-GMA, X96, Y10	274	356	284	363
Ref. 1, Fiber + GMA, X96, Y20	270	356	254	329
Ref. 6, Disk + GMA, X96, PA	276	378	265	373
Ref. 6, Disk + GMA, X96, PC	276	365	267	358
Ref. 6, Disk + GMA, X96, PE	276	364	273	366
Ref. 9, Disk + GMA, X96, 1	251	<b>385</b>	265	<b>385</b>
Ref. 9, Disk + GMA, X96, 2	290	<b>385</b>	285	<b>390</b>
Ref. 9, CO <sub>2</sub> + GMA, X96, 1	280	370	275	362
Ref. 9, CO <sub>2</sub> + GMA, X96, 2	290	<b>384</b>	290	360
Ref. 11, CO <sub>2</sub> + GMA, 12.50	275			
Ref. 11, Fiber + GMA, 12.50	280			
Ref. 1, Fiber + GMA, 12.50, Y10	261	355	283	367
Ref. 1, Fiber + GMA, 12.50, Y20	254	317	276	331
Ref. 6, Disk + GMA, 12.50, PA	271	363	267	363
Ref. 6, Disk + GMA, 12.50, PC	270	354	261	337
Ref. 6, Disk + GMA, 12.50, PE	266	337	261	336
Ref. 6, GMA, X96, PA	272	350	270	350
Ref. 6, GMA, X96, PC	262	338	263	340
Ref. 6, GMA, X96, PE	264	343	254	334
Ref. 7, GMA, X96	240	340	250	
Ref. 6, GMA, 12.50, PA	266	338	264	310
Ref. 6, GMA, 12.50, PC	265	332	258	330
Ref. 7, GMA; 12.50	260	320	240	330
Ref. 8, GMA, 12.50, 1	270	350		
Ref. 8, GMA, 12.50, 2	250	340		

used in the references but only the results carried out at the temperature  $-40^{\circ}\text{C}$  are presented, and the notch was placed in the middle of the weld and on the fusion line. According to the welding procedure standards, the evaluation of toughness should focus on a line fusion area: which measured thus: fusion line  $+1-2\text{mm}$ . The references did not have the values of impact toughness widely available in that specified area, so the toughness values on the fusion line are observed instead (Table IX). The more alloyed the welding filler material is like Union X96, the harder and more brittle the non-tempered martensitic-bainitic microstructure in the weld metal and HAZ is. The impact toughness of the hard martensitic or bainitic microstructure is not as good as the impact toughness of the acicular ferrite which microstructure is formed when the low-alloyed and undermatching filler material, such as G3Si1 is used.<sup>1</sup> As mentioned earlier, the hardness of the weld increases when the cooling rate is short. It is demonstrated in the laser hybrid welding trials that with the use of non- or low-alloyed filler material, the best impact toughness (the highest values: 62J) was achieved and its use can be recommended instead of matching and high alloyed filler materials like Union X96, if the design of the structure permits this. The usability of the Charpy-V impact toughness test for the examinations of laser and laser hybrid welded joints of Optim 960 QC was impugned in some of the Refs. 1 and 5. If the notch is placed in the middle of the weld, the strain is concentrated on the narrow soft weld metal which results in a reduction in impact toughness. The following conclusions are possible to make based to the impact toughness results: optimizing of the groove geometry is essential, e.g., with  $40^{\circ}$  of groove angle and 0.63 kJ/mm welding energy, results 25J of the impact toughness in the fusion

TABLE VIII. Result of transversal bend test.

Reference	Face		Root	
	Passed	Fail	Passed	Fail
Ref. 6, Disk, PA	2	0	2	0
Ref. 6, Disk, PC	0	2	1	1
Ref. 6, Disk, PE	0	2	2	0
Ref. 6, Fiber + GMA, X96, PA	1	1	2	0
Ref. 6, Fiber + GMA, X96, PC	0	2	1	1
Ref. 6, Fiber + GMA, X96, PE	0	2	0	2
Ref. 9, Disk + GMA, X96	0	6	4	2
Ref. 9, CO <sub>2</sub> + GMA, X96	4	3	6	1
Ref. 6, Fiber + GMA, 12.50, PA	0	2	2	0
Ref. 6, Fiber + GMA, 12.50, PC	0	2	1	1
Ref. 6, Fiber + GMA, 12.50, PE	0	2	0	2
Ref. 6, GMA, X96, PA	0	2	1	1
Ref. 6, GMA, X96, PC	0	2	1	1
Ref. 6, GMA, X96, PE	0	2	0	2
Ref. 7, GMA, X96	2	0	1	1
Ref. 6, GMA, 12.50, PA	2	0	0	2
Ref. 6, GMA, 12.50, PC	1	1	1	1
Ref. 7, GMA, 12.51	2	0	0	2



FIG. 9. The bent profile of the weld, left: undermatching filler, right: matching filler material.

line. And when the groove angle is changed to the  $20^\circ$  and  $0.31 \text{ kJ/mm}$  of the welding energy is used, the impact toughness  $25 \text{ J}$  in the fusion line is achieved. With the use of undermatching filler material, it is possible to achieve very good impact toughness on the fusion line.

## V. DISCUSSION

The main welding studies made with Optim 960 QC were examined. The target was to estimate the overall welding quality of the welded joints and also estimate the suitability of modern welding processes like laser and laser hybrid welding to the welding of ultrahigh-strength steels. There were no big differences in the tensile strengths measured for the specimen joined by laser or laser hybrid welding. It is worth of noticing that, in terms of the strength of laser welds, the yield strength of the base material Optim 960 QC was passed with almost no exceptions. The number of bend test specimens was limited but as expected the passing of the test was difficult. The hardness values verified once more the existence of the softened zone in the HAZ-area of welded direct-quenched steel. The width of the zone varied according to the welding energy used. The values of impact results show some deviation but as mentioned, the positioning of the notch place in the specimen is demanding process and among others the traditional Charpy-V impact test is in not the best method for estimating the toughness of modern ultrahigh-strength steels. However, it is possible to achieve a high quality weld with laser processes and the modern low heat input arc sources, but the limits set by steel manufacturers for the cooling rate and the heat input should be observed.

The influence of the cooling time on the HAZ hardness and impact toughness transition temperature of a welded joint is well known. With a short cooling time, the maximum hardness in the HAZ-area reaches a high level due to intensive hardening of the area. However, a short cooling time usually results in good toughness properties. The use of high heat input leads to a long cooling time ( $>15 \text{ s}$ ) and the values of hardness and strength decreases. Some of the hardness values measured from the laser welded specimens were exceptionally

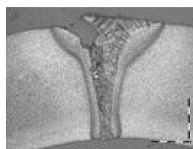


FIG. 10. Laser hybrid-welded bend test specimen after the test.

TABLE IX. Values of the impact toughness. Dimensions of the test specimen  $5 \times 10 \times 55 \text{ mm}$ .

Reference	W (J)	FL (J)	Welding energy (kJ/mm)
Ref. 6, Disk, PA	45	38	0.23
Ref. 6, Disk, PC	49	53	0.23
Ref. 6, Disk, PE	51	57	0.23
Ref. 5, Fiber, 1	17	28	0.20
Ref. 5, Fiber, 2	17	33	0.23
Ref. 5, Fiber, 3	15	32	0.28
Ref. 5, Fiber, 4	18	30	0.38
Ref. 5, Fiber, 5	26	23	0.52
Ref. 5, Fiber, 6	25	34	0.95
Ref. 1, Fiber-GMA, X96, Y10	22	45	0.31
Ref. 1, Fiber + GMA, X96, Y20	15	25	0.63
Ref. 6, Disk + GMA, X96, PA	40	23	0.31
Ref. 6, Disk + GMA, X96, PC	39	42	0.30
Ref. 6, Disk + GMA, X96, PE	40	46	0.30
Ref. 9, Disk + GMA, X96, 1	14	12	0.25
Ref. 9, Disk + GMA, X96, 2	37	27	0.25
Ref. 9, Disk + GMA, X96, 3	34	48	0.25
Ref. 9, Disk + GMA, X96, 4	30	27	0.25
Ref. 9, Disk + GMA, X96, 5	13 <sup>a</sup>	14	0.25
Ref. 9, Disk + GMA, X96, 6	25	24	0.25
Ref. 9, CO <sub>2</sub> + GMA, X96, 1	44	43	0.35
Ref. 9, CO <sub>2</sub> + GMA, X96, 2	32	49	0.35
Ref. 9, CO <sub>2</sub> + GMA, X96, 3	52	40	0.35
Ref. 9, CO <sub>2</sub> + GMA, X96, 4	46	40	0.35
Ref. 9, CO <sub>2</sub> + GMA, X96, 5	42	38	0.35
Ref. 1, Fiber + GMA, 12.50, Y10	67	62	0.31
Ref. 1, Fiber + GMA, 12.50, Y20	12 <sup>a</sup>	47	0.63
Ref. 6, Disk + GMA, 12.50, PA	50	46	0.31
Ref. 6, Disk + GMA, 12.50, PC	24	32	0.31
Ref. 6, Disk + GMA, 12.50, PE	31	26	0.30
Ref. 6, GMA, X96, PA	29	18	0.51
Ref. 6, GMA, X96, PC	30	15	0.56
Ref. 6, GMA, X96, PE	8 <sup>a</sup>	18	0.45
Ref. 7, GMA, X96	31	42	0.57
Ref. 8, GMA, X96, 4	26	21	0.54
Ref. 6, GMA, 12.50, PA	51	48	0.52
Ref. 6, GMA, 12.50, PC	48	51	0.60
Ref. 7, GMA, 12.50	42	54	0.56

<sup>a</sup>Weld defect reported.

high, surpassing the Vickers hardness limit of 380. However, this has no effect on the other mechanical properties of the welds because the changed area is very narrow.

If the cross-weld strength values of the joints are required to meet those specified for the base material,  $t_8/5$  should not exceed  $4 \text{ s}$ . In some of the references the exact values for the minimum and maximum cooling rate were given. To achieve and control these values precisely, the welding process must be automated and the welding power sources should have the possibility to use pulsing and control welding parameters precisely. With the undermatching filler material, relatively high values of yield strength were achieved. The yield strength of OK 12.50 filler material is  $470 \text{ MPa}$  and the highest yield strength value achieved with the use of this undermatching filler together with the laser hybrid process was  $1020 \text{ MPa}$ , and even the lowest values were relatively high  $764 \text{ MPa}$ .

## VI. CONCLUSIONS

This research showed that with the use of modern welding processes like the pulsed arc power source, laser and laser hybrid, it is possible to achieve good mechanical properties in the weld, even if the undermatching filler material is used. The relatively low carbon content and carbon equivalent value of Optim 960 QC steel lead to a low susceptibility of hardening in the weld. With optimized welding parameters, it is possible to achieve the matching joints, even with the undermatching filler material if the laser hybrid process is used.

## ACKNOWLEDGMENTS

The authors would like to thank Ruukki Metals Oy for the opportunity to publish this conference paper, and they appreciate the support given for preparing the conference paper.

<sup>1</sup>J. Siltanen, J. Kömi, R. Laitinen, M. Lehtinen, S. Tihinen, U. Jasnau, and A. Sumpf, "Laser-GMA hybrid welding of 960 MPa steels," in *Proceedings of International Congress on Applications of Lasers & Electro-Optics*, Anaheim (2011).

<sup>2</sup>F. F. Kalkhorani, J. Siltanen, and A. Salminen, "Autogenous high power fiber laser welding of Optim 960QC ultra-high-strength-steel," Master's thesis, Lappeenranta, Finland (2014).

<sup>3</sup>J. Kömi, "Direct—quenched structural steel," Design Manual (2013).

<sup>4</sup>R. Laitinen, J. Kömi, M. Keskitalo, and J. Mälikangas, "Improvement of the strength of welded joints in ultra-high-strength Optim 960 QC using autogenous Yb:YAG laser welding," in *Proceedings of Nolamp Conference*, Lappeenranta, Finland (2007).

<sup>5</sup>K. Farhang Farrokhi, J. Siltanen, and A. Salminen, "High power fiber laser of direct quenched ultra high strength steels—Evaluation of hardness, tensile strength, and toughness properties at subzero temperatures," article proposal, Lappeenranta, Finland, 2014.

<sup>6</sup>J. Siltanen and S. Tihinen, "Position welding of 960 MPA ultra-high-strength-steel," in *Proceedings of International Congress on Applications of Lasers & Electro-Optics*, Anaheim (2012).

<sup>7</sup>A. Balk, "Impact of balance filler material on the strength of welds on Ruukki's Optim 960 QC ultra-high-strength steel," Bachelor's thesis, Kemi, Finland (2011).

<sup>8</sup>R. Ylikangas, "The effect of tack welds on ultra-high-strength Optim 960 QC steel," Master's thesis, Lappeenranta, Finland (2009).

<sup>9</sup>A. Fellman, "Welding of Optim 960 QC steel," Internal Report No. RR038 of Ruukki (2008).

<sup>10</sup>J. Kömi, "Hot-rolled ultra-high-strength steels," *J. Mater.* **1**, 50–51 (2012), [http://www.vuorimiesyhdistys.fi/sites/default/files/materia/pdf/Materia%201-2012\\_0.pdf](http://www.vuorimiesyhdistys.fi/sites/default/files/materia/pdf/Materia%201-2012_0.pdf).

<sup>11</sup>P. Leiviskä, A. Fellman, R. Laitinen, and M. Vänskä, "Strength properties of laser and laser hybrid welds of low alloyed high strength steels," in *Proceedings of Nolamp Conference*, Lappeenranta, Finland (2007).

<sup>12</sup>J. Siltanen, "Utilising laser-GMA hybrid welding in industrial application," in *Proceedings of International Congress on Applications of Lasers & Electro-Optics*, Anaheim (2010).

<sup>13</sup>J. Siltanen, "Fiber laser GMA hybrid welding of telescopic booms," Ruukki Internal Research Report, Hämeenlinna, Finland (2010).

<sup>14</sup>R. Laitinen, M. Lehtinen, A. Fellman, and V. Kujanpää, "Influence of laser and CO<sub>2</sub>-laser-MAG hybrid welding on the strength and toughness of the weld HAX of ultra high strength steel Optim 960 QC," in *Proceedings of Nolamp Conference*, Luleå, Sweden (2005).

## Meet the Authors

Mr. Jukka Siltanen works as a project manager at Ruukki Metals Oy in Hämeenlinna, Finland. His duties include the welding coordination of Ruukki Metals steel service centre in Uusikaupunki, Finland. He received his M.Sc. degree from Lappeenranta University of Technology in the field of mechanical engineering.

Mr. Sakari Tihinen works as a product development engineer at Ruukki Metals Oy in Raahe, Finland.

Mr. Jukka Kömi works as a director of hot rolled product development at Ruukki Metals Oy in Raahe, Finland.

## **Publication III**

Siltanen, J., Skriko, T., and Björk, T.

**Effect of the welding process and filler material on the fatigue behaviour of 960 MPa structural steel at a butt joint configuration**

Reprinted with permission from  
*Journal of Laser Applications*  
Vol. 28 (2), pp. 1-9, 2016  
© 2016, Laser Institute of America





# EFFECT OF THE WELDING PROCESS AND FILLER MATERIAL ON THE FATIGUE BEHAVIOR OF 960 MPA STRUCTURAL STEEL AT A BUTT JOINT CONFIGURATION

Paper 1809

Jukka Siltanen<sup>1</sup>, Tuomas Skriko<sup>2</sup>

<sup>1</sup>SSAB Europe Oy, Harvialantie 420, FI-13300, Hämeenlinna, Finland

<sup>2</sup>Lappeenranta University of Technology, P.O.Box 20, FI-53851, Lappeenranta, Finland

## Abstract

Ultra-high-strength steels are being used more and more frequently in the engineering industry. Normally the welding of these steels is more demanding. The welding requires a controlled heating and cooling rate. In this study, the S-N curves were determined for the laser, the laser-GMA hybrid and the gas-metal-arc welded joints according to the recommendations of the International Institute of Welding (IIW) by using a constant amplitude loading and a stress ratio of  $R = 0.1$ . The frequency of loading varied between 4 and 10 Hz. The tested material was direct quenched steel with a yield strength of 960 MPa and a thickness of 6 mm. The total amount of tested specimens was 51. The fatigue test results proved to be close to the IIW recommendations and the differences between various welding processes were minor. Instead of welding process or filler material, the main factor influencing the fatigue behaviour was the geometry of the weld. Consequently, the proper welding parameters should be applied in every welding process in order to achieve a smooth joint geometry and thus, a high fatigue resistance.

## Introduction

The weldability of ultra-high-strength steels (UHSS) is a widely research area and the information related to the mechanical properties of welded joints has also been presented /1, 2, 3, 4, 5, 6, 8/. However, quite often the results have focused on the static examinations of the welded joints and the amount of the information for the dynamic properties is much more limited. There are several reasons for this, such as the fact that fatigue testing is more time consuming to do and the weld geometry as a dominant factor results in the fact that the welding method used for the joining of the specimens has only a limited effect on fatigue properties. It is assumed that the welding in those cases is done by fully mechanized welding, which eliminates the risk of weld defects that are more common in manual welding. It is estimated that up to 90% of all failures in welded structures are believed to be related to fatigue. The

importance of fatigue is even greater when using high strength steel, because the fatigue strength of a welded joint is the same, regardless of the steel grade /7/.

The long list of benefits when ultra-high-strength steels are utilized has been presented many times in previous studies /1, 2, 3, 4, 5/. Typical applications in the field of heavy engineering where the use of UHSS brings clear benefits are in the structures of load handling and transportation vehicles, and lifting equipment, such as a telescopic boom or crane /11/. The target is to decrease the weight of structures to save fuel or to make the lifting or transportation of higher payloads possible /6/. From the perspective of fatigue, the steel itself does not have a key role. The design, dimensioning, production, and quality are the factors that matter.

The processing of UHSS is more demanding to handle because of the more precise instructions and, for example, a relatively small processing window is set for the welding. In the former studies, the use of laser technology has been proved to produce high quality welds for fulfilling these requirements /2/. SSAB has focused on the manufacturing of special steels and one group is direct quenched steels (QC-steels) which are made by a combination of modern hot strip rolling and direct quenching process. This process differs from the manufacturing process of quenched and tempered steels (QL-steels). QL-steels are made in the conventional way: hot rolling, reheating, quenching and finally tempering (Figure 1).

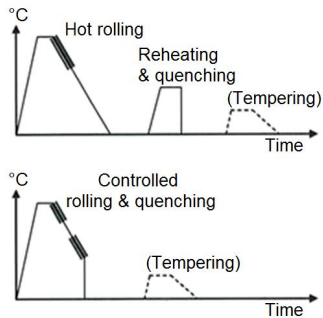


Figure 1. Schematic presentation of UHSS steel manufacturing routes. Temperature diagrams showing the differences between the conventional manufacturing route (upper) and direct quenching (lower) /1/.

The tested steel, S960 MC (former Ruukki brand name: Optim 960 QC, new SSAB brand name Strenx 960 MC) is standardized as a thermo-mechanically rolled steel according to standard EN 10149-1: 2013 /9/. QC-steels are not tempered and they have a lower level of alloying when compared to the conventional quenched and tempered steels with the same yield strengths. The effect of this phenomenon has an impact on the mechanical properties of the direct quenched S960 MC steel, e.g. it has a wider and deeper softened zone in the weld joint area than that of the quenched and tempered S960 QL steel due to the softening of the inter-critical/sub-critical heat-affected zones (ICHAZ/SCHAZ), and the tempered zone in the peak temperature range of 450–850 °C.

The maximum hardness value on the coarse-grained HAZ of the direct quenched S960 MC steel remains at a lower level than on the quenched and tempered QL steel. If the matching strength for joint is targeted, the use of laser and laser-hybrid welding can be recommended. Laser welding and laser-GMA hybrid welding as fully automated welding processes ensure the homogenous welding quality that normally have a positive effect on the fatigue properties of the welded joint. In this study, the thickness of test material was 6 mm, representing the typical thickness of strip steel used in the engineering industry and in welded structures, such as mobile lifting booms. The objective of the study was to investigate the behavior of the weld joint when dynamically loaded by varying the welding method and the filler material used for the welding.

## Experimental set-up

### Test plate and filler materials

The test materials comprised the steel S960 MC with a thickness of 6 mm. Joint preparations information like the groove shape, the groove angle and the depth of root face are presented in Table 1. In all cases, the groove preparation was done by machining. The size of the welded test sample was 600 x 1000 mm. Filler material used for laser-GMA hybrid welding and GMA welding were a matching Union X96 (EN ISO 16834-A-G Mn4Ni2.5CrMo) and an under-matching Esab OK Autrod 12.51 (EN ISO 14341-A-G3Si1). The diameter of the filler wires was a constant being 1.0 mm. The chemical composition and the mechanical properties both for the S960 MC and the filler materials are presented in Tables 2 and 3.

Table 1. Groove preparations of test plates.

Weld method	Groove geometry
GMAW	Single V40° 2 mm root face
LHW	Single V10° 2 mm root face
Laser	Square prep, 0°

Table 2. Chemical composition (wt. %) of the base material (max. specified) and filler wires (typical).

	S960 MC	Union X96	OK 12.51
t [mm]	6	Ø 1	Ø 1
C	0.11	0.1	0.1
Si	0.25	0.81	0.85
Mn	1.2	1.94	1.5
P+S	0.03	0.026	
Ti	0.07	0.058	
B			
Cr		0.52	
Cu		0.06	
Mo		0.53	
Ni		2.28	
V		0.002	
CEV <sub>max</sub>	0.52	0.79	≈ 0.33

Table 3. Mechanical properties of the base metals and filler wires.

Base material/ filler material	t [mm]	R <sub>p0.2</sub> [MPa]	R <sub>m</sub> [MPa]	A [%]	Toughness [J, -50°C]
S960 MC	6	1035	1139	11	55
Union X96	Ø 1	930	980	14	47
OK 12.51	Ø 1	470	560	26	70 (-30°C)

## Welding of test pieces

The laser and laser-GMA hybrid welding experiments were carried out by using a 12 kW disc laser of Trumpf and the laser was equipped with a 400  $\mu\text{m}$  feeding fibre and the welding optics had a 200 mm collimator and a 300 mm of focal length was used. The diameter of the focused laser beam on the surface was 0.6 mm. The arc power source used for laser hybrid and gas-metal-arc welding was a Fronius Time 5000 Digital and welding was realized by using a pulling arc torch with a following laser beam, in other words the arc was leading (Figure 2). The welding was performed by one pass for welding processes and the welding position was a flat position (PA/1G) in all cases.

The main welding parameters are presented in Tables 4, 5 and 6. The cooling rate  $t_{8/5}$  was calculated for the welding processes by using Equations 1 and 2. The value of thermal efficiency for gas-metal arc welding is 0.8 and for laser and laser GMA-hybrid welding 0.75.

Equation 1 is for the 2-dimensional heat conduction and equation 2 is for the 3-dimensional heat conduction.

$$t_{8/5} = (4300 - 4,3T_0) \times 10^5 \times \left(\frac{2 \times E}{d}\right)^2 \times \left\{ \left[ \frac{1}{(500 - T_0)^2} \right] - \left[ \frac{1}{(800 - T_0)^2} \right] \right\} \times F_2 \quad \text{Eq. 1}$$

$$t_{8/5} = (6700 - 5T_0) \times \eta \times E \times \left\{ \left[ \frac{1}{(500 - T_0)} \right] - \left[ \frac{1}{(800 - T_0)} \right] \right\} \times F_3 \quad \text{Eq. 2}$$

where,

$T_0=25^\circ\text{C}$ ,  $\eta$ =thermal efficiency,  $E$ =laser energy (kJ/mm),  $d$ =plate thickness (mm) and  $F_{2/3}$ =joint factor.

If the matching strength is targeted to have in a butt joint, the used welding energy should not exceed the value of 0.4 kJ/mm. In the case of under-matching butt joint, the used welding energy can be even higher but less than 0.8 kJ/mm. This leads to the limitations at cooling rates. If the matching strength is targeted, a cooling time  $t_{8/5}$  should be  $\leq 4$  seconds and in the case of under-matching joint, the time can be longer at max. 15 seconds. The welding energies were following mainly the recommendations except in the case of GMA welding where the limits given were exceeded. In despite of these overruns in the values, the yield strength of the base material was achieved in the welded joints when the matching Union X96 filler material was used.

The shielding gas used in the laser-GMA hybrid welding and the GMA welding experiments was a gas mixture with a content of 92% argon and 8%  $\text{CO}_2$  with a trade name Mison 8 by Linde AGA and the gas flow rate used was 25 l/min. The movement of the welding test was performed with a Kuka KR 30 HA-C industrial

robot. A clamping device was used to fasten the test pieces and those were tack welded by a continuous laser welding before the actual welding with the varying welding processes. The laser power used for the tack welding was 1.5 kW and the approximately length of the tacks were 20 mm.



Figure 2. The GMA welding torch and laser optics. The arrow shows the welding direction.

Table 4. The main welding parameters of GMA welding.

Parameter	Value	
	OK 12.51	Union X96
Filler material	OK 12.51	Union X96
Current [A]	255	256
Voltage [V]	27	26
Welding speed [m/min]	0.8	0.8
Wire feed rate [m/min]	14	14
Torch angle [°]	5	5
Welding energy [kJ/mm]	0,52	0,51
Cooling time $t_{8/5}$ [s]	4,9	4,7

Table 5. The main welding parameters of laser-GMA hybrid welding.

Parameter	Value	
	OK 12.51	Union X96
Filler material	OK 12.51	Union X96
Laser power [kW]	6.5	6.5
Current [A]	140	139
Voltage [V]	20	21
Welding speed [m/min]	1.8	1.8
Wire feed rate [m/min]	7.5	7.5
Focus pos. [mm]	0	0
Torch angle [°]	20	20
Process distance [mm]	2.5	2.5
Welding energy [kJ/mm]	0.31	0.31
Cooling time $t_{8/5}$ [s]	1.5	1.5

Table 6. The main welding parameters of laser welding.

Parameter	Value
Laser power [kW]	4.5
Focus pos. [mm]	0 = surface
Welding speed [m/min]	1.2
Welding energy [kJ/mm]	0.23
Cooling time $t_{8/5}$ [s]	0.8

### Testing of welded joints

The mechanical properties of the welded joints from statistic point of view were widely introduced in 2012 at ICALEO conference by Siltanen et al. where the values for the transversal tensile strengths, the transversal bend tests and the hardness profiles were presented /5/. In addition, the cross-sections of the joints as well as the microstructures of the welds were depicted and discussed. The welded specimens used for the fatigue examinations are identical with the ones that were used for the preparation of ICALEO paper in 2012, several equal specimens were welded at that time. The manufacturing procedures and welding quality was wanted to represent the normal industry quality having for example some variations in the joint geometry and local weld quality. Thus, the cross-sections presented in this paper are from the welded specimens reserved for the fatigue examinations because the actual local weld geometry was needed to know in order to see its influence on the fatigue strength of the welded joint.

### Static testing

The results of the static destructive testing are presented in this paper as in a shortened version because the main focus is in the fatigue properties of welded joints. The results presented in this chapter are collected from the previous conference paper of Siltanen et al. /5/. Before the destructive testing, the welded specimens reserved for the static testing were inspected by radiographic inspection. The weld defects found from those specimens are presented in Table 7.

Table 7. The result of radiographic examination.

Process	Filler material	Imperfection type
GMAW	OK 12.51	porosity, lack of fusion/penetration
GMAW	Union X96	porosity
LHW	OK 12.51	porosity, undercut, excess penetration, incompletely filled groove
LHW	Union X96	porosity lack of penetration, incompletely filled groove
Laser		undercut

### Cross-sections of the welded joints

The cross-sections photos presented are taken from the test specimens reserved for the fatigue testing (Figures 3-7). There are two samples and photos (a/b) taken from each welded joint to show the possible difference in the weld geometry of the joint.

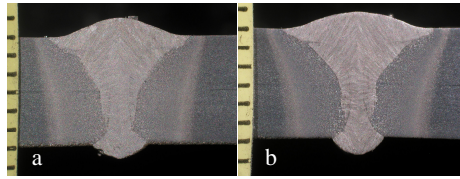


Figure 3. GMA welded joint, filler material: OK 12.51.

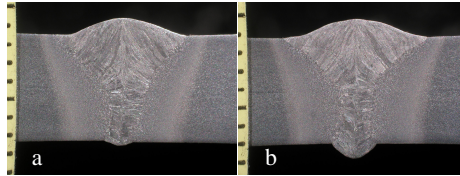


Figure 4. GMA welded joint, filler material: Union X96.

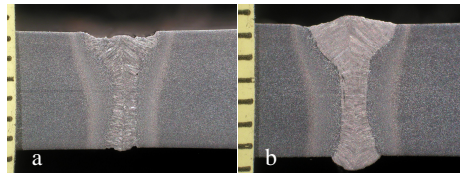


Figure 5. Laser-GMA hybrid welded joint, filler material: OK 12.51.

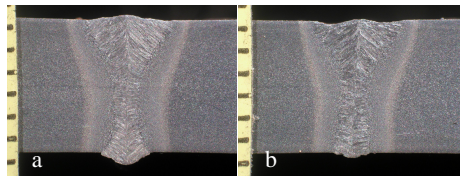


Figure 6. Laser-GMA hybrid welded joint, filler material: Union X96.

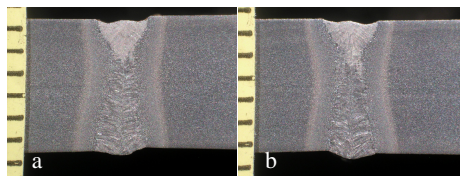


Figure 7. Laser welded joint.

### Transversal tensile strength

The results of tensile strength are presented in Figure 8. The weld reinforcement was removed from tests specimens before testing. It was presented by Siltanen et al. in previous ICALEO conference paper that main breaking point of the samples was located on ICHAZ (Inter-Critical Heat-Affected Zone) /5/. In that paper the welding was performed by using several welding

positions. In addition, the results showed that with the use of under-matching filler material, such as OK 12.51, the place of fracture is on the weld which is logical because that is the weakest part of the joint. The yield strength (1035 MPa) of the base material was not reached in any of the transversal tensile strength tests. In laser welding, almost matching yield strength with the base material was achieved. The values of elongation in every welding test combination remained in low level being a far away from the elongation value of the base material (11%).

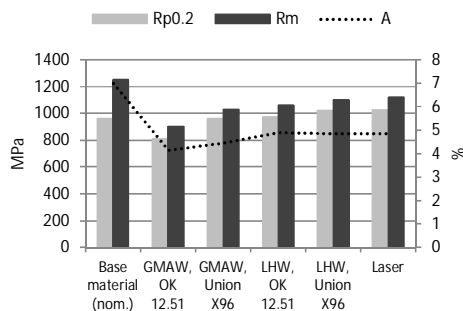


Figure 8. Transversal tensile strength test result.

### Bend test

The results of bend test are shown in Table 8. The only sample that passed both the face and root side testing was a laser welded joint. This problem to pass the standardised bend test with the direct quenched steels joined by a laser or laser hybrid welding methods is discussed earlier [6]. The narrow softened region in HAZ has no capacity to take care of all forming during bending which leads to the cracking on that area.

Table 8. Bend test results (f = face side, r = root side).

Process	Filler material	Bend side	Result
GMAW	OK 12.51	f	passed
		f	passed
		r	fracture 29 mm
GMAW	Union X96	r	fracture 2 mm
		f	fractured
		f	fractured
LHW	OK 12.51	r	passed
		r	fracture 5 mm
		f	fracture 11 mm
LHW	Union X96	f	fractured
		r	passed
		r	passed
Laser		f	fracture 6 mm
		f	passed
		r	passed
Laser		r	passed
		f	passed
		r	passed

### Hardness

The hardness (HV5) values of welded samples were measured (Figures 9-11). The first measuring line (Line 1) was located 1 mm below the surface of the plate and the second line was 1 mm above the bottom surface of the plate. Hardness values are presented in a graphic form in Figures 9-11. The softened region located at the fusion line and heat-affected zone is visible in all the welds. However, in the laser-GMA hybrid and the laser-welded joints, the softened zone is very narrow. This also affects the formability and the elongation which are evident when performing the bend test and the transversal tensile strength test. The figure showing the hardness of laser weld has different amount of measuring points compared to GMA or laser-GMA hybrid welds hardness curves and thus, showing the laser weld wider in the hardness curve than it actually was.

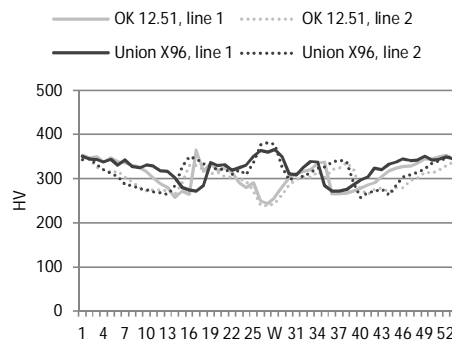


Figure 9. The hardness profiles of GMA welds, filler materials: OK 12.51 and Union X96.

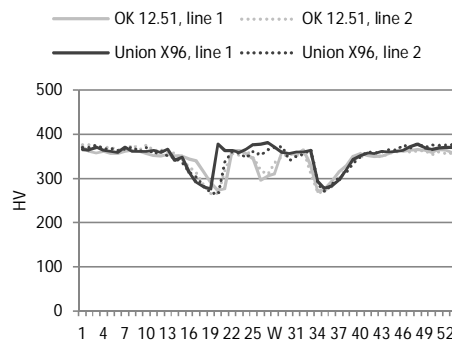


Figure 10. The hardness profiles of laser-GMA hybrid welds, filler materials: OK 12.51 and Union X96.

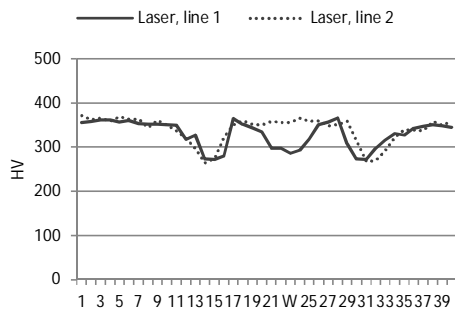


Figure 11. The hardness profiles of laser weld.

The use of under-matching filler material (OK 12.51) created both in the GMA and laser GMA-hybrid welding a softened area also on the weld region (Figures 9 and 10). In the GMA welding and when matching filler material was used, a harder point compared to base material was formed on the weld area (Figure 9). In the case of laser welding there is a softened point in the weld area as well. The cross sections of the laser welds are showing some difference in the microstructure on the top and bottom side of the weld. The top side seems to have a fine-grained microstructure if compared to bottom part where the microstructure has some coarse-graining which leads to a higher value of hardness in lower part of the welds. It is also possible that the measuring line 1 was placed on the line where has happened the phase formation that leads to a local softening.

#### Impact test (Charpy V)

Impact toughness is a measure of how much energy a material can absorb during fracture and a material impact testing is used to find this value of energy. In this study, the Charpy V-Notch (CVN) testing method was used. The place of notch on the impact toughness specimen varied depending of the welding method. For GMA and laser-GMA hybrid welding, the notch was placed at the weld (W), the fusion line (FL), the fusion line + 1 mm (FL + 1mm) and the fusion line + 2mm (FL + 2mm), and for the laser welding the notch was placed at the weld and the fusion line. The dimensions of the impact test piece were 5x10x55 mm. The guaranteed base material (BM) value for the steel S960 MC is 34 J/cm<sup>2</sup> at a temperature -40 °C. The results of impact strengths are presented in Figure 12.

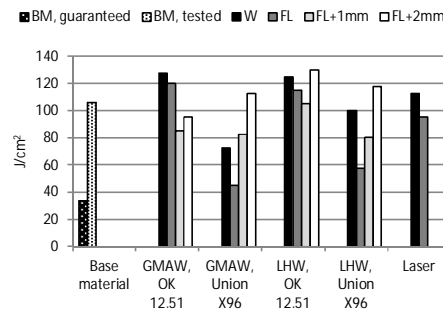


Figure 12. The Charpy-V impact energies [J/cm<sup>2</sup>] of the welded joints (T= -40 °C).

The toughness of the fusion line remains low with matching filler material Union X96 both in GMA and laser-GMA hybrid welded joints. With the under-matching filler material OK 12.51 values were higher than the toughness of the base material. The toughness of the laser weld on the fusion line remained slightly below the toughness of the base material. However, all values of toughness on the welded joints were above the guaranteed toughness of the base material which is usually set as a minimum limit for the acceptance of impact toughness test.

#### Fatigue testing

The fatigue tests were carried out in the Laboratory of Steel Structures at Lappeenranta University of Technology. A servo-hydraulic test rig (Figure 13) was used and during each experiment, the load and displacement values were monitored from the test rig and strain gauges were used to define the structural stresses of each butt joint.

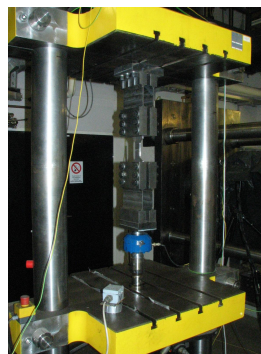


Figure 13. Fatigue test rig and set-up at Lappeenranta University of Technology.

The fatigue properties of the butt welded joints for S960 MC were defined using a constant amplitude cyclic loading where the stress ratio was kept constant ( $R = 0.1$ ) but the applied stress range ( $\Delta\sigma$ ) was varied between different test specimens. According to the recommendations of the International Institute of Welding (IIW) /10/, mean and characteristic S-N curves were determined for different welding processes. The test results are presented in Figures 14-21 where the used stress ranges ( $\Delta\sigma$  [MPa]) of every test specimens are plotted as a function of fatigue life ( $N$  [cycles]). Figure 14 covers all tested specimens and Figures 15 and 16 includes all the fatigue test results of GMA and laser-GMA hybrid welded joints, respectively. In Figures 17-20, the results of GMA and laser-GMA hybrid welded joints are separated more precisely in terms of used filler metal (under-matching or matching) and finally, the fatigue test results of laser welded joints are shown in Figure 21. In addition, the mean and characteristic fatigue resistance (FAT) values of every variations are presented in Table 9.

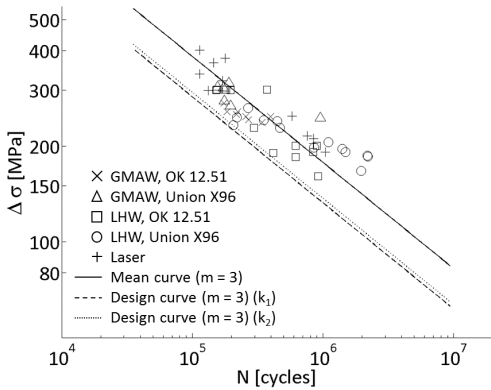


Figure 14. S-N curves for all welded joints.

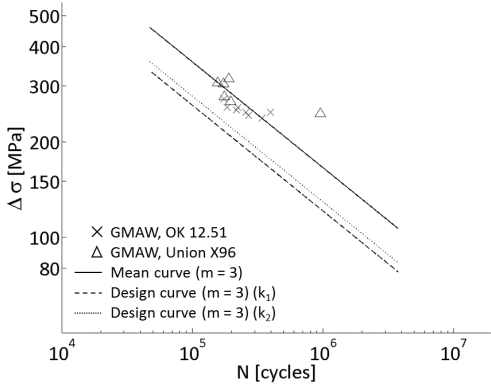


Figure 15. S-N curves for all GMA welded joints.

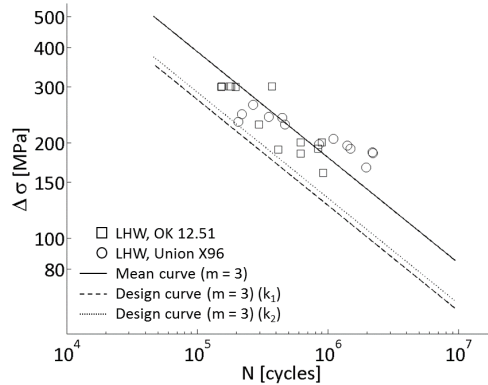


Figure 16. S-N curves for all laser-GMA hybrid welded joints.

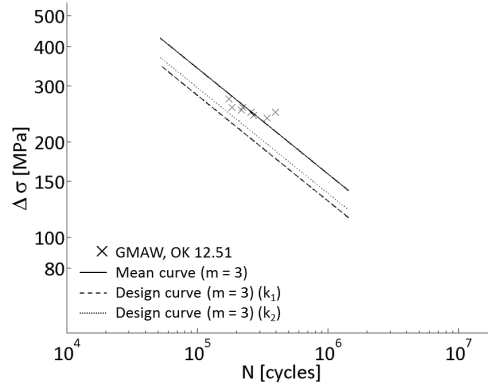


Figure 17. S-N curves for GMA welded joints, filler material: OK 12.51.

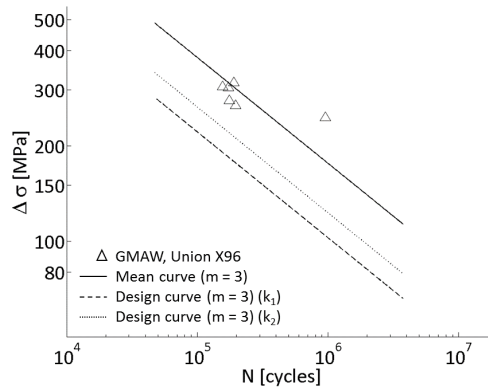


Figure 18. S-N curves for GMA welded joints, filler material: Union X96.



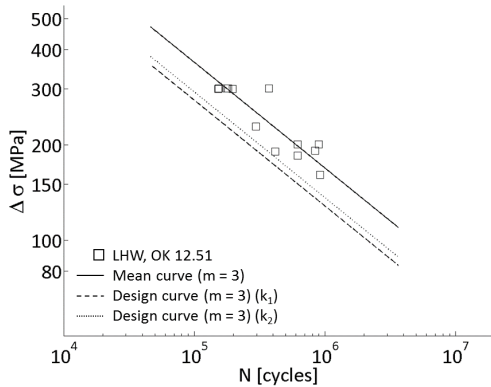


Figure 19. S-N curves for laser-GMA hybrid welded joints, filler material: OK 12.51.

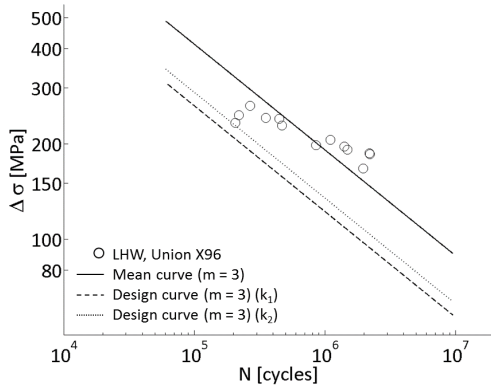


Figure 20. S-N curves for laser-GMA hybrid welded joints, filler material: Union X96.

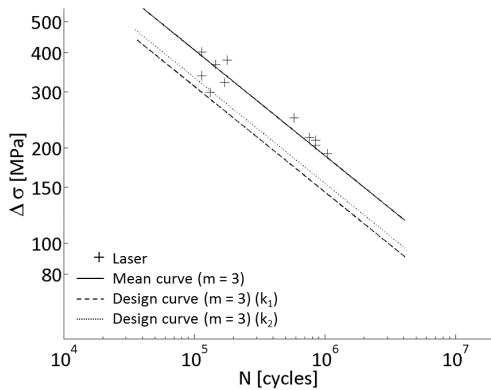


Figure 21. S-N curves for laser welded joints.

Table 9. Mean and characteristic FAT values of different welding processes and variations.

FAT value	All	GMAW	LHW	Laser
FAT <sub>mean</sub> (m = 3)	140	131	142	149
FAT <sub>char</sub> (m = 3) (k <sub>1</sub> )	105	95	100	115
FAT <sub>char</sub> (m = 3) (k <sub>2</sub> )	108	102	106	122

FAT value	GMAW OK 12.51	GMAW Union X96	LHW OK 12.51	LHW Union X96
FAT <sub>mean</sub> (m = 3)	125	139	133	151
FAT <sub>char</sub> (m = 3) (k <sub>1</sub> )	103	81	101	96
FAT <sub>char</sub> (m = 3) (k <sub>2</sub> )	109	97	108	106

## Discussion

The paper is mainly focused to the fatigue properties of welded ultra-high-strength steel S960 MC. However, the static properties were tested as well. The yield strength (1035 MPa) of the base material was not reached in any of the transversal tensile strength tests no matter what welding method or filler material was utilized. The values of elongation remained also in low level if compared to the elongation value of the base material (11%). The bend test was hard to pass by the laser-GMA hybrid and the GMA welding but with the continuous laser welding both the face and root side bending tests were passed. The hardness of the joints was measured as well showing the universal softening in the HAZ area of the welds. The toughness of the welds was tested and in the fusion line, the best results were achieved by using under-matching filler material. It should be noted when welding ultra-high-strength steel, there should be enough know-how in design and manufacturing to optimize the properties of steel structure. In some cases, the high tensile or yield strength are targeted and in the other applications, the high toughness at relative low temperatures is needed.

The fatigue test results indicated minor differences between the characteristic FAT values of different welding processes and all results are close to IIW recommendations where the fatigue resistance against structural hot spot stress for butt welded joints is stated to be 100 MPa/10/. However, the effects of weld cross-section, heat input used in the welding or possible weld defects formed to joints were not possible to specify explicitly. Nevertheless, some light conclusions can be made and in some cases, the factors mentioned earlier might be present directly or indirectly. Laser welded joints showed slightly better FAT values and less deviation compared to GMA and laser-GMA hybrid welds but for example the S-N curves of GMA welded joints are not fully reliable due to few data points and thus, more test results are needed from high-cycle

fatigue region in order to define more precise S-N curves for both under-matching and matching filler materials. In addition, the finite element analyses, the assessment by effective notch stress (ENS) method and the consideration of residual stresses should be performed to all fatigue test specimens and results in the future.

The fixed slope  $m = 3$  seems to be suitable for most S-N curves but when using matching filler material in GMA and laser-GMA hybrid welding, a less steep slope might fit better (Figures 18 and 20). However, this will need more experimental tests and analyses to prove it and based on the results from this study, the filler material does not have a straight effect on the fatigue strength of butt welded joints. The geometrical factors, such as weld toe radius, angular distortion and misalignment, have the major influence on fatigue resistance. In the future, the authors will publish more results where the effects of these above mentioned weld geometrical factors are studied thoroughly and critically.

Fatigue cracks initiated mostly from the root side of welded joints apart from the laser-GMA hybrid welds with under-matching filler material where the fatigue crack propagated almost invariably from weld face side. The reason for this behaviour can be explained by the differences in global and local geometries of welded joints. In GMA welds, the angular distortion was detrimental to weld face side but the local geometry in root side was more abrupt compared to face side so the root side became critical. In laser welds, the incomplete fill was usual in weld face side but an excessive penetration occurred on the root side. In addition, the angular distortion was detrimental to root side as opposed to other welding processes so the root side fatigue fracture was expected. In laser-GMA hybrid welds, the filler material does not necessarily explain why the welds with under-matching filler material failed from the face side and the welds with matching filler material failed from the root side. The angular distortion was detrimental to face side in both variations. In laser-GMA hybrid welds with under-matching filler material, undercuts or incomplete fill were also common on face side so it was more sensitive to fatigue. Whereas in laser-GMA hybrid welds with matching filler material, the face side was filled better and in some cases the weld toe geometry was very smooth which can lead to root side fatigue, despite the angular distortion.

### Conclusions

Based on the experimental procedures, measurements, fatigue tests and analyses, the conclusions are as follow:

1. The fatigue resistance of GMA, laser-GMA hybrid and laser welded S960 MC butt joints are close to

the recommendations of International Institute of Welding.

2. Laser welded butt joints proved to have a slightly higher characteristic FAT value compared to GMA and laser-GMA hybrid welded butt joints.
3. In GMA and laser-GMA hybrid welding processes, the used filler material (under-matching or matching) did not have a direct effect on the attainable fatigue strength.
4. The used welding methods and parameters should be optimized for every process and variation (GMA, laser-GMA hybrid and laser welding) in order to have a high quality and smooth joint geometry and thus, a high fatigue resistance.

### Acknowledgements

The authors would like to acknowledge SSAB Europe Oy and FIMECC/TEKES for the opportunity to publish this conference paper, and also appreciate the support given by several specialists for preparing the conference paper.

### References

#### Conference Paper

- [1] Siltanen J., Kömi J., Laitinen R., Lehtinen M., Tihinen S., Jasna U., Sumpf A. (2011), Laser-GMA Hybrid Welding of 960 MPa Steels, Proceedings of International Congress on Applications of Lasers & Electro-Optics, Anaheim, USA
- [2] Siltanen J. (2010), Utilising Laser-GMA Hybrid Welding in Industrial Application, Proceedings of International Congress on Applications of Lasers & Electro-Optics, Anaheim, USA
- [3] Leiviskä P., Fellman A., Laitinen, Vänskä M. (2007), Strength Properties of Laser and Laser Hybrid Welds of Low Alloyed High Strength Steels, Proceedings of Nolamp Conference, Lappeenranta, Finland
- [4] Laitinen R., Kömi J., Keskitalo M., Mäkikangas J. (2007), Improvement of the Strength of Welded Joints in Ultra-High-Strength Optim 960 QC Using Autogenous Yb:YAG Laser Welding, Proceedings of Nolamp Conference, Lappeenranta, Finland
- [5] Siltanen J., Tihinen S. (2012), Position Welding of 960 MPA Ultra-High-Strength-Steel, Proceedings of International Congress on Applications of Lasers & Electro-Optics, Anaheim, USA
- [6] Siltanen J., Kesti V., Ruoppa R. (2014), Longitudinal bendability of laser welded special steels

in a butt joint configuration, Proceedings of International Congress on Applications of Lasers & Electro-Optics, Anaheim, USA

#### Diploma works

[7] Narimani H. (2010), Fatigue strength of laser-hybrid welded high strength steel, Luleå University of Technology, Sweden

#### Reports

[8] Siltanen J. (2010), Fiber laser GMA hybrid welding of telescopic booms, Ruukki Internal Research Report, Hämeenlinna, Finland

[9] European standard EN 10149-1 (2013), Hot rolled flat products made of high yield strength steels for cold forming. Part 1: General technical delivery conditions

[10] Hobbacher A. (2013), Recommendations for fatigue design of welded joints and components. IIW document XIII-2460-13/XV-1440-13 ex XIII-2151r4-07/XV-1254r4-07

#### Web pages

[11] SSAB steel data (2015), Strenx, [www.strenx.com](http://www.strenx.com)

#### **Meet the Authors**

Mr. Jukka Siltanen works as a specialist at SSAB Europe Oy in Hämeenlinna, Finland. His duties include the welding coordination of SSAB steel service centre in Uusikaupunki, Finland. He received his M.Sc. degree from Lappeenranta University of Technology in the field of mechanical engineering

Mr. Tuomas Skriko works as a doctoral student at Lappeenranta University of Technology in Lappeenranta, Finland. His studies are focused on the welding quality and fatigue strength of ultra-high-strength steel joints, components and structures in terms of both the design and manufacturing aspects.

## **Publication IV**

Farrokhi, F., Siltanen, J., and Salminen, A.

**Fiber laser welding of direct-quenched ultrahigh strength steels: Evaluation of hardness, tensile strength, and toughness properties at subzero temperatures**

Reprinted with permission from  
*Journal of Manufacturing Science and Engineering*  
Vol. 137, pp. 061012-1-10, 2015  
© 2015, ASME



**Farhang Farrokhi<sup>1</sup>**

Department of Mechanical and  
Manufacturing Engineering,  
Aalborg University,  
Aalborg East DK-9220, Denmark  
e-mail: ffk@m-tech.aau.dk

**Jukka Siltanen**

SSAB Europe Oy.,  
Hämeenlinna FI-13300, Finland  
e-mail: jukka.siltanen@ruukki.com

**Antti Salminen**

Professor  
Department of Mechanical Engineering,  
Lappeenranta University of Technology,  
Lappeenranta FI-53851, Finland  
e-mail: antti.salminen@lut.fi

# Fiber Laser Welding of Direct-Quenched Ultrahigh Strength Steels: Evaluation of Hardness, Tensile Strength, and Toughness Properties at Subzero Temperatures

*The recently developed direct-quenched ultrahigh strength steels (UHSS) possess an appropriate combination of high tensile strength and toughness properties at subzero temperatures down to  $-80^{\circ}\text{C}$ , while simultaneously having low carbon contents, which is beneficial for weldability. In this study, butt joints of Optim 960 QC direct-quenched UHSS with a thickness of 8 mm were welded with a 10 kW fiber laser to evaluate the characteristics of the joints within the range of low to high heat inputs possible for this welding process. The mechanical properties of the joints were studied by subjecting the specimens to a number of destructive tests, namely, hardness and tensile testing, as well as impact toughness testing at temperatures of  $-40^{\circ}\text{C}$  and  $-60^{\circ}\text{C}$ . It was found that high quality butt joints with superior tensile strength and good impact toughness properties at  $-40^{\circ}\text{C}$  could be obtained. However, having a high level of all these properties in the joint narrows the process parameters' window, and the heat input needs to be strictly controlled. [DOI: 10.1115/1.4030177]*

**Keywords:** laser welding, fiber laser, ultrahigh strength, impact toughness, arctic materials

## 1 Introduction

UHSSs possess superior tensile strength properties with which it is possible to create lightweight structures. In addition, the continuing oil and gas developments in the Arctic region require steel structures that have high strength, good weldability, and very high toughness properties at temperatures of  $-40^{\circ}\text{C}$  and below [1]. The recently developed direct-quenched UHSSs provide a higher strength for a given chemistry, which means lower carbon equivalents and better weldability at high strength levels. Moreover, due to the combination of thermomechanical rolling and low carbon content, a good combination of strength and toughness is reachable even at  $-80^{\circ}\text{C}$  temperature [2], which distinguishes the direct-quenched UHSSs from the quenched and tempered (QT) UHSSs with the same levels of strength. Therefore, the question that is raised is whether it is possible to take advantage of the excellent strength and toughness properties of direct-quenched UHSSs for structures in harsh and cold environments. More studies are required to evaluate the mechanical properties of UHSS welded joints that have been made by modern welding processes.

Laser welding is a fast and precise technology that takes advantage of keyhole welding and thus benefits from high productivity, deep penetration, and low heat input. The recently developed fiber lasers have multiple advantages, such as high power levels with small beam divergence (high beam quality), flexible beam delivery, high efficiency, and compact size when compared with other laser sources [3–6]. The high power density and high quality beam of fiber lasers may lead to welds with a higher

penetration for a given welding speed [3,7]. However, some critical challenges control the stability of the process and the weld quality when welding at high power levels [8]. For example, it has been anticipated that the high power density beam repeatedly generates metal vapor above the keyhole [9]. The metal vapor can decrease the beam intensity reaching the workpiece surface by absorption, scattering, and refraction mechanisms [10]. More systematic investigations on the applications of high power fiber laser welding are still lacking, and welding procedures must be developed further to overcome the process challenges.

Concerning UHSSs, the difficulties such as a high susceptibility to cracking, heat affected zone (HAZ) softening, and a lack of sufficient toughness and ductility in the joint appear regardless of the welding process and exact alloy used. In general, during laser welding, high thermal strain and stress occur in the weld zone [11] due to the high cooling rates of the welding process. This fact, together with the high hardenability of the steel itself, makes UHSSs to become highly susceptible to cracking at the joints. Particularly, it should be kept in mind that UHSS weld metals mainly consist of untempered martensitic microstructures, which are known to be the most susceptible microstructures for cold cracking [12]. Also, one of the most primary challenges in welding UHSSs is the HAZ softening phenomenon. The presence of a reduced-hardness layer in the HAZ does not only deteriorate the strength of the joint and the entire structure [13–15], but it can also affect the fatigue strength and formability of the welded joint [16–18]. It has been reported in the literature that this very complex phenomenon is affected by the martensite content in the microstructure [14], the chemical composition of the steel [19,20], and the heat input of the welding process [14,15,19].

Recent studies about the fiber laser welding of DP980 thin sheets reveal that the low heat input of high speed fiber laser welding can greatly reduce the formation of harmful soft zones by

<sup>1</sup>Corresponding author.

Contributed by the Manufacturing Engineering Division of ASME for publication in the JOURNAL OF MANUFACTURING SCIENCE AND ENGINEERING. Manuscript received November 16, 2014; final manuscript received March 19, 2015; published online September 9, 2015. Assoc. Editor: Hongqiang Chen.

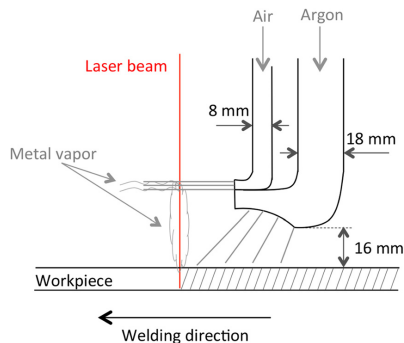


**Fig. 1 Shielding gas and lower cross jet tubes arrangement used in order to protect the weld bead and push the laser induced metal vapor plume away from the laser beam**

narrowing them down significantly, such that almost-matching joints with 96% joint efficiency can be obtained [21,22]. According to the same study [21], the HAZ and fusion zone (FZ) obtained by fiber laser welding are narrower than those formed by welding with alternative lasers, such as CO<sub>2</sub> lasers [23], Nd:YAG lasers [24], and diode lasers [17]. However, this might be achieved at the price of excessive hardness (above 450 HV) in the weld metal, which could potentially raise the risk of cracking. Although, direct-quenched UHSSs that have the same tensile strength are not as prone to these difficulties, due to the low carbon content and carbon equivalent of the base metal [25–27]. In addition, investigations on the effect of welding heat input on the toughness properties of welds in UHSSs show that higher toughness values are obtained with lower heat inputs [28–30]. For example, in one study it was concluded that, in order to assure the impact toughness of the HAZ, the weld heat input must be equal to or less than 2 kJ/mm [29], which is attainable with the low heat input welding methods such as laser and hybrid laser welding. Therefore, the high accuracy and very low heat inputs of fiber laser welding technology are expected to have a positive influence on the mechanical properties of welded joints in this heat-sensitive generation of steels.

A number of investigations on the welding of dual phase (DP) and QT steels with tensile strengths of above 900 MPa have been reported in the literature, including both arc welding and conventional laser welding methods. However, little is known about the characteristics of recently developed direct-quenched UHSS joints welded by fiber lasers, especially when it comes to Arctic applications and operations in cold environments. This experimental report investigates the characteristics of 8 mm butt joints welded by high power fiber lasers. On the basis of the comparative studies mentioned above [21,22], fiber laser has been chosen for the experiments in order to take advantage of its high cooling rates and the fact that it yields the narrowest possible welds. Hardness testing, tensile testing, and impact toughness testing at –40 °C and –60 °C were the destructive tests that were used to assess the mechanical properties of direct-quenched UHSS butt joints and their suitability for cold environment applications. Because of the sensitivity of Optim 960 QC steel to the heat input, the line energy

(laser power/welding speed) of the experiments was also taken into consideration in the results as a critical contributor. However, it should be noted that, due to the limitation of equipment and the length of this article, a number of important factors such as keyhole behavior and molten metal flow in the welding pool have not been considered in this study, even though they are actually crucial concerns in laser welding.

## 2 Experimental Method

The laser used in this study was an IPG Photonics YLS-10,000 Ytterbium fiber laser system providing a 10 kW continuous wave laser beam with a wavelength of 1070 nm. The laser was guided through an optical fiber of 200 μm in diameters to a Precitec YW50 welding head. The welding head was mounted on a gantry, such that the inclination angle of the laser beam was 90 deg to the surface of the workpiece (vertical or flat welding position) and the focal point positioned 1 mm below the workpiece's top surface. The beam parameter product was 11.5 mm mrad after optical fiber. Collimation and focal length of the optic system were 150 mm and 300 mm, respectively, creating a focal point diameter of about 620 μm, and a Rayleigh length of 8.5 mm. A protection air cross jet was located below the focusing lens between the lens and workpiece, to protect the optics from the process' spatters. Another air cross jet with a flow rate of 12 l/min was provided by a copper tube with an outer diameter of 8 mm to avoid the laser induced metal vapor plumes being raised too high. As it has been depicted in Fig. 1, an 18 mm outer diameter shielding gas tube was coupled with the latter cross jet tube to deliver pure argon gas with a flow rate of 24 l/min, in order to avoid oxidization of the weld. A distance of 16 mm was used between the lowest part of the shielding gas tube and the workpiece, such that an appropriate argon flow was delivered on the weld bead while the cross jet air flow was at its minimum possible distance to the keyhole, in order to suppress the plumes more efficiently.

The steel used in this study was direct-quenched Optim 960 QC with a thickness of 8 mm. Tables 1 and 2 contain information regarding the chemical composition and mechanical properties of the steel, respectively. According to the laser welding procedure test, the EN ISO 15614-11 standard [31], steel plates were laser cut to 150 mm × 300 mm pieces and then prepared for butt joints to form a 300 mm × 300 mm blank after welding. Since the information in Table 2 is based on longitudinal specimens, all the plates were cut so that the welds were perpendicular to the rolling direction of the plates. After cutting, the edges were grit blasted with aluminum oxide abrasives to remove the oxide layers of the laser cut edges and also to obtain a more homogeneous surface roughness throughout the entire length of the edge. The average surface roughness ( $R_a$ ) of laser cut and grit blasted edges was measured at about 7.5 μm [32]. Finally, all the edges and surfaces of the specimens were cleaned with oil-free acetone to remove any grease or other dirt prior to welding. Since the air gap tends to open during welding, the plates must be pressed together firmly. Therefore, the plates were clamped tightly and tack welded in both the start and end locations, to avoid the joint opening during welding. Prior to welding, air gaps were measured throughout the length of the edge to make sure that there was no gap larger than 0.05 mm. Figure 2 depicts a schematic of joint dimensions as well as the prepared edges' properties.

After radiography examinations, the surface and macrosection of all specimens were checked for the imperfections that are visually detectable according to the guidance on quality levels of laser

**Table 1 Chemical composition and carbon equivalent value (wt.%) of Optim 960 QC [2]**

Steel	C max.	Si max.	Mn max.	P max.	S max.	Ti max.	CEV <sup>a</sup> typical
Optim 960 QC	0.11	0.25	1.20	0.02	0.01	0.07	0.52

<sup>a</sup>CEV = C + (Mn/6) + ((Cr + Mo + V)/5) + ((Cu + Ni)/15)

**Table 2 Minimum specified tensile and impact properties of Optim 960 QC [2]**

Steel	$R_{0.2}$ (MPa)	$R_m$ (MPa)	$A_5$ (%)	Charpy V, longitudinal, $-40^\circ\text{C}$ J/cm <sup>2</sup>
Optim 960 QC	960	1000	7	34

welds in the EN ISO 13919-1 standard [33]. One macrosection was studied randomly for each weld. In the case of root concavity and incomplete filled groove imperfections, the top and root concavity ( $d_1$  and  $d_2$ ), and the average width of weld ( $w_f$ ) were measured, as per Fig. 3.

Microhardness tests were performed as per hardness testing of laser welded narrow joints in the ISO 22826 standard [34] using a Struers Durascan 70 hardness tester. Before testing, the specimens were polished and etched with Nital ( $\text{HNO}_3 + \text{alcohol}$ ). Vickers hardness measurement profiles were obtained using a 500 g load, so that the hardness indentation points were spaced 0.2 mm and 0.4 mm from each other in the critical area and base metal, respectively. Figure 4 schematically depicts the indentation rows located

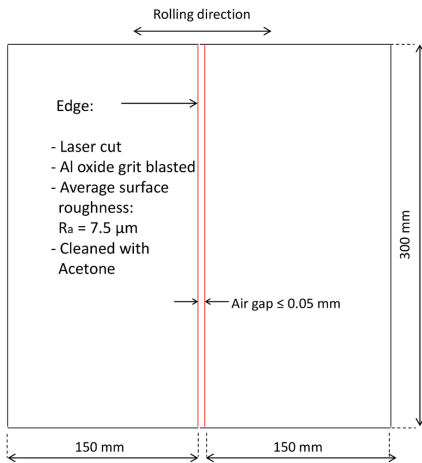


**Fig. 2 Summary of joint configuration and the prepared edges' properties. Size of specimens was chosen according to laser welding procedure test EN ISO 15614-11.**

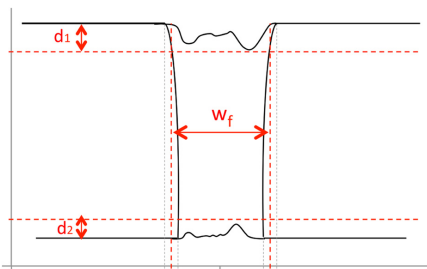


**Fig. 3 Top and root concavity ( $d_1$  and  $d_2$ ) and average width of weld ( $w_f$ ) measured for each specimen**

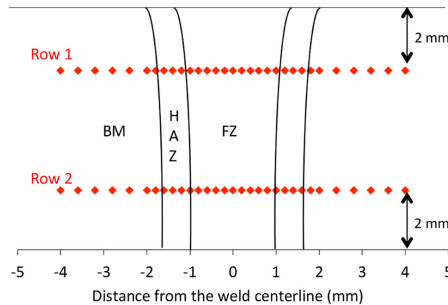


**Fig. 4 Schematic preview of rows of indentation for hardness measurement according to hardness testing of laser welded joints ISO 22826. BM: base metal.**

in lines at a distance of 2 mm on the top and bottom surfaces of the plate. It should be noted that one specimen was cut out randomly from each weld for hardness measurements. The results were evaluated according to the permitted maximum hardness value as per the EN ISO 15614-1 (2012) standard [35] for QT steels (3rd group), defined by CEN ISO/TR 15608 (2013) standard classification [36]. It should be noted that, according to the steel manufacturer (Ruukki's) classification [37], Optim 960 QC could be classified as a QT steel in the third group (3.2 subgroup) of the latter standard.

In order to evaluate the hardness properties of the welds, four key values: average base metal hardness ( $h_b$ ), average FZ hardness ( $h_f$ ), average minimum hardness in HAZ ( $h_m$ ), as well as the average width of soft zone in HAZ ( $w_s$ ) were determined using an arithmetic mean method. These parameters have been depicted schematically in Fig. 5, which shows a typical average of two rows of hardness measurements of laser welded Optim 960 QC butt joints. It should be noted that  $w_s$  is the average of minimum hardness of the soft zone in both sides of the weld ( $w_1$  and  $w_2$ ).

In addition, since these groups of materials are very sensitive to the heat input imposed by any thermal process, softening may already occur during the laser cutting process [38]. If the width of the soft zone exceeds the width of weld (FZ), as may occur in the case of high speed laser welds, this could affect the final hardness distribution of the welded joint. Therefore, two pieces of laser cut Optim 960 QC with a thickness of 8 mm were also prepared for the hardness measurement. Vickers hardness measurement indentations were located within a distance of 0.4 mm to 1.2 mm from the cut edges.

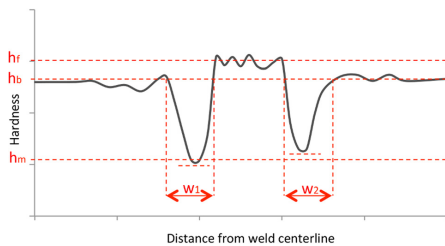


**Fig. 5 Measurement of the average base metal hardness ( $h_b$ ), average FZ hardness ( $h_f$ ), average minimum hardness in HAZ ( $h_m$ ), and the average width of the soft zone of both sides ( $w_1$  and  $w_2$ ) from a schematic average hardness profile**



Two transverse tensile specimens were machined from each weld according to the EN ISO 4136 standard [39] for the evaluation of tensile properties of the joints. The test specimens were taken transversely from the welded joint such that, after machining the weld, the mid-longitudinal axis remained in the middle of the parallel length of the test specimen. Due to the limitation of the testing equipment's load capacity (max. 200 kN), the width of the parallel length was considered to be 20 mm.

A Charpy V impact test was performed at  $-40^{\circ}\text{C}$  and  $-60^{\circ}\text{C}$  as per the EN ISO 148-1 standard [40] to evaluate the toughness properties of the joints at subzero temperatures. A pendulum impact testing machine with maximum impact energy of 150 J was used. Subsize specimens of 55 mm in length and 10 mm and 7.5 mm widths were used for the test. Testing was aimed at evaluating the lowest possible fracture energy of the joints at the two susceptible areas of the FZ and the coarse-grained heat affected zone (CGHAZ). Since laser welds are so narrow that it is almost impossible to locate the notch exactly in the desired area, 45 deg V-notches were machined at the weld centerline and the HAZ in the vicinity of the fusion line (FL). After machining, the etched samples were marked accurately. For the samples notched at the FL, notches were located within 0.5–1 mm distance from the weld centerline, depending on the weld's width. Testing was separately repeated three times for each notch location and test temperature, for a total of 72 samples. In addition, six samples were provided to evaluate the impact toughness of the base metal at each temperature. Based on 27 J toughness requirements for full-thickness specimens, the test results were assessed based on 22 J requirements with a correction factor of 5/6 for  $7.5 \times 10$  mm subsize specimens. Additionally, the measured values were considered as reliable only when the lowest value was not smaller than 70% of the mean value. It should be noted that, although testing at  $-40^{\circ}\text{C}$  was accurate enough as the samples were chilled down to  $-45^{\circ}\text{C}$  prior to testing, in the case of testing at  $-60^{\circ}\text{C}$ , a slight deviation in the actual test temperature was caused, due to the maximum capacity of the chilling equipment of  $-60^{\circ}\text{C}$ .

The experimental parameters were considered to be limited between the maximum welding speed for full penetration welds and the minimum welding speed before HAZ softening leads to a loss of tensile strength in the joint. Based on a number of preliminary experiments with different laser power and welding speed values, it was concluded that the power-speed window is very narrow for fully penetrated and visually acceptable joints, limiting the choice of line energy. The maximum welding speed for full penetration was below 3 m/min and laser power was limited to 9 kW and above. Welding with lower power levels leads to weld discontinuities mainly such as a lack of penetration, root/top underfill, spatter, undercut, and process instabilities. Therefore, with a constant value of 9.5 kW for laser power, four high speed welds were considered within the range of 1.5–2.8 m/min to study the characteristics of the welds with low line energy levels. In addition, two other welds were selected with welding speeds of 1 m/min and below, in order to investigate the effect of moderate and high line energy levels, respectively. Cooling time ( $t_{8/5}$ ) was calculated for variable welding speeds based on the following equation [41] with the assumption of a two-dimensional heat flow and a joint factor ( $F$ ) equal to 1:

$$t_{8/5} = (4300 - 4.3T_0) \cdot 10^5 \cdot \left(\frac{kE^2}{d^2}\right) \cdot \left[\left(\frac{1}{500 - T_0}\right)^2 - \left(\frac{1}{800 - T_0}\right)^2\right] \cdot F$$

where  $k$  is the laser absorption,  $E$  is the laser line energy (kJ/mm),  $T_0$  is the initial temperature ( $^{\circ}\text{C}$ ), and  $d$  is the plate thickness (mm). Laser absorption was considered to be 70%, based on the results of a study about the estimation of the cooling time of disk laser welding of Optim 960 QC steel [26]. In addition, the results

of an experimental study on the fiber laser welding of carbon steel butt joints reveal a correlation between laser energy absorption and edge surface roughness in the joint [42]. As was previously mentioned, the  $R_a$  of the laser cut and grit blasted edges in the current study was measured about  $7.5 \mu\text{m}$ , which corresponds to a 73–74% energy absorption, according to the latter study [42] (Fig. 6). This can approximately estimate and confirm the 70% absorption efficiency considered for the current experiments. It should be noted that, based on studies on the fiber laser welding of stainless steel [43], it has been found that laser absorption decreases significantly as the welding speed increases from 1 to 15 m/min. However, in this study, except for the slowest weld, the variation of absorption would not be that significant within the welding speed range of 1–3 m/min.

The summary of the main test parameters is presented in Table 3, which shows the weld numbers sorted by their line energy and cooling time. Focal point position was determined based on preliminary welding experiments, such that the maximum penetration is obtained at the joint.

### 3 Results and Discussion

**3.1 Visual Properties.** Before visual evaluation, all the welds were exposed to X-ray radiation to evaluate the welds' quality through the thickness. No porosity was observed in the welds except in weld #804 which contained two small pores at its end part. None of the welds contained cracks either visually or identified by X-ray tests. However, more nondestructive tests such as ultrasonic test is needed to assess the welds' quality in terms of crack defects.

First, as was expected, the width of weld increased from 1 to about 2.5 mm as the welding speed decreased, since with the higher line energy more material is melted in the joint. This is illustrated clearly in Fig. 7 in which the measured weld width values and their corresponding line energy are shown. However, at higher line energy levels, the increasing rate in the welds' widths seems to be close to zero, as the welds' widths remained almost constant in welds #805 and #806.

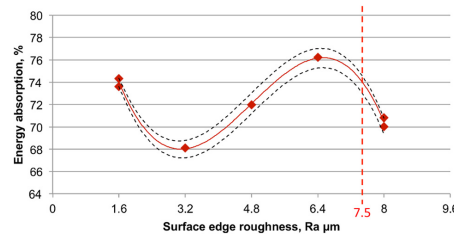


Fig. 6 Energy absorption at different roughness levels [42]. The vertical dashed line denotes the average edge surface roughness for the current study.

Table 3 Main parameters of the experiments and their corresponding line energy and estimated cooling time, calculated with the equation above. Laser power was measured at the workpiece.

	#801	#802	#803	#804	#805	#806
Laser power (kW)	9.5	9.5	9.5	9.5	9.5	9.5
Welding speed (m/min)	2.8	2.5	2.0	1.5	1.1	0.6
Line energy (kJ/mm)	0.20	0.23	0.28	0.38	0.52	0.95
Line energy level <sup>a</sup>	Low	Low	Low	Low	Moderate	High
Cooling time $t_{8/5}$ (s)	0.36	0.45	0.70	1.26	2.34	7.85

<sup>a</sup>Relative scale within the experimental range.

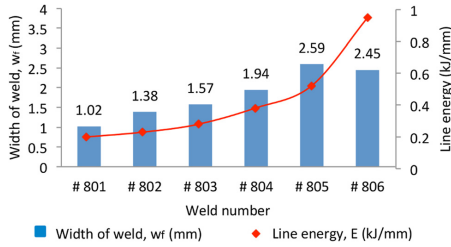


Fig. 7 The width of weld ( $w_f$ ) increased as the energy input increased

Generally, all the welds were almost uniform and fully penetrated throughout the weld bead without major defects. Spattering occurred mainly in high speed weld #801 (see Fig. 8). However, as can be seen in Fig. 8, a significant root concavity appeared in the joints welded with high line energy. Figure 9 compares the measured concavity in both top and root sides of the macrospecimen of joints. Based on these measurements, despite the presence of a minor concavity in the low line energy welds, all the welds except #806 were classified as B quality level, according to EN ISO 13919-1.

However, these measurements mentioned for concavity can be considered for the overall concavity of the welds as well, only if the welds are thoroughly uniform. Despite the acceptable uniformity of the welds, some local instabilities leading to more severe concavities were observed in low speed welds. These instabilities can be ascribed to the laser induced metal vapor plumes that occasionally appeared during the process. So, even though the cross jet and shielding gas tubes were carefully designed to avoid this phenomenon and it was significantly suppressed during the experiments, it was not completely prevented. According to the visual inspection results, it can be said that the degree of instability increased at the root side as the welding speed decreased. The high line energy weld #806 was most unstable on the root side, while the welds with moderate and low line energies were considerably more stable (see Fig. 10). However, except for the high line energy weld #806, the local concavities did not exceed the specified critical limit of the standard.

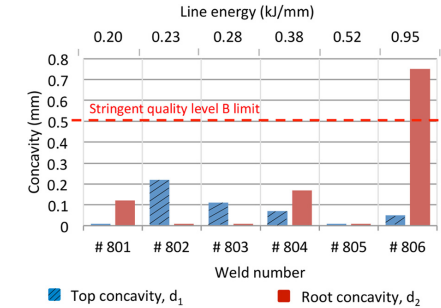


Fig. 9 Measured concavity in the top and root sides of the macrospecimen of welds. Apart from weld #806, all values were below the specified critical limit for quality level B according to EN ISO 13919-1.

**3.2 Hardness Properties.** The hardness profiles of the top side and root side of the fastest and slowest welds (#801 and #806) have been shown in Fig. 11. It is clear from the figure that the welds with the lowest line energy (solid curve) were narrower in both FZ and HAZ compared to the welds with the highest line energy (dashed curve). As was expected, softening occurred in all welds due to the heat input of the process, which may lead to microstructural changes in the HAZ.

It should be noted that, when speaking about HAZ softening, this phenomenon is characterized by two measures of: (i) the width of soft zone and (ii) the minimum hardness of the soft zone. However, numerical finite element simulations and experimental tests show that they are both responsible for the decrease in the overall strength and ductility of the welded joints [44]. The width and the average maximum hardness drop in the soft zone of the HAZ of all experiments have been illustrated in Fig. 12. As can be seen, they both increased as the line energy increased. The width of the soft zone was very narrow, as a result of high speed fiber laser welding process. The average values varied from about 0.5 to 0.8 mm for the high speed low line energy welds. Even in the case of the highest line energy weld, the soft zone width did not

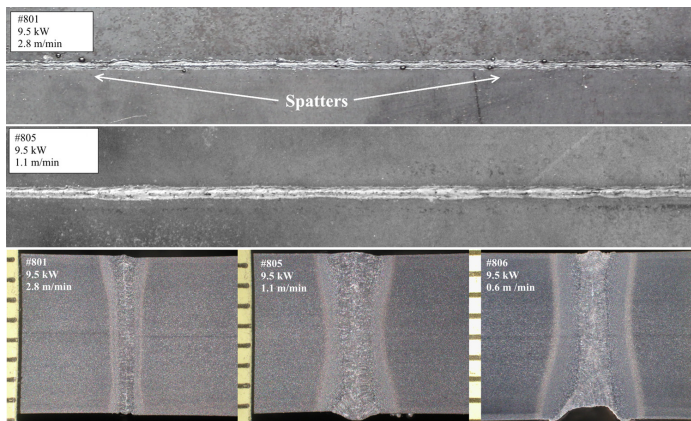


Fig. 8 Visual comparison of top side (half-length) and cross section of the welds welded with highest and lowest welding speeds

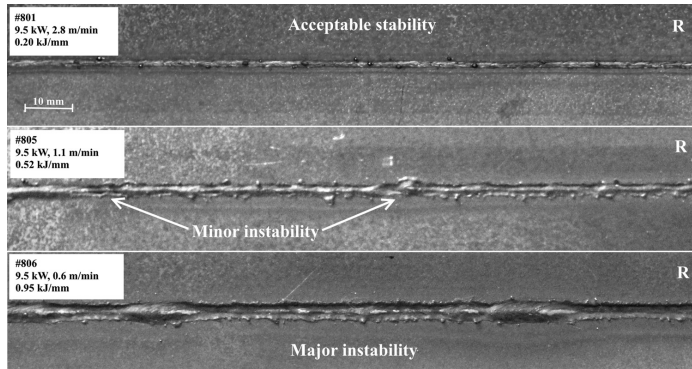


Fig. 10 Comparison of root sides of the stable fast welds with the unstable slow welds (half-length images)

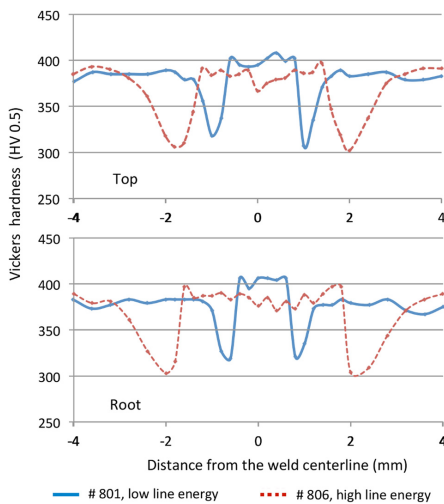


Fig. 11 Hardness profile of top side (upper) and root side (lower) of the welds with lowest and highest line energy

exceed from 1.1 mm. However, the hardness drop was significant, even when the soft zone was so narrow, and the values varied within only 15 HV from about 65 to 80 HV.

As was mentioned earlier, the hardness of the FZ can be problematic in laser welded UHSSs, as the highest cooling rate occurs in this region, and therefore it may lead to excessive hardness and microstructures susceptible to cracking at that location. Figure 13 shows the average hardness of the FZ for each weld of the current study, compared with the average base metal hardness and the critical hardness level. The upper dashed line in the figure represents the permitted maximum hardness value according to the EN ISO 15614-1 standard. As is shown in Fig. 13, despite the very high cooling rates of the fiber laser welding process, hardness in the FZ was increased only slightly with respect to the hardness of the base metal. Thanks to the low carbon content of the steel, the average hardness in the FZ was significantly lower than the

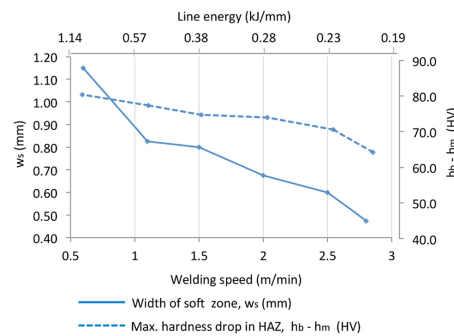


Fig. 12 Soft zone width ( $w_s$ ) and the degree of softening ( $h_b - h_m$ ) decreased as the welding speed increased

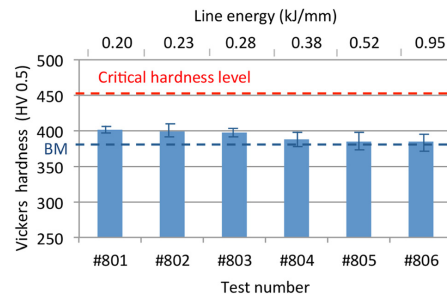
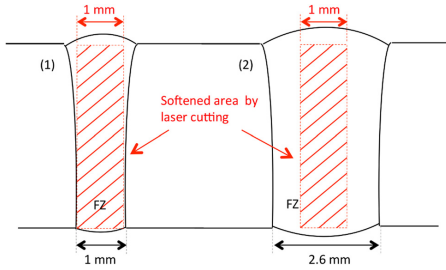


Fig. 13 Average hardness in the FZ ( $h_f$ ) with a standard deviation varying between 5 and 10 HV

critical hardness value and even barely reached 400 HV in the case of the lowest line energy welds. However, a similar study on the high speed fiber laser welding of butt joints showed that the average FZ hardness even reaches the 450 HV critical hardness level in DP steels with the same strength level (DP980) [21].



**Fig. 14** Laser cut softened area overlapping with the narrowest weld (1) and the widest weld (2). Width of laser cut softened area was narrower than the welds.

Furthermore, results of hardness measurements of the laser cut samples revealed that laser cut Optim 960 QC is softened within 0.5 mm of the vicinity of the cut edge, due to the heat of the thermal cutting process that is imposed. This means that, if the width of the FZ in a butt joint is narrower than 1 mm, the remaining softened area on the edge may affect the HAZs properties during welding. However, according to the visual measurement of the weld width and the hardness profiles, one can conclude that the softening induced by laser cutting did not affect the hardness properties of the laser welds, as the width of the lowest line energy weld was not narrower than 1 mm. Figure 14 depicts a schematic of the softened area overlapping with the FZ in the case of the narrowest and widest welds, assuming that the joint did not open during welding (this would be seen in the overall weld quality in the form of missing material).

**3.3 Tensile Properties.** The tensile strength of all welds was higher than the guaranteed minimum tensile strength of the base metal specified by the steel manufacturer (see Table 4). Even the specimen welded with the slowest speed (#806), in which the width of the soft zone reached 1.15 mm, withstood tensile stresses up to above 1000 MPa. This means that the degree of softening was not severe enough to cause a loss of strength, even in the case of the highest line energy weld with an estimated cooling time of 7.8 s. Based on the tensile strength results, it can be said that tensile strength decreased from 1130 to 1030 MPa as the welding speed decreased. However, according to the linear prediction trend line of the average tensile strength values (Fig. 15) and variation trends of the degree of softening (Fig. 12), one could argue that cooling times longer than 11.7 s or line energies higher than 1.16 kJ/mm could lead to a loss of strength in the joint, as a consequence of excessive softening in the HAZ. Aside from the degree of softening influences, it has been well accepted in the literature that a smoother weld bead profile shows better strength under tension compared to other weld bead geometries, as the stress concentrations are increased with concavity or convexity shapes at the weld zone [45]. Therefore, the severe root concavity in the

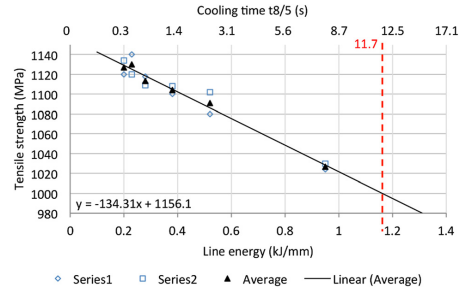


**Fig. 15** Tensile test results. Linear trend line of the average values predicts the maximum line energy and cooling time before the loss of strength occurs in the joints.

weld #806 has also a considerable contribution in the decreasing of tensile strength in the joint.

Surprisingly, the tensile ductility of the joints was influenced by concavity rather than the softening induced by the process' line energy. According to Table 4, except for the weld with high line energy, almost all the joints reached around 7% elongation, which is the minimum elongation specified for the base metal. However, the high line energy welds had a lower elongation down to 62% of the base metal. This could be due to the fact that the severe root concavity of the weld led to the concentration of plastic deformation in the weld, which caused a reduction in the overall specimen elongation and the premature failure of the weld.

**3.4 Toughness Properties.** As was expected, the fine grained base metal showed very good impact properties, as the average energy absorbed in the base metal was 68 J and 54 J at  $-40$  and  $-60$  °C temperatures, respectively, for subsize samples. However, toughness properties of the joints were not as good as that of the base metal. Figures 16 and 17 show the results of impact tests at  $-40$  and  $-60$  °C temperatures, respectively. The error bars shown in dashed red correspond to the test series in which the lowest value was smaller than 70% of the mean value. However, only three test series from a total of 24 showed such low reliability. Despite the higher impact toughness values of the HAZ, the impact energy absorbed was significantly lower in the weld metal and brittle fractures occurred in either the weld metal or the HAZ of the samples. The higher impact toughness of the HAZ (FL) can be attributed to the narrowness of the coarse-grained HAZ (see Fig. 18) and the lower carbon content of the steel, as these lead to a lower hardness of the coarse-grained HAZ compared to that typically is encountered in QT steel joints [2]. Although all the joints passed the 22 J requirement in the HAZ (70% of 27 J), acceptable toughness values were obtained at  $-40$  °C only in the case of the two moderate and high line energy welds with cooling times above 2 s, as the moderate and high line energies of the process provided optimized toughness properties in the entire joint.

**Table 4** Results of tensile test

Item no.	Yield strength (MPa)			Ultimate tensile strength (MPa)			Elongation (%)		
	Test1	Test2	Average	Test1	Test2	Average	Test1	Test2	Average
#801	N/A	1080	1080	1119	1135	1127	7.5	7.3	7.4
#802	1094	1088	1090	1142	1118	1130	6.5	N/A	6.5
#803	1065	1035	1050	1118	1109	1113	7.9	7.4	7.6
#804	1046	1065	1055	1100	1108	1104	7.0	6.6	6.8
#805	1034	N/A	1034	1080	1102	1091	7.1	6.4	6.7
#806	N/A	1008	1008	1024	1030	1027	4.7	3.9	4.3

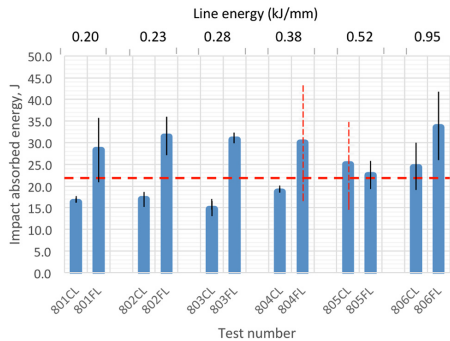


Fig. 16 Absorbed impact energy at  $-40^{\circ}\text{C}$  of each joint and their corresponding standard deviation (vertical lines). The horizontal dashed line depicts the minimum toughness requirement of 22 J. CL: weld centerline and FL: fusion line.

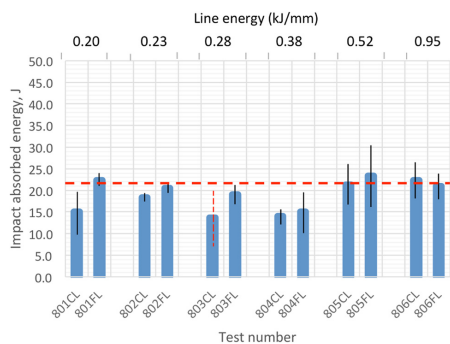


Fig. 17 Absorbed impact energy at  $-60^{\circ}\text{C}$  of each joint and their corresponding standard deviation (vertical lines). The horizontal dashed line depicts the minimum toughness requirement of 22 J. CL: weld centerline and FL: fusion line.

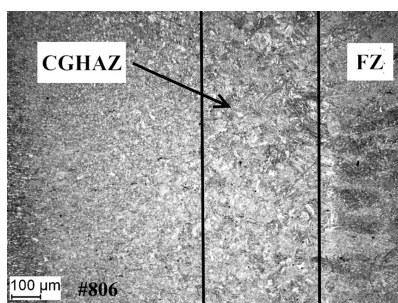


Fig. 18 Width of CGHAZ in the vicinity of the welds was about 0.3 mm at its maximum in the case of the widest weld

However, at  $-60^{\circ}\text{C}$ , impact values barely reached the minimum requirement of 22 J, even in the case of the two slowest welds with low cooling rates. Except for the two slowest welds, none of the low line energy joints passed the 22 J requirements, neither in the HAZ nor in the weld. Fracturing energy decreased significantly in the weld metal down to  $\sim 80\%$ .

In the literature, it was noted that the mechanical properties of the welds in Optim 960 QC steel depend on the line energy of welding process. Figure 19 summarizes all the aspects of this study by illustrating the experimental areas according to their corresponding cooling time and welding speed, and the critical cooling times for the required tensile and toughness properties. As goes without saying, there is no challenge in obtaining matching joints within the range of low to high speed experiments. However, one should also note that joints with better quality could be obtained by taking advantage of the process' better stability at higher speeds. Therefore, as long as impact toughness requirements are not involved, the low line energy and overmatching joints may be preferable, since the low carbon content of the steel guarantees the absence of excessive hardness in the joint.

On the other hand, if high quality joints having both high strength and toughness properties at  $-40^{\circ}\text{C}$  temperatures are required, the welding parameter window is limited to a narrow range of moderate line energy weld with welding speeds of around 1 m/min. However, with the consideration of weak impact toughness properties at extreme low temperatures ( $-60^{\circ}\text{C}$ ), and the fact that acceptable impact toughness properties were obtained only in the case of the welds #805 and #806, one could argue that the very low line energy values of fiber laser welding were probably not beneficial in terms of impact toughness properties. In fact, this could indicate that there is only a certain range of heat input, which leads to the best attainable impact toughness properties. According to the literature and the results of this study, the optimum range for obtaining acceptable impact toughness properties might be limited between the lowest possible heat inputs by arc welding and the highest possible heat inputs by fiber laser welding. Therefore, one can conclude that hybrid laser arc welding technology with which the mentioned range of heat input is attainable could potentially be an appropriate solution for this challenge.

As was mentioned in Sec. 2, the experimental data points of this study were selected in accordance with the limitations of a narrow power-speed parameter window during the preliminary experiments. As a result, it was not possible to provide any experimental data to evaluate if welding with the same line energies but

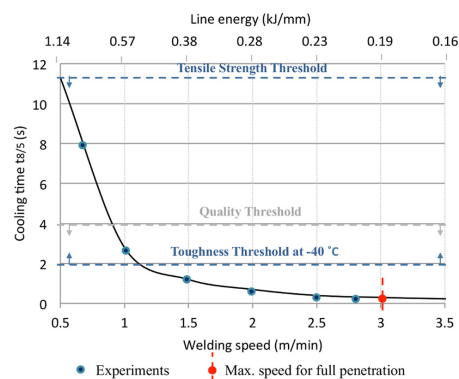


Fig. 19 Summary of the study, showing the experiments within the acceptable thresholds of cooling times ( $t_{9/5}$ ) for tensile strength and impact toughness properties. Quality threshold was estimated approximately.

different parameters (e.g., 1/2x laser power and 1/2x welding speed) would have the same result. Therefore, it is important to note that the term “line energy” in this paper actually refers to the “appropriate/possible line energies” for visually acceptable joints according to the preliminary experiments. However, considering the plate thickness of 8 mm, further studies can be carried out with higher power lasers, in order to provide more choices of line energy for a better evaluation.

Additionally, the results of this study show that with autogenous fiber laser welding it is possible to obtain joints which have weld metal properties close to the properties of the base material. In other words, joints with acceptable quality can be made without the use of filler material, which is one of the main expenses in every welding process. Therefore, the possibility of using this process should be considered as a cost effective solution when mass production is concerned.

#### 4 Conclusions

The present research was designed to determine the weldability of Optim 960 QC UHSS in a butt joint configuration welded by fiber lasers. The aim was to study the visual, hardness, tensile, and impact toughness properties of the joints with respect to the limited choices of possible line energies for visually acceptable joints. The following conclusions can be drawn:

- High quality butt joints with superior tensile properties can be obtained by the application of high power fiber laser welding within a wide range of low to moderate line energies, thanks to the combination of the low carbon content of direct-quenched Optim 960 QC and the high quality beam of fiber lasers. However, in the case of the slowest weld with a line energy of 0.95 kJ/mm, root concavity noticeably increased and the welding process became more unstable.
- Excessive hardness does not occur in the FZ of laser welded direct-quenched Optim 960 QC, due to the low carbon content and carbon equivalent of the steel. Therefore, the risk of cracking as a result of excessive hardness in the FZ is considerably lower in direct-quenched Optim 960 QC laser welds than in other commercial DP and QT UHSSs with the same strength levels.
- Despite the presence of a low degree of HAZ softening in the joints, all the joints passed the tensile requirements as the softened area was narrow. It was concluded that as long as the cooling time ( $t_{8/5}$ ) is approximately below 11.7 s or the line energy is less than 1.16 kJ/mm, matching joints are guaranteed.
- Laser cutting seems to be an appropriate method for the preparation of the joints, as the softening induced by laser cutting of the plates had no considerable effect on the hardness properties of the laser welds.
- Tensile ductility of the joints was influenced by concavity rather than the process' line energy. In the case of low and moderate line energy, the average elongation was not reduced significantly in the joints compared with that of the base metal. However, a high degree of root concavity in the high line energy welds led to a 38% lowering of ductility in the joint.
- It is possible to obtain fiber laser welded butt joints meeting both strength and impact toughness requirements at  $-40^{\circ}\text{C}$ , but the line energy should be above 0.52 kJ/mm, as long as the excessive line energy does not deteriorate the weld quality. The narrowness and the low hardness in coarse-grained HAZ compared to that typically encountered in QT steels' joints led to high impact values in the HAZ. However, it was concluded that the fusion area of the weld is the most susceptible to impact fractures, due to the high cooling rates which occur in high speed fiber laser welding.
- At  $-60^{\circ}\text{C}$ , the impact values barely reached the minimum requirement of 22 J only when the line energy was above

0.52 kJ/mm. Despite the very high impact toughness values of the fine grained base metal, brittle fracture occurred in the joints. However, due to the narrowness of the fiber laser welds, the performance of Charpy V impact testing demands great accuracy, and alternative toughness testing methods should be performed as well to increase the reliability of the results.

#### Acknowledgment

This study was supported by the Arctic Materials Technologies Development project, which was cofunded by the European Union, Finnish industries, Lappeenranta University of Technology, and the Russian Federation. The steel plates for the experimental work were provided by the Rautaruukki Corporation. In addition, the authors would like to thank the staff of Lappeenranta University of Technology, especially the staff of the Laboratory of Laser Materials Processing and the Laboratory of Steel Structures for carrying out the experimental work.

#### References

- [1] Horii, Y., Ohkita, S., Shinada, K., and Koyama, K., 1995, “Development of High-Performance Welding Technology for Steel Plates and Pipe for Structural Purposes,” Nippon Steel, Report No. 65.
- [2] Hemmälä, M., Hirvi, A., Kömi, J., Laitinen, M., Mikkonen, P., Porter, D., Savola, J., and Tihinen, S., 2010, *Technological Properties of Direct-Quenched Structural Steels With Yield Strength 900-960 MPa as Cut Length and Hollow Sections*, Rautaruukki Corporation, Helsinki, Finland.
- [3] Quentino, L., Costa, A., Miranda, R., Yapp, D., Kumar, V., and Kong, C. J., 2007, “Welding With High Power Fiber Lasers: A Preliminary Study,” *Mater. Des.*, **28**(4), pp. 1231–1237.
- [4] Ion, J., 2005, *Laser Processing of Engineering Materials: Principles, Procedure and Industrial Application*, Elsevier Butterworth-Heinemann, Burlington, MA.
- [5] Canning, J., 2006, “Fibre Lasers and Related Technologies,” *Opt. Lasers Eng.*, **44**(7), pp. 647–676.
- [6] Salminen, A., Lehtinen, J., and Harkko, P., 2008, “The Effect of Welding Parameters on Keyhole and Melt Pool Behavior During Laser Welding With High Power Fiber Laser,” 27th International Conference on Applications of Lasers and Electro Optics ICALOE2008, Temecula, CA, pp. 354–363.
- [7] Shi, S., and Westgate, S., 2008, “Laser Welding of Ultra High Strength Steels for Automotive Applications,” PICALO 2008, Beijing.
- [8] Kaplan, A. F. H., Westin, E. M., Wiklund, G., and Norman, P., 2008, “Imaging in Cooperation With Modeling of Selected Defect Mechanisms During Fiber Laser Welding of Stainless Steel,” ICALOE, Temecula, CA, pp. 789–798.
- [9] Kawahito, Y., Kinoshita, K., Matsumoto, N., Mizutani, M., and Katayama, S., 2008, “Effect of Weakly Ionized Plasma on Penetration of Stainless Steel Weld Produced With Ultra High Power Density Fiber Laser,” *Sci. Technol. Weld. Joining*, **13**(8), pp. 749–753.
- [10] Daley, W. W., 1999, *Laser Welding*, Wiley, New York.
- [11] Yilbas, B. S., and Akhtar, S., 2013, “Laser Welding of AISI 316 Steel: Microstructural and Stress Analysis,” *ASME J. Manuf. Sci. Eng.*, **135**(3), p. 031018.
- [12] Losz, J., and Challenger, K., 1999, “HAZ Microstructures in HSLA Steel Weldments,” First United States-Japan Symposium on Advances in Welding Metallurgy, Yokohama, Japan, pp. 207–225.
- [13] Zeman, M., 2009, “Assessment of Weldability of WELDOX 1100 High-Strength Quenched and Tempered Steel,” *Weld. Int.*, **23**(2), pp. 73–82.
- [14] Xia, M., Biro, E., Tian, Z., and Zhou, Y., 2008, “Effect of Heat Input and Martensite on HAZ Softening in Laser Welding of Dual Phase Steels,” *ISIJ Int. J.*, **48**(6), pp. 809–814.
- [15] Mohandas, T., Madhusudan Reddy, G., and Satish Kumar, B., 1999, “Heat Affected Zone Softening in High Strength Low Alloy Steels,” *J. Mater. Process. Technol.*, **88**(1), pp. 284–294.
- [16] Farabi, N., Chen, D., and Zhou, Y., 2011, “Microstructure and Mechanical Properties of Laser Welded Dissimilar DP600/DP980 Dual-Phase Steel Joints,” *J. Alloys Compd.*, **509**(3), pp. 982–989.
- [17] Xia, M., Sreenivasan, N., Lawson, S., Zhou, Y., and Tian, Z., 2007, “A Comparative Study of Formability of Diode Laser Welded in DP980 and HSLA Steels,” *ASME J. Eng. Mater. Technol.*, **129**(3), pp. 446–452.
- [18] Farabi, N., Chen, D., and Zhou, Y., 2010, “Fatigue Properties of Laser Welded Dual-Phase Steel Joints,” *Procedia Eng.*, **2**(1), pp. 835–843.
- [19] Biro, E., McDermid, J., Embury, J., and Zhou, Y., 2010, “Softening Kinetics in the Subcritical Heat-Affected Zone of Dual-Phase Steel Welds,” *Metall. Mater. Trans. A*, **41**(9), pp. 2348–2356.
- [20] Baltazar Hernandez, V., Nayak, S., and Zhou, Y., 2011, “Tempering of Martensite in Dual Phase Steels and Its Effects on Softening Behavior,” *Metall. Mater. Trans. A*, **42**(10), pp. 3115–3129.
- [21] Xu, W., Westerbaan, D., Nayak, S., Chen, D., Goodwin, F., and Zhou, Y., 2012, “Tensile and Fatigue Properties of Fiber Laser Welded High Strength Low Alloy and DP980 Dual-Phase Steel Joints,” *Mater. Des.*, **43**, pp. 373–383.

- [22] Xu, W., Westerbaan, D., Nayak, S., Chen, D., Goodwin, F., Biro, E., and Zhou, Y., 2012, "Microstructure and Fatigue Performance of Single and Multiple Linear Fiber Laser Welded DP980 Dual-Phase Steel," *Mater. Sci. Eng. A*, **553**, pp. 51–58.
- [23] Kim, C.-H., Choi, J.-K., Kang, M.-J., and Park, Y.-D., 2010, "A Study on the CO<sub>2</sub> Laser Welding Characteristics of High Strength Steel up to 1500 MPa for Automotive Application," *J. Achiev. Mater. Manuf. Eng.*, **39**(1), pp. 79–86.
- [24] Sreenivasan, N., Xia, M., Lawson, S., and Zhou, Y., 2008, "Effect of Laser Welding on Formability of DP980 Steel," *ASME J. Eng. Mater. Technol.*, **130**(4), p. 041004.
- [25] Leiviskä, P., Fellman, A., Laitinen, R., and Vänskä, M., 2007, "Strength Properties of Laser and Laser Hybrid Welds of Low Alloyed High Strength Steels," 11th Conference Nordic Laser Materials Processing, Lappeenranta, Finland, pp. 173–184.
- [26] Laitinen, R., Kömi, J., Keskitalo, M., and Mäkkikangas, J., 2007, "Improvement of the Strength of Welded Joints in Ultra High Strength Optim 960 QC Using Autogenous Yb:YAG Laser Welding," Nordic Laser Materials Processing, NOLAMP 11, Lappeenranta, Finland, pp. 204–215.
- [27] Siltaanen, J., and Tihinen, S., 2012, "Position Welding of 960 MPa Ultra-High-Strength-Steel," ICALAO, Anaheim, CA, pp. 464–473.
- [28] Zeman, M., 2009, "Properties of Welded Joints Made of Weldox 1100 Steel," *Weld. Int.*, **23**(2), pp. 83–90.
- [29] Juan, W., Li, Y., and Liu, P., 2003, "Effect of Weld Heat Input on Toughness and Structure of HAZ of a New Super-High Strength Steel," *Bull. Mater. Sci.*, **26**(3), pp. 301–305.
- [30] Shi, Y., and Han, Z., 2008, "Effect of Weld Thermal Cycle on Microstructure and Fracture Toughness of Simulated Heat-Affected Zone for a 800MPa Grade High Strength Low Alloy Steel," *J. Mater. Process. Technol.*, **207**(1), pp. 30–39.
- [31] EN ISO 15614-11, 2002, *Specification and Qualification of Welding Procedures for Metallic Materials-Welding Procedure Test-Part 11: Electron and Laser Beam Welding*, Finnish Standard Association SFS, Helsinki, Finland, Report No. SFS-EN ISO 15614-11.
- [32] Farrokhi, F., 2014, "Autogenous High Power Fiber Laser Welding of Optim 960 QC Ultra High Strength Steel," Masters thesis, Lappeenranta University of Technology, Lappeenranta, Finland.
- [33] EN ISO 13919-1, 1996, *Welding: Electrons and Laser Beam Welded Joints. Guidance on Quality Levels for Imperfections. Part 1: Steel*, Finnish Standard Association SFS, Helsinki, Finland, Report No. SFS-EN ISO 13919-1.
- [34] ISO 22826, 2005, *Destructive Tests on Welds in Metallic Materials-Hardness Testing of Narrow Joints Welded by Laser and Electron Beam (Vickers and Knoop Hardness Tests)*.
- [35] ISO 15614-1:2004/Amd, 2012, *Specification and Qualification of Welding Procedures for Metallic Materials-Welding Procedure Test-Part 1: Arc and Gas Welding of Steels and Arc Welding of Nickel and Nickel Alloys-Amendment 2*, Finnish Standard Association SFS, Helsinki, Finland, SFS-EN ISO 15614-1/A2.
- [36] CEN ISO/TR 15608, 2013, *Welding: Guidelines for a Metallic Materials Grouping System*, Finnish Standard Association SFS, Helsinki, Finland, CEN ISO/TR 15608.
- [37] Raukki Metals Oy., 2013, *Welding General: Hot-Rolled Steel Sheets: Plates and Coils*, Rautaruukki Corporation, Helsinki, Finland.
- [38] Hemmilä, M., Laitinen, R., Liimatainen, T., and Porter, D., 2005, *Mechanical and Technological Properties of Ultra High Strength Optim Steels*, Rautaruukki Corporation, Helsinki, Finland.
- [39] EN ISO 4136, 2012, *Destructive Tests on Welds in Metallic Materials. Transverse Tensile Test*, Finnish Standard Association SFS, Helsinki, Finland, SFS-EN ISO 4136.
- [40] EN ISO 148-1, 2009, *Metallic Materials-Charpy Pendulum Impact Test-Part 1: Test Method*, Finnish Standard Association SFS, Helsinki, Finland, SFS-EN ISO 148-1.
- [41] Degenkolbe, J., Uwer, D., and Wegmann, H., 1984, "Characterisation of Welding Thermal Cycles With Regard to Their Effect on the Mechanical Properties of Welded Joints by Cooling Times t8/5 and Its Determination," IIW Document, International Institute of Welding, London.
- [42] Sokolov, M., Salminen, A., Somonov, V., and Kaplan, A. F., 2012, "Laser Welding of Structural Steels: Influence of the Edge Roughness Level," *Opt. Laser Technol.*, **44**(7), pp. 2064–2071.
- [43] Kawahito, Y., Matsumoto, N., Abe, Y., and Katayama, S., 2013, "Laser Absorption Characteristics in High-Power Fiber Laser Welding of Stainless Steel," *Weld. Int.*, **27**(2), pp. 129–135.
- [44] Panda, S., Sreenivasan, N., Kuntz, M., and Zhou, Y., 2008, "Numerical Simulations and Experimental Results of Tensile Test Behavior of Laser Butt Welded DP980 Steels," *ASME J. Eng. Mater. Technol.*, **130**(4), p. 041003.
- [45] Marimuthu, S., Eghlio, R. M., Pinkerton, A. J., and Li, L., 2013, "Coupled Computational Fluid Dynamic and Finite Element Multiphase Modeling of Laser Weld Bead Geometry Formation and Joint Strengths," *ASME J. Manuf. Sci. Eng.*, **135**(1), p. 011004.

## **Publication V**

Siltanen, J., Minkkinen, A., and Järn, S.  
**Laser welding of coated press-hardened steel 22MnB5**

Reprinted with permission from  
*Physics Procedia*  
Vol. 89, pp. 139-147, 2017  
© 2017, Elsevier







Available online at [www.sciencedirect.com](http://www.sciencedirect.com)

ScienceDirect

Physics Procedia 89 (2017) 139 – 147

Physics

Procedia

Nordic Laser Materials Processing Conference, NOLAMP\_16, 22-24 August 2017, Aalborg University, Denmark

## Laser welding of coated press-hardened steel 22MnB5

Jukka Siltanen<sup>a\*</sup>, Ari Minkkinen<sup>a</sup>, Sanna Järn<sup>a</sup>

<sup>a</sup>SSAB Europe Oy, Harvialantie 420, Hämeenlinna 13300, Finland

### Abstract

The press-hardening process is widely used for steels that are used in the automotive industry. Using ultra-high-strength steels enables car manufacturers to build lighter, stronger, and safer vehicles at a reduced cost and generating lower CO<sub>2</sub> emissions. In the study, laser welding properties of the coated hot stamped steel 22MnB5 were studied. A constant 900°C temperature was used to heat the steel plates, and two different furnace times were used in the press-hardening, being 300 and 740 seconds. Some of the plates were shot blasted to see the influence of the partly removed oxide layer on the laser welding and quality. The welding set-up, welding, and testing of the weld specimens complied with the automotive testing code SEP 1220.

© 2017 The Authors. Published by Elsevier B.V. This is an open access article under the CC BY-NC-ND license (<http://creativecommons.org/licenses/by-nc-nd/4.0/>).

Peer-review under responsibility of the scientific committee of the Nordic Laser Materials Processing Conference 2017

*Keywords:* Laser welding, 22MnB5

### 1. Introduction

The overview of hot stamping steels written by Rendón et al (2013) for internal use in SSAB gives a thoughtful description of the production, processing, and usage of this steel grade. The following text in the introduction chapter includes several references from that report and those are separated by quotation marks in the following text.

“The automotive industry is continuously developing the car body to achieve an optimal structure that combines at least a light weight and superior crash performance. This can be achieved by the use of lightweight materials and modern, advanced, high-strength steels. 22MnB5 is an example of a high-strength steel that, after hot stamping, has a fully martensitic microstructure together with a high ultimate strength of up to 1500 MPa or even higher. There is a trend to get even higher strength levels for press-hardening steels, and a strength level as high as 2000 MPa is

\* Corresponding author. Tel.: +358-40-542-8214.

E-mail address: [jukka.siltanen@ssab.com](mailto:jukka.siltanen@ssab.com)

targeted. This is done by adding alloying elements such as carbon and boron. The 22MnB5 steel is usually used for safety-related automotive body parts such as A- and B-pillars, roof rails, and door-beams.”

“The 22MnB5 steel is further processed by a forming process called many names, such as hot stamping, press hardening, or hot forming, to gain the properties mentioned above. Hot stamping is a non-isothermal process for sheet metals, in which forming and quenching take place in the same forming step. The steel sheets are heated typically for 5-10 minutes in a furnace until reaching a temperature of about 900-950°C, which changes the steel structure to fully austenitic. The forming process takes advantage of the good formability at high temperatures. The fully martensitic structure is formed when the pressing machine is kept closed for about 20 seconds while the sheet is cooled down with a velocity of about 27°C/s.”

In the hot stamping process, the steel is usually heated in the atmosphere containing oxygen which then assists the forming of a scale on the surface of 22MnB5 steel during the hot stamping. To prevent this, the steel can be coated. Nowadays the most commonly used coating is aluminium–silicon (AlSi), but competing coatings are available, such as galvanized zinc-iron coating (ZnFe). The AlSi and ZnFe coated steels are produced in a continuous coating line by dipping the steel in a bath filled with the desired coating mixture. The steel can be further processed by adding an additional heat treatment process in galvanising line to make the base material and coating react, as in the manufacture of galvanized steel (ZnFe). Fan et al. (2007) have written that AlSi-coated steel has the best properties for hot stamping and a galvanized steel sheet has similar properties. Both are superior to uncoated cold-rolled steel.

Gerhards et al. (2015) reported that the hot stamped steel 22MnB5 is a very good material for automotive construction and parts. However, as good as this steel may be as construction material, there are several issues when it comes to joining. Heat inputs produced in welding are harmful to the properties of hot stamped steel. Despite the low heat input and high welding speed that are typical for laser welding, the previous phenomenon still occurs. The result is a loss of hardness and strength in the heat-affected zone. Siltanen et al. (2015) showed about a 200 Vickers decrease in hardness and 200 MPa decrease in yield strength for the coated 22MnB5 material after laser welding. The motivation to prepare this conference paper on the Nolamp 16 conference has been the better results achieved from laser welding tests if compared the previous conference paper of Siltanen et al. (2015) and the objective to understand better the factors influencing on the weld quality.

## 2. Experimental set-up

In the study, the test material was coated hot stamped 22MnB5 steel, and the coating was an iron-zinc alloy. This steel is commercially known as galvanized, and the abbreviation ZF is used to identify this coating type. The mass of the coating was 180 g/m<sup>2</sup> on both surfaces, and therefore the thickness of the coating was 13µm per surface. The thickness of the test material was 1.5 mm. The mechanical properties of the test material are depicted in Table 1 and the typical chemical composition in Table 2.

Table 1. Typical mechanical properties of 22MnB5 steel as rolled and after hot stamping.

Material	Yield strength R <sub>p</sub> (N/mm <sup>2</sup> )	Tensile strength R <sub>m</sub> (N/mm <sup>2</sup> )	Elongation A (%)
22MnB5, rolled	400	600	22
22MnB5, hot stamped	1200	1600	11

Table 2. Typical volumes of leading alloying elements of 22MnB5 steel in the percentages of weight.

Material	C	Si <sub>max</sub>	Mn	Cr	B
22MnB5	0.2-0.25	0.4	1.1-1.4	0.1-0.3	0.0008-0.0050

The test samples were hot stamped with a laboratory scale furnace and hot stamping equipment. The temperature in the furnace was a constant and the target temperature for the heated specimen was 900°C before hot stamping. Two furnace times were used: 300 and 740 seconds (s). This means the time the test pieces were in the furnace before the hot stamping process took place. With the short furnace time there are two regions in the coating, an upper layer consisting of Zn-Fe phases with  $\alpha$ -Fe(Zn) phases and a  $\alpha$ -Fe(Zn) solid solution layer under this first layer. With longer heating times coating has completely transformed to  $\alpha$ -Fe(Zn) solid solution. The oxide layer is formed on the surface of a material during heating, and the thickness of the layer depends on the heating time. With a longer furnace time, the thickness of the oxide layer grows, as well as the thickness of the coating. The influence of an oxidation layer located on the surface of the test material on welding quality was studied. The oxide layer was partly removed from the surface of some test plates by means of shot blasting, to compare the influence of surface conditions.

The coating characteristics for a hot stamped test material are shown in Figures 1 and 2. The figures depict the surfaces for furnace times of 300 and 740 seconds. Metallographic sections were prepared for coating, oxide-layer thickness measurement, and microstructural examinations. After etching an optical microscope was used to measure coating thickness and perform microstructural examinations. Coating thickness was calculated as an average from 15 points in 3 pictures. A scanning electron microscope was used for the surface structure examination and coating elemental composition identification. The zinc content of the coating was calculated as an average of 15 evenly distributed measuring points. The zinc content of the coating decreased from 32% to 25% when the furnace time increased from 300 seconds to 740 seconds. The shot-blasting process removed and flattened the remaining oxide layer to some degree, but a remarkable amount of oxide still existed on the surface after shot blasting.

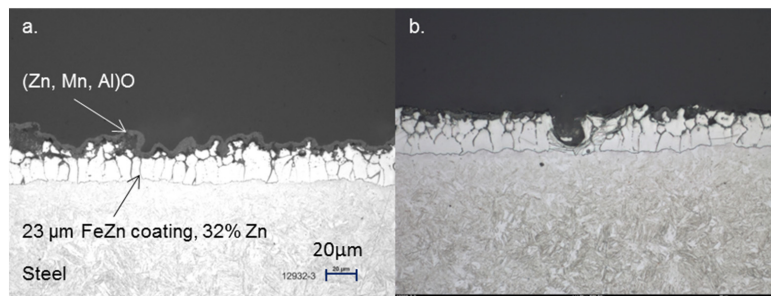


Figure 1. SEM micrographs showing the coating structure of the material after 300 seconds in the furnace: (a) hot stamped, (b) hot stamped and shot blasted (same scaling is used in the both figures).

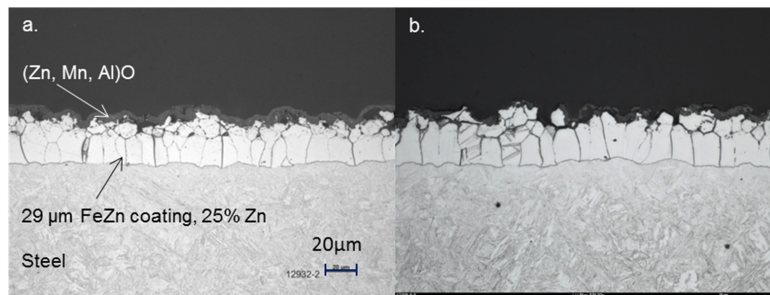


Figure 2. SEM micrographs showing the coating structure of the material after 740 seconds in the furnace: (a) hot stamped, (b) hot stamped and shot blasted (same scaling is used in the both figures).

The joint types used were a butt and a lap joint. The movement of the welding test was performed using a KUKA KR 30 HA (high accuracy) industrial robot. The actual welding tests were performed according to SEP 1220-3 when applicable. Therefore, the sheets were adjusted with a 16 mm overlap, and the width and length of the sheets were 200 x 300 mm with a thickness of 1.5 mm, as mentioned earlier. The welding was performed using a 10 kW disk laser, with a configured 4 kW laser power and the laser welding was done by using a continuous wave mode. The diameter of the fibre used was 400  $\mu\text{m}$ , the welding optics had a 200 mm collimator, and a focal length of 300 mm was used. The diameter of the focused laser beam on the surface was 0.6 mm, and the focus was positioned on the surface ( $\pm 0\text{mm}$ ) in both joint configurations. No active process gases were used in welding; just cross-jet blowing compressed air was used to protect the welding optics. The butt and the lap joint configurations were continuously welded without tack welds. In the welding of the lap joint configuration, a foil of 0.1 mm thickness was placed between the test plates to guarantee an open escape route for the zinc fumes formed during welding. The foil remained unmelted and it was removed after welding. The main laser welding parameters used are presented in Table 3.

Table 3. Laser welding parameters.

Joint type	Welding speed (m/min)	Welding energy (kJ/mm)
Butt joint	8000	0.02
Lap joint	2600	0.07

### 3. Testing

The testing included visual and radiographic inspection of welded specimens, followed by the destructive tests such as a transversal tensile strength test, hardness evaluation, metallography, and cross-sections of the welds. The visual inspections of the welds showed improved weld quality compared to the weld quality of the previous study by Siltanen et al. (2015), in which the welds showed intensive incomplete penetration and a filled groove in both butt and lap joint configurations. In this new study, the visual examination did not reveal any major defects in the lap joints. The correctly placed and shaped foil between the plates helped the vaporized zinc to escape from the joint, ensuring the production of an almost defect-free weld. However, there were some defects, like the incomplete penetration and filled groove in the lap joints, but the critical level was not exceeded. The groove preparation of the butt joints was done by a mechanical shear cutter, producing a poor edge quality, which led to the presence of a gap between the edges of the plates and therefore influenced the weld quality. The radiographic inspection revealed some single pores in the lap joints. The butt joints were not inspected by the X-rays. The places for destructive testing were selected from the areas representing an equal weld quality.

#### 3.1. Cross-sections

The cross-sections of lap and butt joints for the steel sheets with a 300 and 740 seconds furnace times are presented in Figures 3 to 6. The figures of the lap joint visualise the influence of the foil between the plates. The overall shape of the weld is good, and much better than in the previous welding tests that Siltanen et al. (2015) performed. The cross-sections did not show any clear differences resulting from the different state of the surface, whether shot blasted or not. It should be noted that the geometry of laser welds is good; the waists of welds are wide, with a positive influence on the strength properties of the joints.

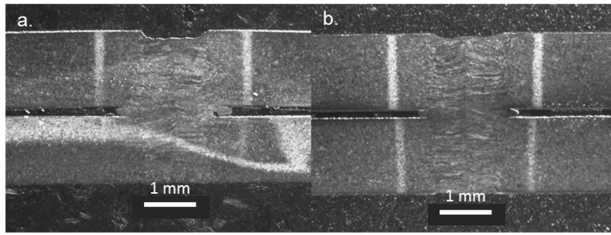


Figure 3. Lap joint, 740 s: (a) shot blasted, (b) without shot blasting.

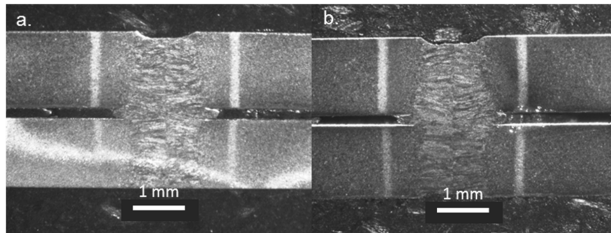


Figure 4. Lap joint, 300 s: (a) shot blasted, (b) without shot blasting.

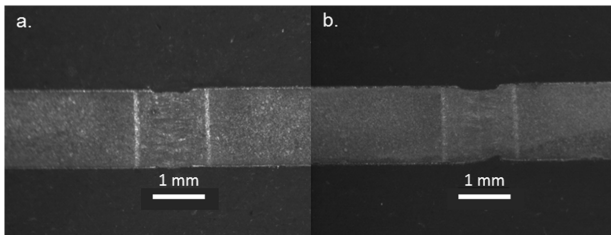


Figure 5. Butt joint, 740 s: (a) shot blasted, (b) without shot blasting.

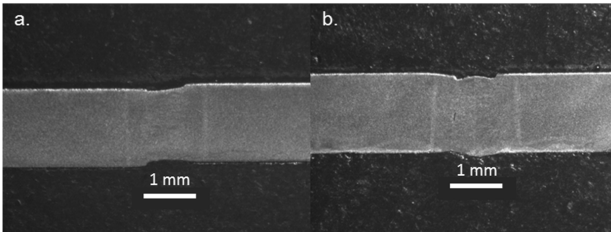


Figure 6. Butt joint, 300 s: (a) shot blasted, (b) without shot blasting.

### 3.2. Microstructure

The analysing of microstructures is unfinished and therefore the following information about formed microstructures is based on the observations of Jia et al. (2014) and Siltanen et al. (2015). That information should be relevant because the same test material and welding method is used. However, the microstructures of welds will be analysed and compared on the previous tests results.

Jia et al. (2014) and Siltanen et al. (2015) observed that the microstructure of 22MnB5 steel is fully martensitic after the hot stamping, despite the different furnace times used. In the laser welding of hardened 22MnB5 steel, the fast cooling rate typical of this welding process produces a hard and brittle martensitic structure in the weld metal and in parts of the HAZ, where the temperature has reached the upper part of the austenitisation area where complete austenitisation takes place. The HAZ can be split into three parts (starting from the weld direction): quenched HAZ, incompletely tempered HAZ, and tempered HAZ. In the quenched HAZ closest to the weld metal, the temperature is high enough for complete transformation to austenite; the structure will be completely martensitic after cooling and no softening will take place. In laser welding, this zone is relatively narrow because of the low heat input. In the incompletely tempered HAZ, the maximum temperature stays below the limit that is required for full austenitisation, and therefore the final microstructure consists of martensite and ferrite, because some amount of the original martensite is transformed into ferrite rather than austenite. This zone is also relatively narrow, like the previous zone. In the tempered HAZ, the maximum temperature never exceeds the temperature at which transformation to austenite starts. In that area, after cooling, the microstructure consists of martensite, tempered martensite, ferrite, and probably some bainite. The width of this area is the widest of the three. The softening detected in hardness values is located in the complete HAZ area, where all these previously named zones exist.

### 3.3. Hardness

The hardness of the lap joints and butt joint was measured in HV1 by following the instructions of SEP. The distance between the measurement points was 0.2 mm. The hardness measurement line goes from the base material, over the weld, and ends on the other side of the base material. Figure 7 depicts hardness profiles of the butt joints, and Figure 8 shows similar for the lap joints. The figures include values for both shot-blasted and oxidized surfaces without shot blasting when data was available. The location of weld (WM) and heat affected zone (HAZ) are depicted in Figure 7. The profiles of the lap joints show some differences in the hardness of the base materials. The reason for this is insufficient grinding after the laser-cutting that was used to remove a test specimen from the welded sheet. A typical reduction in hardness in the heat-affected zone (HAZ) is visible, as well as the hardening of a weld area for both joint types. Table 4 depicts the minimum and maximum values of hardness in the weld area (weld metal + fusion line + HAZ). It was assumed that there are no clear differences in the hardness values between materials with different conditions on the surface, because the coating interacts just on the surface area and invariable welding parameters were used. The materials with furnace times of 300 and 740 seconds, with both surface conditions, confirm this; the hardness values are equal for both joint types. The values in oxidized conditions follow the values of measurements for other furnace times.

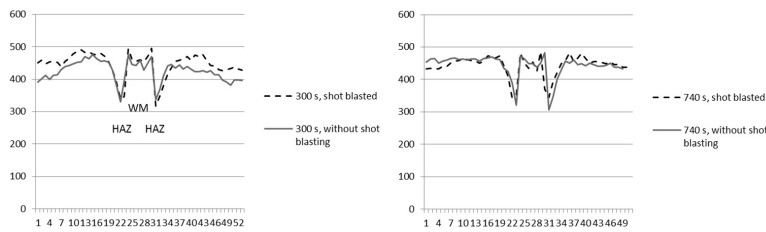


Figure 7. Butt joint: Hardness (HV1): 300 and 740 seconds furnace time.

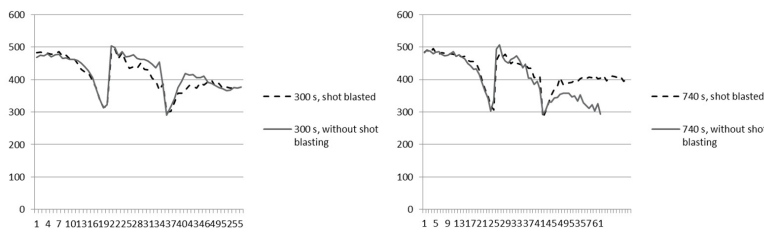


Figure 8. Lap joint: Hardness (HV1): 300 and 740 seconds furnace time.

Table 4. The minimum and maximum hardness values.

Specimen ID	Butt joint		Lap joint	
	HV1 <sub>min</sub>	HV1 <sub>max</sub>	HV1 <sub>min</sub>	HV1 <sub>max</sub>
740 s, shot blasted	343	485	283	495
740 s, without shot blasting	306	483	294	506
300 s, shot blasted	318	496	300	494
300s, without shot blasting	331	476	290	503

### 3.4. Shear tensile strength

The shear tensile strength of the lap joints was tested in accordance with SEP 1220 and ISO standard 14273. The width of the test specimen was 45 mm, and two tests were performed for a single specimen. Instead of the five test specimens that SEP requires, just two specimens were tested. Table 5 shows the average values for shear tensile strength at fracture ( $F_{max}$ ) and elongation/deflection at fracture ( $S_{Fmax}$ ).

Table 5. Shear tensile strength results of the lap joints.

Specimen ID	$F_{max}$ (kN)	$S_{Fmax}$ (mm)	$R_m$ (N/mm <sup>2</sup> )	Place of fracture
740 s, sandblasted	46.77	10.41	1299	HAZ
740 s, without shot blasting	45.68	7.42	1269	HAZ
300 s, sandblasted	44.91	9.83	1248	HAZ
300s, without shot blasting	46.60	7.92	1294	HAZ



It is very hard to find correlations between the tested materials and their properties, and the results of the shear tensile strength test. The location of the fracture was in the HAZ in all tests. In addition, the values of ultimate strengths ( $R_m$ ) were calculated using an approximation that the width of welds was 0.8 mm when measured from the waist of the welds, and the length of the weld was 45 mm, and therefore the calculated area for every weld was the same, at 36 mm<sup>2</sup>. If we compare the ultimate strength values with the results published by Siltanen et al. (2015), the difference between the calculated values (mean value: 1277 N/mm<sup>2</sup>) and the actual tested values (mean value: 1347 N/mm<sup>2</sup>) is approximately 120 N/mm<sup>2</sup>. The tensile strength of the base material is 1600 N/mm<sup>2</sup>.

#### 4. Conclusions

The laser welding trials for coated boron steel 22MnB5 were performed. The weld joint types were a butt and a lap joint. The thickness of the test material was 1.5 mm. Based on the welding tests and analysis of the non-destructive and destructive testing, the following statements can be made.

- Boron steels are alloyed and heat treated to give a tensile strength of up to 2000 MPa. With these steels, there is a potential risk of cold cracking during welding. This is normally true when uncoated material is used. In the performed tests with the coated 22MnB5 hot stamped steel, no cracking was evident. In the previous welding test of the same steel by Siltanen et al. (2015), a lot of weld defects were indicated after the visual and radiographic examinations. In this study, more attention was given to the welding set-up. For example, the vaporization of zinc was ensured by adding some extra base between the test plates, and some holes were cut in the foil to increase the volume between the plates. The positive influence of this change was concretely proved during the welding tests: the amount of spatter was much smaller than in the previous tests, and the radiographic examination discovered just a few localised pores. It is essential to follow the SEP guidelines to guarantee weld quality. The oxide layer removal by shot blasting did not show any visually demonstrable influence on welding tests, and the layer conditions had no clear effect on any test results.
- The cross-sections show the shape of the beads and also how the foil between the plates is placed in the lap joint. There are no differences in the geometry of cross-sections between the different materials (furnace time and oxide layer). The width of the weld is important because it influences the strength properties of the joint. In this case, there is minor deviation between the strength values, which indicates that the weld quality is relatively equal. On the other hand, the welded joints have low values of elongation. The heat forming in the laser-welding process will cause local softening in the HAZ, and all plasticity in the joints concentrates on that area. The low heat input of laser welding keeps that area narrow, and therefore the overall strength properties of the welds are good.
- The microstructure was analysed by utilising some references. The HAZ has three zones with variable microstructures. Based on the first analysis the conditions of the coatings seemed not to have any influence on the microstructures of welds.
- The hardness profile shows the typical reduction in hardness values. The softened zones influence the weld properties as described earlier. Neither the furnace times nor the surface conditions have an influence on hardness. The minimum and maximum values were very similar.

- The shear tensile test of the overlap welds shows that the oxide layer or its removal has no clear influence on the strength properties of welds. The ultimate strength values were calculated and compared to the results of earlier studies. Those showed minor differences but were at a good level.
- In future studies, it is recommended to perform welding tests with variable welding parameters, to see if the furnace time or condition of coating has an influence on those.
- Some welding tests are planned to do by using specimens which has been hot stamped by using a shorter furnace time than that of 300 seconds to see its influence of that on the formation of oxidation during the hot stamping process and later on the welding results. This will deepen the scientific part of the project.

#### **Acknowledgements**

The authors would like to acknowledge SSAB Europe Oy and their colleagues in both Finland and Sweden for the support and the opportunity to publish the conference paper.

#### **References**

- SEP 1220-3, 2010. Testing and documentation guideline for the joinability of thin sheet of steel - Part 3: Laser beam welding.
- Gerhards, B., Engels, O., Olschok, O., Reising, U., 2015. Laser beam welding of press hardened ultra-high-strength 22MnB5 steel. Lasers in manufacturing conference, Munich, Germany, paper 247.
- Siltanen, J., Minkinen, A., Lepikko, E., Järvenpää, M., 2015. Preliminary laser welding tests of 22MnB5 steel with a butt joint and lap joint configurations. Proceedings from International Congress on Applications of Lasers & Electro-Optics. Atlanta, USA, paper 1804. p. 799-808.
- Rendón, J., 2013. Review of hot stamping and press hardening, SSAB Internal report.
- Fan, D.W., Kim, H., Biroasca, S., De Cooman, B.C., 2007. Critical review of hot stamping technology for automotive steels. Proceedings from the Materials Science & Technology Conference, Detroit, USA p. 99-108.
- Jia, A., Yang, S., Ni, W., Bai, J., Lin, Y., 2014. Microstructure and properties of fiber laser welded joints of ultrahigh-strength steel 22MnB5 and its dissimilar combination with Q235 steel, ISIJ International, 54 No. 12, p. 2881-2889.



## ACTA UNIVERSITATIS LAPPEENRANTAENSIS

- 1038.** INGMAN, JONNY. Evaluation of failure mechanisms in electronics using X-ray imaging. 2022. Diss.
- 1039.** LIPIÄINEN, SATU. The role of the forest industry in mitigating global change: towards energy efficient and low-carbon operation. 2022. Diss.
- 1040.** AFKHAMI, SHAHRIAR. Laser powder-bed fusion of steels: case studies on microstructures, mechanical properties, and notch-load interactions. 2022. Diss.
- 1041.** SHEVELEVA, NADEZHDA. NMR studies of functionalized peptide dendrimers. 2022. Diss.
- 1042.** SOUSA DE SENA, ARTHUR. Intelligent reflecting surfaces and advanced multiple access techniques for multi-antenna wireless communication systems. 2022. Diss.
- 1043.** MOLINARI, ANDREA. Integration between eLearning platforms and information systems: a new generation of tools for virtual communities. 2022. Diss.
- 1044.** AGHAJANIAN, SOHEIL. Reactive crystallisation studies of CaCO<sub>3</sub> processing via a CO<sub>2</sub> capture process: real-time crystallisation monitoring, fault detection, and hydrodynamic modelling. 2022. Diss.
- 1045.** RYYNÄNEN, MARKO. A forecasting model of packaging costs: case plain packaging. 2022. Diss.
- 1046.** MAILAGAHA KUMBURE, MAHINDA. Novel fuzzy k-nearest neighbor methods for effective classification and regression. 2022. Diss.
- 1047.** RUMKY, JANNATUL. Valorization of sludge materials after chemical and electrochemical treatment. 2022. Diss.
- 1048.** KARJUNEN, HANNU. Analysis and design of carbon dioxide utilization systems and infrastructures. 2022. Diss.
- 1049.** VEHEMAANPERÄ, PAULA. Dissolution of magnetite and hematite in acid mixtures. 2022. Diss.
- 1050.** GOLOVLEVA, MARIA. Numerical simulations of defect modeling in semiconductor radiation detectors. 2022. Diss.
- 1051.** TREVES, LUKE. A connected future: The influence of the Internet of Things on business models and their innovation. 2022. Diss.
- 1052.** TSERING, TENZIN. Research advancements and future needs of microplastic analytics: microplastics in the shore sediment of the freshwater sources of the Indian Himalaya. 2022. Diss.
- 1053.** HOSEINPUR, FARHOOD. Towards security and resource efficiency in fog computing networks. 2022. Diss.
- 1054.** MAKSIMOV, PAVEL. Methanol synthesis via CO<sub>2</sub> hydrogenation in a periodically operated multifunctional reactor. 2022. Diss.
- 1055.** LIPIÄINEN, KALLE. Fatigue performance and the effect of manufacturing quality on uncoated and hot-dip galvanized ultra-high-strength steel laser cut edges. 2022. Diss.

1056. MONTONEN, JAN-HENRI. Modeling and system analysis of electrically driven mechatronic systems. 2022. Diss.
1057. HAVUKAINEN, MINNA. Global climate as a commons — from decision making to climate actions in least developed countries. 2022. Diss.
1058. KHAN, MUSHAROF. Environmental impacts of the utilisation of challenging plastic-containing waste. 2022. Diss.
1059. RINTALA, VILLE. Coupling Monte Carlo neutronics with thermal hydraulics and fuel thermo-mechanics. 2022. Diss.
1060. LÄHDEAHO, OSKARI. Competitiveness through sustainability: Drivers for logistics industry transformation. 2022. Diss.
1061. ESKOLA, ROOPE. Value creation in manufacturing industry based on the simulation. 2022. Diss.
1062. MAKARAVA, IRYNA. Electrochemical recovery of rare-earth elements from NdFeB magnets. 2022. Diss.
1063. LUHAS, JUKKA. The interconnections of lock-in mechanisms in the forest-based bioeconomy transition towards sustainability. 2022. Diss.
1064. QIN, GUODONG. Research on key technologies of snake arm maintainers in extreme environments. 2022. Diss.
1065. TAMMINEN, JUSSI. Fast contact copper extraction. 2022. Diss.
1066. JANTUNEN, NIKLAS. Development of liquid–liquid extraction processes for concentrated hydrometallurgical solutions. 2023. Diss.
1067. GULAGI, ASHISH. South Asia's Energy [R]evolution – Transition towards defossilised power systems by 2050 with special focus on India. 2023. Diss.
1068. OBREZKOV LEONID. Development of continuum beam elements for the Achilles tendon modeling. 2023. Diss.
1069. KASEVA, JANNE. Assessing the climate resilience of plant-soil systems through response diversity. 2023. Diss.
1070. HYNNINEN, TIMO. Development directions in software testing and quality assurance. 2023. Diss.
1071. AGHAHOSSEINI, ARMAN. Analyses and comparison of energy systems and scenarios for carbon neutrality - Focus on the Americas, the MENA region, and the role of geo-technologies. 2023. Diss.
1072. LAKANEN, LAURA. Developing handprints to enhance the environmental performance of other actors. 2023. Diss.
1073. ABRAMENKO, VALERII. Synchronous reluctance motor with an axially laminated anisotropic rotor in high-speed applications. 2023. Diss.
1074. GUTIERREZ ROJAS, DANIEL. Anomaly detection in cyber-physical applications. 2023. Diss.
1075. ESANOV, BAKHTIYOR. Adaptive user-controlled personalization for virtual journey applications. 2023. Diss.





ISBN 978-952-335-937-6  
ISBN 978-952-335-938-3 (PDF)  
ISSN 1456-4491 (Print)  
ISSN 2814-5518 (Online)  
Lappeenranta 2023